

# **Evaluation of SSEA-4 as a CAR T cell therapeutic target for the treatment of chemoresistant triple negative breast cancers**

## **Dissertation**

der Mathematisch-Naturwissenschaftlichen Fakultät

der Eberhard Karls Universität Tübingen

zur Erlangung des Grades eines

Doktors der Naturwissenschaften

(Dr. rer. nat.)

vorgelegt von

Dipl. Biochem. Rita Pfeifer

aus Borodulicha/Kasachstan

Tübingen

2018

Gedruckt mit Genehmigung der Mathematisch-Naturwissenschaftlichen Fakultät der  
Eberhard Karls Universität Tübingen.

Tag der mündlichen Qualifikation:	27.07.2018
Dekan:	Prof. Dr. Wolfgang Rosenstiel
1. Berichterstatter:	Prof. Dr. Stefan Stevanović
2. Berichterstatter:	Prof. Dr. Hans-Georg Rammensee

**Parts of the thesis are from a prepared manuscript intended for publication:**

**Pfeifer, R.,** Al Rawashdeh, W., Brauner, J., Lock, D., Kaiser, A., Hardt, O., Bosio, A., Assenmacher, M., Johnston, I.C.D.

“Targeting stage-specific embryonic antigen 4 (SSEA-4) in TNBC by CAR T cells reveals unforeseen on target/off tumor toxicities in adult mice”

**Conference presentations:**

**Poster presentation: Pfeifer, R.,** Al Rawashdeh, W., Brauner, J., Lock, D., Kaiser, A., Hardt, O., Bosio, A., Assenmacher, M., Johnston, I.C.D. “Establishment of an Animal Toxicity Model for the Prediction of Clinical Utility of CAR T Cell Therapies and Technologies.” Third CRI-CIMT-EATI-AACR International Cancer Immunotherapy Conference. 2017. Mainz, Germany

**Poster presentation: Pfeifer, R.,** Lock, D., Aloia, A., Bosio, A., Johnston, I.C.D. “Targeting Glycolipid Stage-Specific Embryonic Antigen 4 (SSEA4) by CAR T cells for the treatment of solid cancers.” American Society of Gene & Cell Therapy (ASGCT). 2016. Washington, D.C., USA

**Poster presentation: Pfeifer, R.,** Lock, D., Kaiser, A., Hardt, O., Bosio, A., Assenmacher, M., Johnston, I.C.D. “Development of a CAR T cell therapy against TNBC by targeting SSEA-4”. European Society of Gene & Cell Therapy (ESGCT). 2016. Florence, Italy

**Oral presentation:** “Sialyl Glycolipid Stage-Specific Embryonic Antigen 4 (SSEA4) – a novel target for CAR T cell therapy of solid cancers.” 14<sup>th</sup> Cancer Immunotherapy (CIMT) Annual Meeting. 2016. Mainz, Germany

# Table of contents

Summary.....	I
Zusammenfassung.....	II
List of figures.....	IV
List of tables.....	VI
List of abbreviations.....	VII
1 Introduction.....	1
1.1 Breast cancer.....	1
1.1.1 Breast cancer subtypes.....	2
1.1.1.1 Luminal A breast cancer.....	2
1.1.1.2 Luminal B breast cancer.....	2
1.1.1.3 HER2-enriched breast cancer.....	2
1.1.1.4 Triple negative breast cancer.....	3
1.1.2 Treatment options for TNBC: current status and future trends.....	3
1.1.3 Expression of SSEA-4 by a chemoresistant subpopulation in TNBC.....	5
1.2 Targeted immunotherapy of cancer with chimeric antigen receptor-expressing T cells.....	7
1.2.1 Historical overview of CAR T cell therapy development.....	8
1.2.1 Generation of CAR T cells for clinical applications.....	13
1.2.2 CAR T cell therapy in the solid tumor setting.....	16
1.2.3 CAR T cell therapy-mediated toxicity.....	22
1.2.3.1 Anaphylaxis.....	23
1.2.3.2 Cytokine release syndrome.....	24
1.2.3.3 Insertional mutagenesis.....	24
1.2.3.4 Neurological toxicity.....	24
1.2.3.5 On target/off tumor recognition.....	25
1.3 Aims of the study.....	26
2 Material and Methods.....	27
2.1 Materials.....	27

2.1.1	Animals and animal facility products.....	27
2.1.2	Antibodies .....	27
2.1.2.1	Biotinylated antibodies .....	27
2.1.2.2	Fluorescence-labeled antibodies.....	28
2.1.3	Buffer and solutions.....	31
2.1.3.1	Ready-to-use buffers and solutions.....	31
2.1.3.2	Self-prepared buffers and solutions.....	32
2.1.4	Cell lines .....	33
2.1.4.1	Prokaryotic cells.....	33
2.1.4.2	Eukaryotic cells .....	33
2.1.5	Cell culture media and supplements.....	34
2.1.5.1	Media and supplements for prokaryotic cell cultures .....	34
2.1.5.2	Media and supplements for eukaryotic cell cultures .....	34
2.1.6	Enzymes and enzyme reaction buffers.....	34
2.1.6.1	Enzymes .....	34
2.1.6.2	Enzyme reaction buffers.....	35
2.1.7	Disposables .....	35
2.1.8	Laboratory equipment .....	36
2.1.9	Plasmids .....	38
2.1.10	Ready-to-use kits .....	39
2.1.11	Reagents and chemicals .....	39
2.1.12	Software.....	41
2.2	Methods .....	43
2.2.1	Molecular biology methods.....	43
2.2.1.1	Plasmid transformation and amplification .....	43
2.2.1.2	Plasmid preparation .....	43
2.2.1.3	Restriction of plasmid DNA.....	43
2.2.1.4	Agarose gel electrophoresis and isolation of DNA.....	44
2.2.1.5	Quantitation of DNA .....	45
2.2.1.6	Ligation .....	45

2.2.1.7	Sequencing of DNA.....	45
2.2.2	Cell biology methods.....	46
2.2.2.1	Cultivation of adherent cell lines.....	46
2.2.2.2	Passaging of adherent cells.....	46
2.2.2.3	Cryopreservation of cells.....	46
2.2.2.4	Thawing of cells.....	47
2.2.2.5	Cell quantitation.....	47
2.2.2.6	Transfection of HEK293T cells for CAR expression.....	47
2.2.2.7	Transfection of HEK293T cells for lentiviral vector production.....	48
2.2.2.8	Titration of lentiviral vectors.....	49
2.2.2.9	Isolation of human PBMCs.....	50
2.2.2.10	Pan T cell isolation.....	50
2.2.2.11	T cell activation, transduction and expansion.....	51
2.2.2.12	Selection of $\Delta$ LNNGFR-expressing cells.....	52
2.2.2.13	Bead-based cytokine detection.....	52
2.2.2.14	Live cell imaging-based kinetic cell lysis assay.....	53
2.2.2.15	Concurrent detection of degranulation and production of IFN $\gamma$ and TNF $\alpha$ .....	53
2.2.2.16	Flow Cytometry.....	54
2.2.3	In vivo study methods.....	56
2.2.3.1	Animal model and housing conditions.....	56
2.2.3.2	Tumor inoculation.....	57
2.2.3.3	T cell injections.....	57
2.2.3.4	Physical tumor measurements.....	57
2.2.3.5	Bioluminescent imaging of mice.....	58
2.2.3.6	Preparation of blood plasma.....	58
2.2.3.7	Preparation of single cell suspensions for flow cytometry.....	58
2.2.3.8	Flow cytometric analysis of ex vivo organ preparations.....	60
2.2.4	Statistics.....	60
3	Results.....	61
3.1	Construction of SSEA-4-specific chimeric antigen receptors.....	61

3.2	Expression analysis of SSEA-4-directed CAR variants in HEK293T cells.....	63
3.3	Generation of lentiviral vectors encoding SSEA-4 CAR variants and T cell engineering .....	64
3.4	Comparison of different flow cytometric CAR detection methods before and after $\Delta$ LNGFR enrichment .....	67
3.5	Surface expression of SSEA-4 on breast cancer cell lines .....	70
3.6	Functional in vitro characterization of SSEA-4-directed XS, S, and L spacer CAR T cells.....	71
3.7	Establishment of in vivo tumor xenograft models with MDA-MB-231 and MCF-7 ...	78
3.8	Functional in vivo characterization of SSEA-4 directed XS, S, and L spacer CAR T cells.....	80
3.9	Characterization of the in vivo toxicities mediated by SSEA-4-directed CAR T cells.. .....	84
3.9.1	Identification of SSEA-4-expressing cells in bone marrow.....	88
3.9.2	Identification of SSEA-4-expressing cells in lung.....	91
4	Discussion.....	93
4.1	Comparison of different CAR T cell detection methods .....	94
4.2	Impact of the spacer region on CAR function .....	95
4.3	Choice of animal model for testing in vivo toxicity of SSEA-4-directed CAR T cells	97
4.4	Characterization of SSEA-4-expressing subpopulations targeted by CAR T cells ..	98
4.5	Conclusions.....	100
5	References.....	102
	Acknowledgement.....	130

## Summary

Triple negative breast cancer (TNBC) is an aggressive subtype of breast cancer that accounts for 15-20% of breast cancer incidences. Since it lacks estrogen receptor, progesterone receptor and HER2 overexpression, therapy options are limited to surgery, radiation and chemotherapy, which are curative only to a small fraction of TNBC patients. Accordingly, TNBC has the highest rates of metastatic disease and the poorest overall survival of all breast cancer subtypes. Recently, the sialoglycolipid stage-specific embryonic antigen 4 (SSEA-4) has been identified as an epitope whose overexpression in TNBC strongly correlates with metastasis and chemoresistance. As TNBC patients are typically exposed to multiple rounds of chemotherapy and SSEA-4-positive cells have been found to be enriched in residual tumors surviving this treatment, a sequential therapeutic approach using chemotherapy followed by SSEA-4-directed chimeric antigen receptor (CAR) T cell administration holds great promise to improve the therapeutic outcome of TNBC patients. Consequently, the aim of this study was to develop and evaluate an SSEA-4-directed CAR T cell-based treatment modality for TNBCs. In order to explore the optimal CAR configuration, five second generation chimeric receptors that differed in type and length of the spacer region were generated. All receptors contained a human/mouse cross-reactive single chain variable fragment which allowed a preclinical on target/off tumor toxicity profiling due to the correlated antigen expression between the mouse and the human organism. The three lead candidates, that showed good surface expression, activated T cells in an antigen-specific manner as characterized by T cell degranulation, secretion of inflammatory cytokines and effective killing of SSEA-4-expressing target cells *in vitro*. The efficacy of T cell activation was not uniform between the constructs and no direct correlation between CAR potency and CAR spacer length was observed. When the SSEA-4-directed CAR T cells were adoptively transferred into mice with subcutaneous TNBC cell line xenografts (MDA-MB-231), only the CAR variant that showed the strongest *in vitro* bioactivity could control tumor growth. No anti-tumor effect was detectable in mice cohorts receiving the other CAR T cell variants. In parallel to the tumor burden control, mice receiving T cells incorporating the most potent CAR variant exhibited toxicity symptoms and cachexia. It was found that the administered CAR T cells proliferated primarily in the lungs and in bone marrow with the latter demonstrating hypocellularity and a strong decrease of the CD45<sup>+</sup>Sca-1<sup>bright</sup> population upon therapy. In bone marrow, hematopoietic multipotent progenitor cells were identified to express SSEA-4 which were likely co-targeted by the CAR T cells. In the lungs, the SSEA-4-positive subset was found to co-express CD44, CD81, CD98, and Prominin-1 suggesting an epithelial pluripotent population. The severe side-effects observed in this study raise safety concerns for therapies targeting SSEA-4-positive tumor cells, as a high risk exists to collaterally damage vital pluripotent cells within the organism. Therefore, great care has to be invested in SSEA-4-directed immunotherapies to avoid life threatening side effects.

## Zusammenfassung

Das dreifach negative Mammakarzinom (engl. *triple negative breast cancer*, TNBC) ist ein aggressiver Brustkrebsstyp, der in 15-20% der Brustkrebsfälle vorkommt. Da es weder eine Expression von Östrogen- oder Progesteronrezeptoren noch eine Überexpression von HER2 aufweist, beschränken sich die therapeutische Maßnahmen auf Operation, Bestrahlung und Chemotherapie. Diese sind allerdings nur für einen kleinen Teil der TNBC Patienten kurativ, weshalb bei ihnen – im Vergleich zu anderen Brustkrebsformen – die höchste Metastasierungsrate und die niedrigste Überlebenserwartung auftreten. Vor kurzem wurde das Sialoglykolipid Stadienspezifische embryonale Antigen-4 (SSEA-4) als Epitop identifiziert, dessen Überexpression stark mit den metastasierenden und chemoresistenten Eigenschaften im TNBC korreliert. Da Krebspatienten mehrere Chemotherapiezyklen durchlaufen und SSEA-4-positive Zellen in Tumoren angereichert werden, die diese Behandlung überstehen, verspricht ein sequentieller Therapieansatz aus Chemotherapie und einer darauffolgenden SSEA-4-gerichteten chimären Antigenrezeptor (CAR) T-Zelltherapie, das Behandlungsergebnis zu verbessern und die Gesamtüberlebensdauer der Krebspatienten zu erhöhen. Demnach war das Ziel dieser Studie die Entwicklung und Evaluation einer SSEA-4-gerichteten Behandlungsmethode für TNBC, die auf einer CAR T-Zelltherapie basiert.

Zur Untersuchung der optimalen CAR-Konfiguration wurden 5 Rezeptoren der zweiten Generation entwickelt, die sich in Typ und Länge der Distanzregion zwischen der antigenbindenden Domäne und der Transmembranregion unterschieden. Da die Antigenexpression zwischen Maus und Mensch korreliert, wurde zur Antigenerkennung ein Einzelkettenfragment der variablen Region eines SSEA-4-spezifischen Antikörpers eingebaut, das kreuzreaktiv zum humanen und murinen Epitop ist und somit eine *on target/off tumor* Toxizitätsanalyse bei einem Mausmodell erlaubte. Die drei Kandidaten, welche die beste Oberflächenexpression zeigten, aktivierten T-Zellen auf eine antigenspezifische Weise, was sich in Form von Degranulation von T-Zellen, Sekretion von inflammatorischen Zytokinen und Abtötung von SSEA-4-positiven Zielzellen zeigte. Die Effizienz der T-Zellaktivierung war bei den Konstrukten nicht einheitlich und es ließ sich keine direkte Korrelation zwischen der CAR-Wirksamkeit und der Distanzdomänenlänge der Rezeptoren beobachten.

Nach adoptivem Transfer von SSEA-4-spezifischen CAR T-Zellen in Mäuse mit subkutanen Tumoren einer TNBC-Zelllinie (MDA-MB-231) konnte nur dasjenige CAR-Konstrukt das Tumorstadium kontrollieren, welches zuvor die stärkste *in vitro*-Bioaktivität gezeigt hatte. Bei den Mauskohorten, die die anderen CAR T-Zellgruppen erhielten, trat kein Antitumoreffekt auf. Neben der Tumorkontrolle konnten bei den Mäusen auch Toxizitätssymptome und Kräfteverfall beobachtet werden. Die verabreichten CAR T-Zellen proliferierten vorrangig in Lunge und Knochenmark, wobei bei letzterem Hypozellularität sowie eine starke Abnahme der

CD45<sup>+</sup>Sca-1<sup>high</sup> Population infolge der Therapie auftraten. Es stellte sich heraus, dass hämatopoetische multipotente Vorläuferzellen eine SSEA-4-Expression aufweisen, weshalb diese mit hoher Wahrscheinlichkeit von den CAR T-Zellen ebenfalls angegriffen werden. In der Lunge zeigte die antigenpositive Subpopulation eine Koexpression von CD44, CD81, CD98 und Prominin-1, was darauf hindeutet, dass es sich um epitheliale pluripotente Zellen handelte. Die gravierenden Nebeneffekte, die in dieser Studie beobachtet wurden, geben Anlass zu Sicherheitsbedenken für Therapien, die auf die Zerstörung SSEA-4-positiver Tumorzellen abzielen, da hohes Risiko besteht, hierbei auch essenzielle pluripotente Stammzellen innerhalb des Organismus zu zerstören. Aufgrund dieser lebensbedrohlichen Kollateralschäden ist bei SSEA-4-bezogenen immuntherapeutischen Ansätzen große Vorsicht geboten.

## List of figures

Figure 1: Clinical classification of breast cancers based on receptor expression. ....	2
Figure 2: Overall survival by tumor type and response status. ....	3
Figure 3: Expression of SSEA-4 in TNBC. ....	6
Figure 4: Evolution of chimeric antigen receptors (CARs). ....	11
Figure 5: Timeline of the preclinical and clinical development of CAR T cell therapy. ....	13
Figure 6: A step-by-step breakdown of the CAR T cell manufacturing procedure. ....	15
Figure 7: <i>In vivo</i> application of CARs. ....	23
Figure 8: Detection of MACSPlex cytokine capture bead populations. ....	52
Figure 9: Illustration of the binding sites of Protein L. ....	55
Figure 10: Organisation of the pairwise significant matrix for group comparison. ....	60
Figure 11: Schematic representation of the lentiviral transfer vectors used in this study and construction of SSEA-4-directed CAR variants. ....	62
Figure 12: Expression of $\Delta$ LNGFR and second generation XS, S, M, L, and XL spacer CAR variants on HEK293T cell surface. ....	64
Figure 13: Expression of $\Delta$ LNGFR and second generation XS, S, M, L, and XL spacer CAR variants on T cell surface. ....	65
Figure 14: Expression of $\Delta$ LNGFR on CD4 <sup>+</sup> and CD8 <sup>+</sup> T cells after transduction of Pan T cells with XS, S, and L spacer CAR encoding lentiviral vectors. ....	66
Figure 15: Comparison of different flow cytometric methods for the detection of CAR expression on the T cell surface before $\Delta$ LNGFR enrichment (pre) and after $\Delta$ LNGFR enrichment and expansion (post). ....	69
Figure 16: Surface expression of SSEA-4 on the breast cancer cell lines MCF-7, MDA-MB-231, SK_BR_3, and BT-474. ....	70
Figure 17: Degranulation of T cells after stimulation with MDA-MB-231 and MCF-7. ....	72
Figure 18: Dynamic monitoring of CAR T cell-mediated cytotoxicity. ....	73
Figure 19: Cytokine secretion by CAR transduced T cells following antigen stimulation. ....	74
Figure 20: Expression of PD-L1 and PD-L2 on MDA-MB-231 and MCF-7. ....	75
Figure 21: Heterogeneity of IFN $\gamma$ and TNF $\alpha$ production of cytolytic CAR T cells. ....	77
Figure 22: Characterization of MDA-MB-231 and MCF-7 tumor growth in subcutaneous xenograft models. ....	79
Figure 23: <i>In vivo</i> activity of SSEA-4-directed CAR T cells. ....	81
Figure 24: Frequency of CAR (human CD45 <sup>+</sup> $\Delta$ LNGFR <sup>+</sup> ) and untransduced (human CD45 <sup>+</sup> ) control T cells in mouse peripheral blood over the course of therapy. ....	82
Figure 25: Organ infiltration by CAR-expressing or untransduced control T cells. ....	83
Figure 26: Body weight development in tumor-free NSG <sup>TM</sup> mice following adoptive transfer of SSEA-4-directed CAR T cells. ....	85

Figure 27: Blood serum levels of human IFN $\gamma$ , IL-2, and TNF $\alpha$  in NSG<sup>TM</sup> mice. ....86

Figure 28: Localization of SSEA-4-CAR T cell activity following adoptive transfer in NSG<sup>TM</sup> mice.....88

Figure 29: Bone marrow toxicity following SSEA-4 CAR T cell therapy and phenotypic characterization of bone marrow-resident SSEA-4-expressing cells. ....90

Figure 30: Phenotypic characterization of SSEA-4-expressing cells in lung tissue. ....92

## List of tables

Table 1: Summary of solid tumor target antigens for CAR T cell therapy in clinical and preclinical evaluation. ....	19
Table 2: Biotin-conjugated primary antibodies used within the scope of this study. ....	27
Table 3: Fluorochrome-conjugated antibodies used within the scope of this study. ....	28
Table 4: Prokaryotic cells used for cloning.....	33
Table 5: Eukaryotic cell lines used within the scope of this study.....	33
Table 6: Laboratory equipment used within the scope of this study. ....	36
Table 7: Softwares used within the scope of this study.....	41
Table 8: Composition of analytical and preparative restriction reactions.....	44
Table 9: Cell numbers and volumes for different cell culture vessels.....	51
Table 10: Overview of cargo length and obtained titers for lentiviral vectors encoding XS, S, M, L, and XL spacer CAR variants.....	65
Table 11: Expression efficiency of XS, S, M, L, and XL spacer CAR on the T cell surface normalized to $\Delta$ LNGFR.....	66

## List of abbreviations

### A

aa	amino acid(s)
ALL	acute lymphoblastic leukemia
APC	Allophycocyanin

### B

BLI	bioluminescent imaging
bp	base pairs
BSA	bovine serum albumin

### C

CAIX	carbonic anhydrase IX
CAR	chimeric antigen receptor
CDR	complementarity determining region(s)
C <sub>H</sub>	constant heavy chain
C <sub>L</sub>	constant light chain
CLL	chronic lymphocytic leukemia
CR	complete response
CRS	cytokine release syndrome
CO <sub>2</sub>	Carbon dioxide

### D

°C	degree Celsius
ddH <sub>2</sub> O	double-distilled water
ΔLNGFR	truncated low affinity nerve growth factor receptor
DMEM	Dulbecco's modified Eagle's medium
DMSO	dimethyl sulfoxide
DNA	Deoxyribonucleic acid

### E

<i>E. coli</i>	<i>Escherichia coli</i>
e.g.	<i>exempli gratia</i> , for example
EDTA	Ethylenediaminetetraacetic acid
ER	estrogen receptor
et al.	<i>et alii</i> , and others
EGFR	epidermal growth factor receptor
EGFRvIII	variant III of the epidermal growth factor receptor
EtBr	ethidium bromide

### F

Fab	fragment for antigen-binding
FAP	fibroblast activation protein

Fc	fragment crystallizable region	IU <sub>HT1080</sub>	infectious units titrated on HT1080
FCS	fetal calf serum	i.p.	intraperitoneal
FcR	Fc receptor	i.v.	intravenous
FDA	Food and Drug Administration	<b>L</b>	
FSC	forward scatter	L	liter
FSC-A	forward scatter area	LAMP-1	lysosome associated membrane protein 1
FSC-H	forward scatter height		
FITC	fluorescein isothiocyanate	LDL-R	low affinity density lipoprotein receptor
<b>G</b>		luc	luciferase
G	glycine; Gauge	<b>M</b>	
g	gram; gravity acceleration	μ	micro
GFP	green fluorescent protein	M	molar
GMP	good manufacturing practice	m	mouse
<b>H</b>		mAb	monoclonal antibody
h	hours; human	MACS <sup>®</sup>	magnetic-activated cell sorting (registered trademark)
HEK	human embryonic kidney	MHC	major histocompatibility complex
HER2	ERBB2, human epidermal growth factor 2	min	minute(s)
<b>I</b>		MOI	multiplicity of infection
IFN	Interferon	mRNA	messenger ribonucleic acid
Ig	Immunoglobulin		
IL	Interleukin		
IU	international units		

**N**

n	nano
NHL	non-Hodgkin's lymphoma
NK cell	Natural killer cell
NSG	NOD.scid.IL2 $\gamma^{-/-}$

**O**

ORF	open reading frame
ORR	Overall response rate

**P**

p	Plasmid
P2A	porcine teschovirus-1 2A peptide
PpL	<i>Peptostreptococcus magnus</i> Protein L
PBMC	peripheral blood mononuclear cells
PD-1	programmed cell death protein 1
PD-L1	programmed cell death 1
PD-L2	programmed cell death 2
PE	Phycoerythrin
PEB	PBS/EDTA/BSA
PMA	Phorbol myristate acetate
pre-B-ALL	pre-B cell acute lymphoblastic leukemia

**R**

RBC	red blood cells
RCC	renal cell carcinoma
REA	REAffinity antibody

**P**

PBS	phosphate-buffered saline
PR	progesterone receptor
ROI	region of interest

**S**

S	serine
s	second(s)
s.c.	subcutaneous
scFv	single-chain antibody variable fragment
SCID	severe combined immunodeficiency
SD	standard deviation
SEM	standard error of the mean
SPF	specific pathogen free
SSC	side scatter
SUMC	single use mouse cage
SSEA-4	stage-specific embryonic antigen-4

**T**

TCR	T cell receptor
TNBC	triple negative breast cancer
TNF	tumor necrosis factor
TNFR	tumor necrosis factor receptor

**V**

v	volume
VEGFR-2	vascular endothelial growth factor 2
V <sub>H</sub>	variable heavy chain
V <sub>L</sub>	variable light chain
VSV-G	vesicular stomatitis virus glycolipid

Parts of the data and text in this thesis have been directly taken or slightly modified from a prepared manuscript intended for publication (Pfeifer et al., 2018). The text has been originally written by myself.

# 1 Introduction

## 1.1 Breast cancer

Breast cancer represents the most common neoplasm in women worldwide and is the number one cause of cancer death in females (Anderson et al., 2006; Bray et al., 2004). Each year, more than 1.6 million new cases are diagnosed of which less than 1% affect men (Ferlay et al., 2015; Ghoncheh et al., 2016; Korde et al., 2010). Interestingly, while the incidence of breast cancer is on the rise, the mortality rates have dramatically declined since the 1980s. This decrease is attributed to technological advancements in screening and increased use of targeted therapy directed against dysregulated hormone or growth factor receptor signaling (Berry et al., 2005). Nevertheless, breast cancer still imposes a considerable health and economic burden making it a major public health concern. There are more than twice as many new breast cancer cases diagnosed each year than new incidences of cancer at any other site (Stewart and Wild, 2014). Its etiology has been described to be multifactorial, although increased levels of estrogen are attributed to play a key role in the development of breast tumors. On the basis of epidemiological studies it was found that women with early menarche and late menopause exhibit an increased risk due to longer exposure to endogenous estrogen. In addition, late age of first pregnancy further augments the possibility for developing mammary tumors (Clemons and Goss, 2001).

In terms of genetic factors, germline mutations in the two tumor suppressor genes breast cancer gene 1 (*BRCA1*) and/or breast cancer gene 2 (*BRCA2*) were shown to contribute up to 80% increased lifetime risks of developing breast cancer until the age of 70. Alterations in these genes are associated with 15-20% of familial breast cancers and comprise 2-3% of all breast cancer incidences (Venkitaraman, 2002). Accordingly, somatic mutations are still perceived as the most common causes driving breast carcinogenesis (Nik-Zainal et al., 2016). The most prevalent somatic alterations were described to occur in tumor protein 53 (*TP53*), retinoblastoma 1 (*RB1*), GATA binding protein 3 (*GATA3*), phosphatase and tensin homolog (*PTEN*), phosphatidylinositol-4,5-bisphosphate 3-kinase subunit  $\alpha$  (*PI3CA*), cyclin D1 (*CCND1*), fibroblast growth factor receptor 1 (*FGFR1*), mitogen-activated protein kinase kinase kinase 1 (*MAP3K1*), and Erb-b2 receptor tyrosine kinase 2 (*ERBB2*) (Nik-Zainal et al., 2016).

Around 522,000 women succumb to the disease per year (Ferlay et al., 2015). In this context, metastasis is a very important clinical challenge as it attributes to 90% of all breast cancer related deaths (Chaffer and Weinberg, 2011; Cummings et al., 2014). Although the majority of patients is diagnosed with localized disease, around 30-50% receiving therapy for early stage disease will develop metastatic lesions (Cardoso et al., 2012; Henderson, 2013). Solutions to improve metastatic disease prevention are therefore urgently needed and an active area of current research.

### 1.1.1 Breast cancer subtypes

Breast cancer is a heterogeneous disease with different pathological features and different therapeutic response patterns. In clinical practice, it is therefore routinely categorized into 4 subtypes based on the immuno-histochemical staining levels for the expression of estrogen receptor (ER), progesterone receptor (PR), human epidermal growth factor receptor 2 (HER2) and the proliferation marker Ki67 (Figure 1).

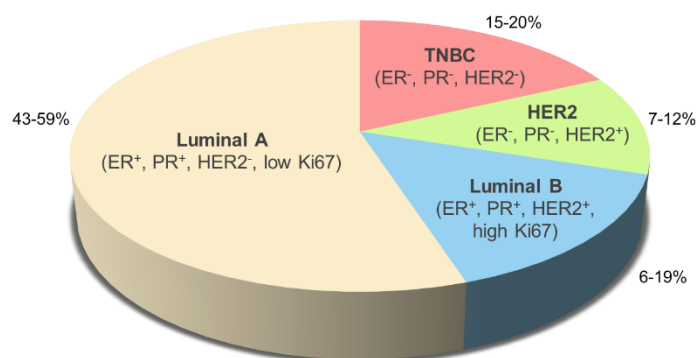


**Figure 1: Clinical classification of breast cancers based on receptor expression.** Pie slice sizes represent fractions of breast cancer incidences. ER, estrogen receptor; PR, progesterone receptor; HER2, human epidermal growth factor receptor 2; TNBC, triple negative breast cancer. Figure modified from Kumar et al. (2012).

Classification into subtypes helps to stratify patients into groups with divergent prognosis and optimize therapeutic treatment (Hennigs et al., 2016; Perou et al., 2000).

#### 1.1.1.1 Luminal A breast cancer

Luminal A is the most common subtype of breast cancers which accounts for 43-59% of all tumors diagnosed. These cancers are characterized by high expression of ER and/or PR but a lack of HER2 amplification (HER2-negative). They are relatively slow growing as seen by low levels of Ki67 expression, less likely to spread and respond well to anti-hormonal therapy. Therefore, patients with luminal A tumors have the most favorable prognosis with high survival and low recurrence rates (Peppercorn et al., 2008; Voduc et al., 2010).

#### 1.1.1.2 Luminal B breast cancer

Luminal B type of breast cancer encompasses 6-19% of the total cases and is defined by a weaker expression of ER and/or PR compared to luminal A breast cancer and an over-expression or amplification of the HER2 gene product (HER2-positive). Based on increased expression of Ki67, these tumors display a higher cell proliferation rate than luminal A cancers and have a slightly worse prognosis (Parise and Caggiano, 2014). Besides chemotherapy, first-line treatment options are anti-hormonal and HER2-directed therapies (Ades et al., 2014).

#### 1.1.1.3 HER2-enriched breast cancer

The HER2-enriched subtype is characterized by absent expression of both hormonal receptors, but an amplified expression of the HER2 oncogene. It has a prevalence of about 7-12% and is

susceptible to early and frequent recurrence and metastasis (Blows et al., 2010). The use of targeted therapies directed against the HER2 gene product, however, has reversed much of the adverse prognostic impact of HER2 overexpression (Baselga, 2010).

#### 1.1.1.4 Triple negative breast cancer

Approximately 15-20% of breast cancer patients develop lesions that are clinically described as “triple negative” due to their negativity for expression of ER and/or PR and lack of overexpression for HER2. This subtype of breast cancers differs from others in its predilection to primarily affect women below the age of 40 (Bauer et al., 2007) and a disproportionate number of metastatic cases and cancer deaths (Dent et al., 2007; Pal et al., 2011). Patients with triple negative breast cancer (TNBC) display a distinct pattern of metastasis with higher rates of distant recurrence to brain and lungs, but less likely to bones (Dent et al., 2007; Liedtke et al., 2008). The 5-year survival rate of TNBC patients (77%) is significantly lower compared to non-TNBC patients (93%) (Bauer et al., 2007).

#### 1.1.2 Treatment options for TNBC: current status and future trends

TNBC is one of the most complicated types of breast cancer to treat. Compared to other breast cancers, triple negative tumors are more aggressive and display an increased likelihood of local and distant metastasis (Dent et al., 2009; Fulford et al., 2007). Initially, TNBC patients respond well to standard care chemotherapy with anthracyclines, taxanes, and/or platinum compounds, however, only

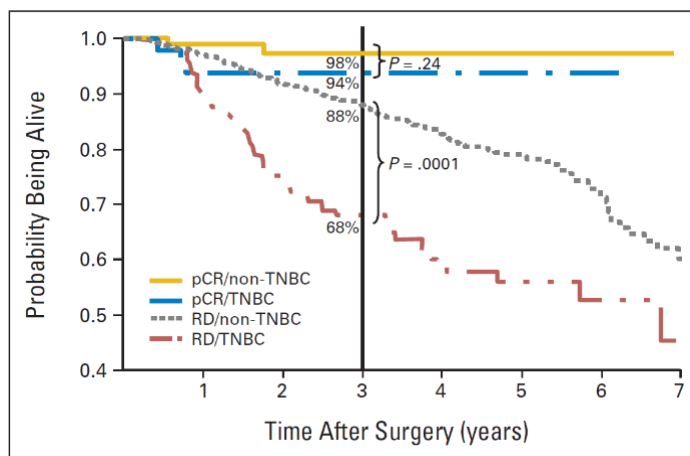


**Figure 2: Overall survival by tumor type and response status.** TNBC, triple negative breast cancer; pCR, pathological complete response; RD, residual disease. Figure adapted from Liedtke et al. (2008).

30-45% achieve a pathological complete response and survival rates similar to other breast cancer subtypes (Balko et al., 2014; Liedtke et al., 2008; Masuda et al., 2011). When residual disease remains, the prognosis is worse than for patients without pathological complete response from other subtypes of breast cancer (Liedtke et al., 2008) (Figure 2). This is largely due to the fact that no oncogenic alterations are known that could be therapeutically targeted across a significant fraction of triple negative tumors. Inhibition of epidermal growth factor

receptor (EGFR), the only target that was found so far to be expressed in ~70% of TNBC, failed in a cetuximab-based targeting approach in clinical trials (ClinicalTrials.gov identifier: NCT00232505) (Carey et al., 2012). It was later discovered that EGFR inhibition rewires the cell to activate AKT and ERBB<sub>3</sub> signaling pathways, which ultimately mediate resistance (Sergina et al., 2007).

Taking into consideration that novel therapies for this type of breast cancer are essential and urgent, large scale genomic and proteomic analyses have identified at least four molecularly distinct subtypes of TNBC (Balko et al., 2014; Burstein et al., 2015; Cabezón et al., 2013; Lawrence et al., 2015; Lehmann et al., 2011). These findings in turn have enabled the identification of possible targets specific for each subtype. Currently, several therapies have entered clinical trials for the treatment of TNBC, including

- poly-ADP ribose polymerase (PARP) inhibitors (e.g. olaparib (NCT026815562, NCT03205761), veliparib (NCT02849496), talazoparib (NCT02401347), and rucaparib (NCT01074970)), anti-androgen receptor agents (e.g. bicalutamide (NCT03055312, NCT03090165), CR1447 (NCT02067741), darolutamide (NCT03383679), enzalutamide (NCT01889238, NCT02457910, NCT02689427, NCT02750358), enobosarm (NCT02971761), seviteronel (NCT02580448), and ortelonel (NCT01990209)),
- histone deacetylase (HDAC) inhibitors (e.g. entinostat (NCT01349959, NCT02708680, NCT03361800), panobinostat (NCT01105312, NCT01194908, NCT02890069), romidepsin (NCT02393794), and tinostamustine (NCT03345485)),
- serine-threonine kinase mammalian target of rapamycin (mTOR) inhibitors (e.g. AZD2014 (NCT02583542, NCT02208375), PQR309 (NCT02723877), everolimus (NCT00499603), and PF-05212384 (NCT01920061)),
- angiogenesis inhibitors (e.g. sunitinib (NCT00887575, NCT00246571), sorafenib (NCT02624700), and bevacizumab (NCT00528567, NCT00472693, NCT01201265 and others)), as well as
- drug combinations that target several signaling pathways (Pal and Mortimer, 2009).

While most studies are still ongoing, initial results remain modest thus highlighting the challenges of intra- and intertumoral heterogeneity and the danger of therapy resistance development (Kalimutho et al., 2015).

In recent years, studies of immune infiltration in breast tumors have shown that aggressive breast cancers such as HER2-enriched breast cancer and TNBC have the greatest incidence of patients with a robust immune infiltrate. Elevated levels of either intratumoral or stromal T cells were associated with improved disease-free and overall survival as well as pathologic complete response in the neoadjuvant setting (Adams et al., 2014; Ibrahim et al., 2014; Loi et

al., 2013, 2014). Interestingly, TNBC was more likely to have lymphocyte infiltration greater than 50% of the total tumor mass indicating that this subtype is more immunogenic than other breast cancers. These findings advocated the potential use of therapeutic immunomodulation and clinical trials have now been attempting to assess immune checkpoint inhibition as a new treatment modality for TNBC. Several options are currently being investigated, specifically

- cytotoxic T lymphocyte-associated antigen 4 (CTLA-4) inhibition by ipilimumab (NCT03326258) or tremelimumab (e.g. NCT02527434) as well as
- the blockade of the programmed cell death 1 (PD-1)/PD-1 ligand 1 (PD-L1) axis by atezolizumab (e.g. NCT02425891), avelumab (e.g. NCT02926196), durvalumab (e.g. NCT02489448), nivolumab (NCT02393794), pembrolizumab (e.g. NCT02447003), and PDR001 (NCT02404441).

Preliminary results indicate a tolerable safety profile of this treatment modality and a response-rate of 10-19% (Bianchini et al., 2016; Kwa and Adams, 2018).

In parallel to these activities, a phase I clinical trial study is evaluating antibody targeting of CD73 as an alternative treatment option to TNBC (NCT03454451). CD73 is a membrane-associated enzyme that converts adenosine monophosphate (AMP) into adenosine with the latter being an immuno-suppressive metabolite that protects tissues against excessive inflammation (Eltzschig, 2013). In the tumor microenvironment, adenosine suppresses antitumor immunity essentially through A2a (Sitkovsky et al., 2014) and A2b (Mittal et al., 2016) adenosine receptors. Overexpression of CD73 was shown mainly in metastatic TNBC and is linked to worse prognosis and resistance to chemotherapy (Loi et al., 2013).

Additional immune targets such as the cancer/testis antigens melanoma associated antigens (MAGE-A) A3 and A4 as well as New York esophageal squamous cell carcinoma 1 (NY-ESO-1) are currently being evaluated in preclinical studies as their expression was shown in a substantial proportion of TNBC cells (Badovinac Črnjević et al., 2012; Curigliano et al., 2011; Turner et al., 2010). Other attractive immunotherapeutic targets in preclinical evaluation for TNBC treatment are the glycosylated form of mucin 1 (MUC-1) and mesothelin. Consequently, while still work in progress, the future therapeutic approaches to TNBC are expected to implement immune modulatory strategies to achieve successful treatment results.

### **1.1.3 Expression of SSEA-4 by a chemoresistant subpopulation in TNBC**

First-line treatment of TNBC is predominantly a combination chemotherapy with several genotoxic drugs (Davis et al., 2014). TNBC patients who present residual disease after such a treatment have in general very poor outcome and alternative treatment options with a favorable

efficacy and safety profile are urgently needed. In an attempt to identify novel targetable biomarkers of chemoresistant cells in TNBC, Aloia et al. performed a flow cytometry-based cell surface marker screening with patient-derived TNBC tumor xenografts treated in mice with standard care chemotherapy of doxorubicin and cyclophosphamide. The authors found that upon chemotherapy treatment, a subpopulation of tumor cells becomes enriched with an overexpression of a glycosphingolipid, commonly known as stage-specific embryonic antigen-4 (SSEA-4) (Aloia et al., 2015)

(Figure 3A). The molecule is part of the globoseries family and is composed of a hexameric carbohydrate structure that is linked to a ceramide moiety (Figure 3B). Currently, it is widely used as a marker to identify pluripotent embryonic and mesenchymal stem cells that rapidly disappears upon cell differentiation (Breimer et al., 2017; Gang et al., 2007; Pittenger, 1999; Riekstina et al., 2009; Shinohara et al., 2015). In their work, Aloia et al. identified a fraction of ~10-30% of SSEA-4-positive cells in TNBC tumors, whose frequency increased by 2-3-fold upon genotoxic treatment. More important, the overall number of SSEA-4-positive cells was not augmented upon therapy, rather these cells showed more resistance to drug toxicity. Besides doxorubicin and cyclophosphamide, these observations were also made with other commonly used chemo-therapeutic drugs such as cisplatin, mafosfamide, and 5-fluorouracil. Interestingly, when the tumors were allowed to regrow after chemotherapy, some tumor xenografts retained a high frequency of SSEA-4-positive cells, while in other tumors this subpopulation returned to pretreatment levels indicating that these cells do not have a general growth advantage. Gene expression analysis and functional assays linked antigen positivity to a mesenchymal phenotype of the cancerous cells, a state which is broadly accepted to be associated with increased resistance to a variety of cell death-inducing signals and strong metastatic potential (Creighton et al., 2009; O'Reilly et al., 2015; Thiery, 2002). The mesenchymal characteristics along with an increased migratory potential of SSEA-4-positive tumor cells were further confirmed by an independent study of Sivasubramaniyan et al.

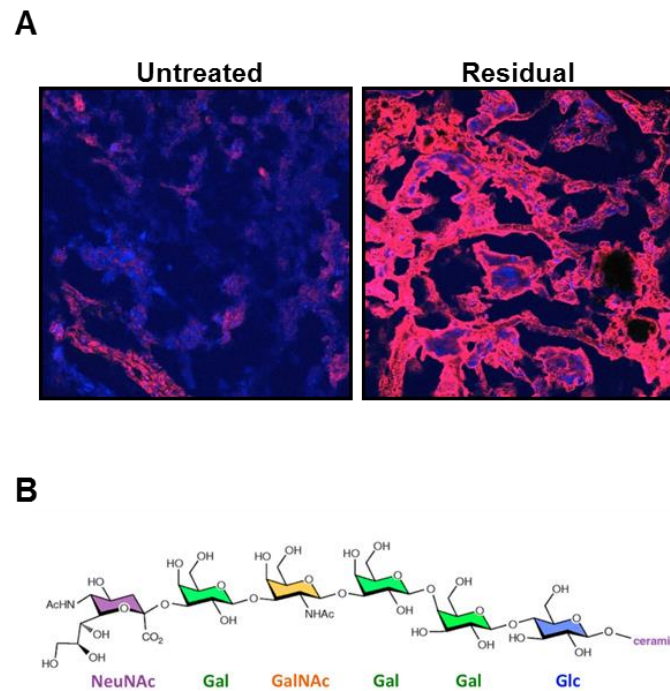


**Figure 3: Expression of SSEA-4 in TNBC.** (A) Immunohistochemical analysis of SSEA-4 expression in untreated and chemotherapy-treated TNBC tumor (red, SSEA4; blue, 4',6-diamidino-2-phenylindole). Figure modified from Aloia et al. (2015). (B) Structure of SSEA-4. Glc, glucose; Gal, galactose; GalNAc, N-acetyl-galactosamin, NeuNAc, N-acetyl-neuraminic acid.

(Sivasubramaniyan et al., 2015). Using a different clone and an antibody of the Immunoglobulin (Ig) M class (instead of IgG as by Aloia et al.), the authors found SSEA-4-positive subpopulations in an array of solid tumor cell lines but not leukemic blasts. Upon further characterization, they identified SSEA-4-positive cells to be enriched for additional pluripotent embryonic stem cell markers such as SSEA-3, Tra-1-60, and Tra-1-81 suggesting their low differentiation status. Furthermore, imaging approaches revealed that the glycolipid predominantly accumulates in filopodia and invadopodia, cellular protrusions that are associated with degradation of the cellular matrix in cancer invasiveness and metastasis. These findings suggest a role of SSEA-4 in the metastatic cascade of neoplastic cells. Collectively, the data sets of two independently working groups using two different antibodies compliantly identified SSEA-4 as a marker for intratumoral heterogeneity and the acquisition of a mesenchymal state by antigen-positive cells. The high metastatic potential along with chemoresistant properties of cells expressing the glycolipid suggest an essential role of this molecule in cancer progression making it an attractive target for immunotherapeutic approaches in TNBC treatment. Moreover, the fact that the expression of SSEA-4 is limited in healthy tissue showing only restricted antigen positivity by subpopulations in placenta, testis, skin, and small intestine (internal data, not shown) further supports a therapeutic targeting strategy.

## **1.2 Targeted immunotherapy of cancer with chimeric antigen receptor-expressing T cells**

Immunotherapeutic treatment of cancer using chimeric antigen receptor (CAR)-expressing T cells is a relatively new approach in adoptive cell therapy. The strategy is based on genetically equipping T cells with novel synthetic receptors that consist extracellularly of an antibody-type recognition domain and intracellularly of T cell signaling modules (Figure 4). The direct identification of intact antigens that is provided by the antibody-derived binding domain of the receptor enables T cells to bypass restrictions of the major histocompatibility complex (MHC)-mediated antigen recognition, so that a given CAR can be used in any patient regardless of its MHC haplotype. Furthermore, the MHC independence endows the CAR T cells with a fundamental anti-tumor advantage, as some tumor cells downregulate MHC expression to escape the T cell receptor (TCR)-mediated immune response (Garrido et al., 1993). T cells that are engineered to express the CAR of interest, on the other hand, are still able to recognize and eradicate these escaping tumor cells. Moreover, by using CAR T cells, the range of potential tumor targets can be broadened to epitopes that are beyond the scope of TCR-based recognition, e.g. it is possible to include not only proteins but also carbohydrates

(Mezzanzanica et al., 1998) and glycolipids (Yvon et al., 2009) for tumor targeting. One limitation of the current CAR T cell strategies, however, is that they are restricted to extracellular antigens on the cancer cells and are unable to target the intracellular proteome.

### 1.2.1 Historical overview of CAR T cell therapy development

The development of CAR T cell therapy has been a multistep process with a series of ups and downs and the significant historical events are summarized in Figure 5. Originally, the concept of providing T cells with antibody-type specificity was described by Eshhar and colleagues at the Weizmann Institute of Science in Israel in 1989 (Gross et al., 1989). In an endeavor to overcome the MHC restriction for T cell activation, they replaced the  $V\alpha$  and  $V\beta$  extracellular domains of the TCR chains with their homologs of immunoglobulin variable light chain ( $V_L$ ) and variable heavy chain ( $V_H$ ) this way giving rise to two chimeric TCR chains ( $C\alpha V_H:C\beta V_L$  or  $C\alpha V_L:C\beta V_H$ ) that functioned independently of their natural ligand partners (Figure 4). When stimulated with an antigen, the fusion proteins induced T cell effector function which provided evidence that stimuli through the TCR:CD3 complex can activate T cells in an MHC-independent manner (Goverman et al., 1990; Gross et al., 1989). As the practicability of this approach suffered from laborious gene engineering as well as inefficient surface expression of the chimeras, the scientists pioneered in 1993 a one-polypeptide-chain design that incorporated a single-chain variable fragment (scFv) of a given antibody as the antigen recognition unit, an extracellular spacer and a transmembrane region as structural features, and a cytoplasmic CD3 $\zeta$  or FcR $\gamma$  domain for T cell activation (Eshhar et al., 1993). This linear arrangement has been termed 'first generation' CAR (Figure 4) and showed antigen-dependent activation of T cell signaling events that eventually resulted in the induction of the cytolytic machinery and Interleukin(IL)-2 production (Eshhar et al., 1993; Eshhar, 2008). Since then, efforts have been made to improve the quality, strength, and duration of the signals delivered by the CAR through incorporation of co-stimulatory domains into the design. The first successful attempt in generating a dual signaling domain containing chimeric receptor was described by Finney et al. from Celltech Therapeutics, Ltd. in 1998. By engineering the single chain variable fragment (scFv) in line to the hinge, transmembrane, and intracellular domains of CD28 followed distally by the CD3 $\zeta$ , they were able to show increased antigen-stimulated IL-2 production compared to first generation CAR T cells (Finney et al., 1998). This finding was further supported by Maher et al. in 2002 who reported that CD28 co-stimulation confers both enhanced IL-2 secretion and robust expansion of the gene-modified immune cells *in vitro* (Maher et al., 2002). Of note, both studies demonstrated that the orientation of the signaling

domains is important and positioning the CD28 co-stimulus downstream of CD3 $\zeta$  abrogates the superior function of the CAR (Finney et al., 1998; Maher et al., 2002).

In parallel to activities with CD28 co-stimulation, reports testing 4-1BB as a co-stimulatory domain in CAR design described that increased antigen-triggered IL-2 secretion was also observed for this alternative co-signaling moiety and – additionally – 4-1BB introduction equipped T cells with superior cytolytic ability when compared to first generation CAR T cells (Imai et al., 2004). Intriguingly, 4-1BB incorporating CAR T cells showed lower levels of IL-4 and IL-10 production and conferred the longest leukemia-free survival in a pre-B cell acute lymphoblastic leukemia (pre-B-ALL) mouse model when compared side-by-side to CD28 co-stimulated CAR T cells (Carpenito et al., 2009; Milone et al., 2009). In these years, CAR constructs harboring a co-stimulatory signaling domain in tandem with CD3 $\zeta$  became known as ‘second generation’ CARs (Figure 4).

Besides intracellular signaling units, the extracellular CAR spacer region was also subjected to extensive research. Initially, it was introduced into the receptor’s single-chain architecture as a structural element that allowed the scFv to extend beyond the dense glycocalyx of the T cell thus ensuring better antigen accessibility (Moritz and Groner, 1995). For this purpose, a variety of spacer regions was simultaneously designed which were primarily based on the immunoglobulin domains of the crystallizable fragments (Fc) of antibodies (Cooper et al., 2003; Hombach et al., 1998; Weijters et al., 1998). This repertoire was quickly expanded by immunoglobulin-like domains derived from the extracellular portions of CD8 $\alpha$ , CD28, TCR $\beta$  chain, or NKG2D (Barber et al., 2008; Darcy et al., 1998; Eshhar et al., 2001; Morgenroth et al., 2007; Niederman et al., 2002; Zhang et al., 2005; Zhang et al., 2007), but without comparative analyses. However, the fact, that the spacer domain can have an impact on CAR function had been previously shown by Patel et al. in 1999. In their work they demonstrated that varying the spacer region within otherwise identical CAR framework resulted in significant changes of receptor stability and ligand affinity leading to differences in cytokine secretion and killing efficacy of the modified T cells (Patel et al., 1999). Moreover, in recent years it was found that efficient antigen recognition by CAR-expressing T cells not only depends on the nature of the spacer region, but also on the epitope position of the antigen. Membrane-distal epitopes are well engaged by CARs with short spacer elements, whereas effective recognition of membrane-proximal epitopes requires receptors with a long spacer region (Guest et al., 2005; James et al., 2008; Krenciute et al., 2016; Haso et al., 2013; Hudecek et al., 2013) suggesting the biological requirements of optimal T cell:target cell distance for accurate effector cell activation. More recently, studies have found out that the commonly used immunoglobulin G (IgG) Fc spacer domains engage with Fc $\gamma$  receptors (Fc $\gamma$ R) expressed by myeloid cells resulting in activation which induced death of T cells and limited persistence *in vivo*. To block the undesired interactions, deletions and mutations have been engineered into the receptors’

IgG Fc spacer domains leading to increased anti-tumor activity and CAR T cell persistence (Hombach et al., 2010; Hudecek et al., 2015; Jonnalagadda et al., 2015).

In 2006, while second generation CARs were at the preclinical stage, two first generation CAR T cell therapies have gone through clinical trials – with disappointing results. Treatment of ovarian carcinoma with folate receptor-redirectioned CAR T cells led to no tumor burden reduction in any of the patients receiving the therapy. It was found that the administered CAR T cells failed to home to the tumor site and quickly declined to undetectable levels within the first 30 days after adoptive transfer (Kershaw et al., 2006). A separate center targeted carbonic anhydrase IX (CAIX) for the treatment of metastatic renal cell carcinoma (RCC). The antigen had been shown to be highly expressed in RCC with a limited presence in healthy kidneys or other tissues. Moreover, the antibody from which the CAR scFv was derived was previously proven to be safe in RCC patients (Bleumer et al., 2004). The initial 4 to 5 CAR T cell infusions were well tolerated by the patients, however, afterwards grade 2-4 hepatotoxicity and a mild anti-scFv-directed antibody response became apparent, leading to termination of treatment in 2 out of 3 patients. Later on, biopsies revealed low level CAIX expression in bile duct epithelial cells with infiltration of CAR T cells suggesting that CAIX-targeted destruction of these cells resulted in the hepatotoxicity (Lamers et al., 2006, 2007, 2013, 2016). This incidence was the first documented clinical evidence of on target/off tumor toxicity elicited by CAR T cells. In an attempt to circumvent the observed hepatotoxicity, the protocol was adjusted to include pre-treatment with low dose of CAIX blocking antibody in subsequent cohorts which abrogated the on target/off tumor toxicity. However, with regard to tumor burden, no clinical responses were detected (Lamers et al., 2013).

The lack of persistence of first generation CAR T cells observed in the clinical trials as well as the demonstration of improved functional efficacy of second generation CAR T cells were directed development efforts to integrate two co-stimulatory domains into the CAR design. In 2007, Wang et al. described a ‘third generation’ CAR (Figure 4) with three tandem intracellular signaling domains, one derived from CD3 $\zeta$  and the other two from CD28 and 4-1BB (Wang et al., 2007). Compared to first and second generation CAR T cells, T lymphocytes incorporating the third generation CAR demonstrated superior cytotoxicity, cytokine secretion, and proliferation ability *in vitro*. This observation was further confirmed by the June group in 2009. Using also CD28 and 4-1BB as co-stimuli, they demonstrated an improved activity of this CAR architecture among all tested constructs, but were unable to show that this enhanced potency translated into a statistically significant survival benefit in a mouse model when compared with a 4-1BB-based second generation CAR (Carpenito et al., 2009; Milone et al., 2009). Additional work on third generation CARs was contradictory. While Kochenderfer et al. showed that second generation, CD28-costimulated CAR T cells targeting CD19 produced more cytokines than their third generation, CD28 and 4-1BB co-stimulated counterpart (Kochenderfer et al.,

2009), Tammana et al. demonstrated a superior functionality of umbilical cord blood cells containing a third generation anti-CD19 CAR incorporating signaling domains of CD28, 4-1BB, and CD3 $\zeta$  compared with second generation CARs containing CD3 $\zeta$  with CD28 or 4-1BB (Tammana et al., 2010). Using *in vivo* models, the group showed further that its third generation CAR T cells conferred prolonged survival in both intraperitoneal and systematic models of xenografted B cell tumors (Tammana et al., 2010). The discrepancies in these results may be attributed to experimental differences such as the choice of scFv fragments, the detailed architecture of the receptors, method of transgene delivery into cells, and inconsistencies in the materials and methods applied by the different investigators.

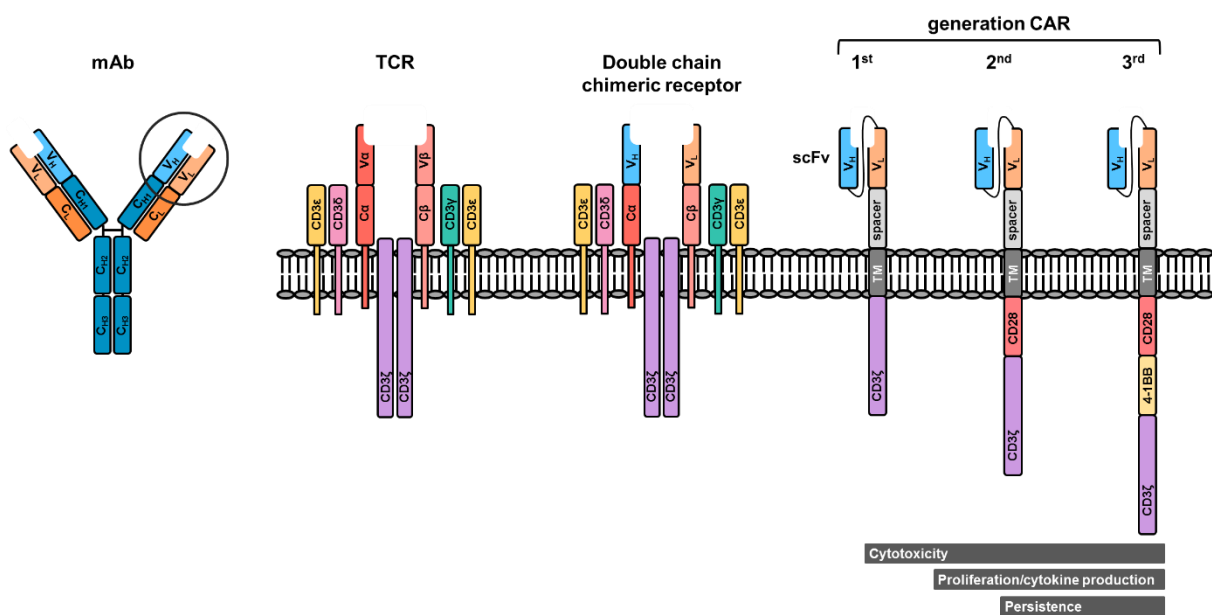


**Figure 4: Evolution of chimeric antigen receptors (CARs).** CARs are fusion proteins that combine antigen recognizing regions from antibodies with intracellular T cell signaling domains. In the original CAR design, the V<sub>H</sub> and V<sub>L</sub> chains of immunoglobulins were engineered to the constant regions of the TCR  $\alpha$ - or  $\beta$ -chains, giving rise to double chain chimeric receptors. Over time, a one-single-chain approach was introduced that combined the targeting and signaling motifs into one polypeptide. First generation CARs contain CD3 $\zeta$  for T cell stimulation, whereas second generation CARs additionally possess a co-stimulatory domain, e.g. CD28 or 4-1BB. Third generation CARs consist of two co-stimulatory domains linked to CD3 $\zeta$ . Co-stimulation enhances the overall survival as well as proliferation, cytokine production, and persistence of activated T cells. mAb, monoclonal antibody; scFv, single-chain variable fragment; TCR, T cell receptor; TM, transmembrane domain.

As preclinical work was further focused on improving the efficacy of CAR technology, the first third generation CAR entered the clinical trial setting only three years after its initial description. One female patient with metastatic colon cancer was treated with a HER2-directed CAR incorporating CD28, 4-1BB, and CD3 $\zeta$  as signaling moieties. The antigen-binding domain was derived from the therapeutically approved monoclonal antibody trastuzumab, which had previously shown a favorable safety profile in HER2-positive breast cancer patients. Without conservative dose-escalation strategies, the patient received a single high-dose infusion of

$10^{10}$  CAR T cells, upon which she developed respiratory distress within 15 min and multiple cardiac arrests over the course of 5 days eventually resulting in mortality. CAR T cell infiltration was found in the lung, abdominal and mediastinal lymph nodes, and at low levels in the heart, but not in tumor metastases. Serum cytokine profiling starting 4 hours after CAR T cell administration revealed strong increases in granulocyte-macrophage colony-stimulating factor (GM-CSF), Interferon  $\gamma$  (IFN $\gamma$ ), IL-6, IL-10, and Tumor necrosis factor  $\alpha$  (TNF $\alpha$ ). It is believed that the observed toxicity was due to HER2 recognition in lung epithelium leading to inflammatory cytokine release syndrome (CRS), which in turn caused lethal multi-organ failure (Morgan et al., 2010).

While the initial attempts in treating solid tumors with CAR T cells were doomed to failure, treatment of B cell hematological malignancies experienced a therapeutic breakthrough using this technology. Emily Whitehead, in 2011 a 6 year old pre-B-ALL patient who stopped responding to conventional treatment, was the first child to receive a CD19-targeted CAR T cell therapy using a second generation construct with 4-1BB and CD3 $\zeta$  signaling domains. CD19 is a transmembrane glycoprotein that is found exclusively on cells of the B lineage and on most B cell-derived leukemias or lymphomas thus representing a suitable target. Upon receiving the third CAR T cell dose, the patient developed high fever and respiratory failure induced by CRS as a result of intensive CAR T cell activation. Her clinical status did not improve, despite administration of high-dose steroids and TNF $\alpha$ -directed therapy. It was then noted that the serum levels of IL-6 were also elevated and tocilizumab, an IL-6 receptor blocking antibody, was administered leading to rapid improvement in her clinical status. B cell aplasia, which developed as a result of on target/off tumor recognition, was mitigated with regular immunoglobulin infusions. The patient has been now in remission for 7 years.

Following this initial CAR T cell therapeutic success, treatments of pediatric and adult relapsed or refractory B-ALL, chronic lymphocytic leukemia (CLL), and B-cell non-Hodgkin lymphoma (NHL) using CD19-directed CAR T cell therapy have consistently demonstrated high anti-tumor efficacy with complete remissions ranging from 70-94% in different clinical trials (Brentjens et al., 2013; Davila et al., 2014; Grupp et al., 2013; Lee et al., 2015; Maude et al., 2014; Maher, 2013). Based on these results, the Food and Drug Administration (FDA) approved two immunotherapies with CD19-directed CAR T cells, Kimriah™ (tisagenlecleucel; containing 4-1BB and CD3 $\zeta$  signaling domains; approved in August 2017) as a second-line treatment for patients up to 25 years of age with ALL and Yescarta™ (axicabtagene ciloleucel, containing CD28 and CD3 $\zeta$  signaling domains; approved in October 2017) for the treatment of adult patients with relapsed or refractory B cell lymphoma. These advancements have reinforced the scientific interest to transfer the CAR technology beyond B cell malignancies. In fact, currently, 727 trials are testing or are due to open CAR T cell and natural killer (NK) cell therapies worldwide, of which 549 trials target non-hematological malignancies (according to

ClinicalTrials.gov, accessed April 1, 2018). Hotspots for clinical CAR research are the United States and China (Hartmann et al., 2017).

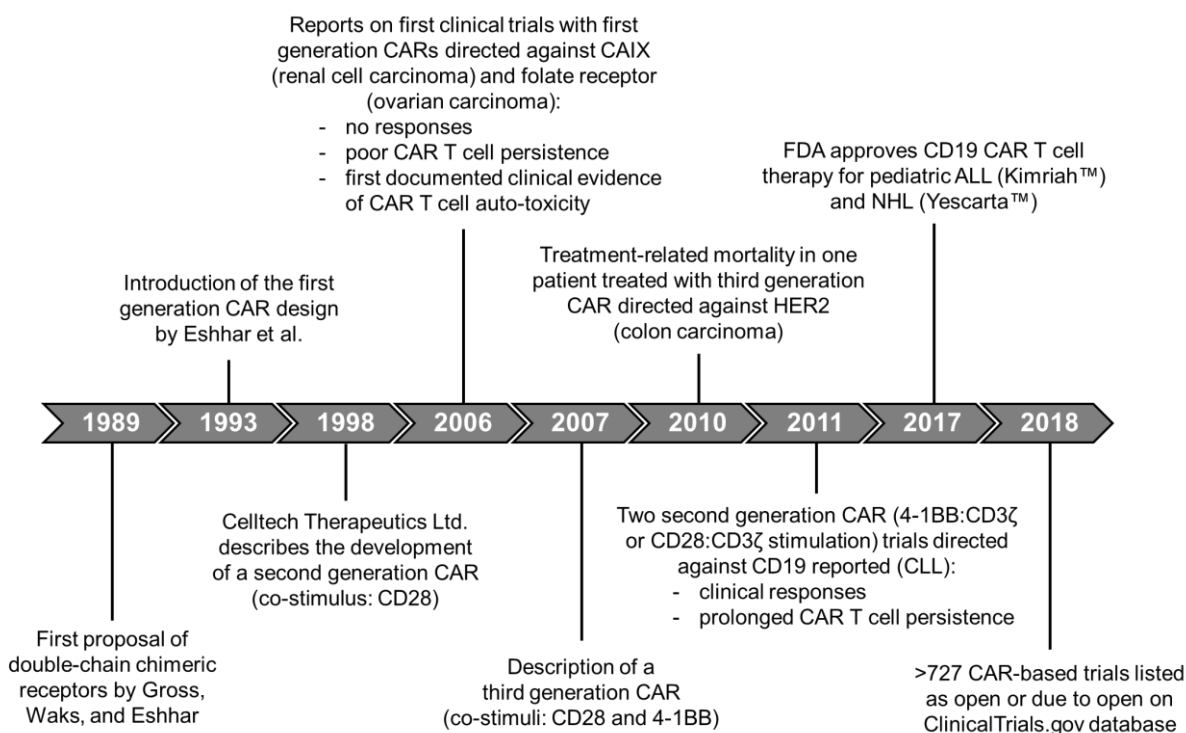


**Figure 5: Timeline of the preclinical and clinical development of CAR T cell therapy.** Milestones and throwbacks in the history of CAR development are listed. Figure modified from Gilham et al. (2012). Key references: 1989: Gross et al.; 1991: Irving and Weiss, Romeo and Seed, Letourneur and Klausner; 1993: Eshhar et al.; 1998: Finney et al.; 2006: Kershaw et al., Lamers et al.; 2007: Wang et al.; 2010: Morgan et al.; 2011: Kalos et al.; Brentjens et al.; Porter et al.; 2017: Approval letter for Kymriah™: <https://www.fda.gov/downloads/Biologics/BloodVaccines/CellularGeneTherapyProducts/ApprovedProducts/UCM574106.pdf>; Approval letter for Yescarta™: <https://www.fda.gov/downloads/biologicsbloodvaccines/cellulargenetherapyproducts/approvedproducts/ucm581259.pdf>.

### 1.2.1 Generation of CAR T cells for clinical applications

As CAR T cell therapy is mostly an autologous treatment, generation of the medicinal product begins with the collection of leukocytes from the patient's blood via leukapheresis. The cell product is subsequently further processed by density gradient centrifugation to obtain peripheral blood mononuclear cells (PBMCs). In the most simplistic approach, CAR T cells are generated from the bulk PBMC population, while more elaborated protocols include a selection step for T cell subsets prior to gene modification, e.g. by enrichment of CD4<sup>+</sup> and CD8<sup>+</sup> (Gardner et al., 2017; Turtle et al., 2016), virus-specific (Ahmed et al., 2017), or CD62L<sup>+</sup> (Wang et al., 2012) populations using fluorescence or magnetic activated cell sorting. To achieve efficient subsequent transgene delivery and *ex vivo* expansion, the cellular product is stimulated through T cell-specific signaling pathways. In this context, primarily monoclonal CD3- and CD28-directed antibodies, either in soluble state or immobilized to a colloidal matrix

or artificial antigen presenting cells (aAPCs), are used. Alternatively, cell-based aAPCs are applied that express a manifold of T cell stimulatory ligands (Huls et al., 2013).

During the activation process, T cells are genetically modified with either a  $\gamma$ -retroviral or lentiviral vector encoding the CAR. Both viral systems are structurally similar but biologically different in that lentiviral vectors are more efficient in transducing non-dividing cells. Moreover,  $\gamma$ -retroviral vectors generally use the native virus promoter for CAR expression, while lentiviruses depend on an internal promoter (Geldres et al., 2016). Though very efficient in transgene delivery, one limitation of these systems is their relatively costly production, which is why non-viral gene modification approaches such as sleeping beauty (Maiti et al., 2013) and piggyBac (Saha et al., 2012) transposon/transposases are being further investigated. These are plasmid-based expression systems that transfer the CAR gene encoded on a vector to the host's genome via an enzymatic cut-and-paste mechanism (Hackett et al., 2010). The relatively simple manufacturing procedure of these methods renders them economically advantageous, however, they suffer from low efficiency of deoxyribonucleic acid (DNA) integration requiring more time for T cell expansion to reach sufficient therapeutic cell numbers. In addition to the above mentioned systems, messenger ribonucleic acid (mRNA) electroporation has been used to permit transient expression of the CAR molecule where desired (Maus et al., 2013).

Following effective transgene introduction, T cells are subjected to an expansion phase to achieve significant numbers of cells for treatment. The most widely used growth factor to support T cell propagation is IL-2, however, it is increasingly replaced by a combination of IL-7 and IL-15. Culture conditions with the latter two cytokines have been shown to increase the frequencies and expansion of T cells with various memory phenotypes, while IL-2 drives effector T cell differentiation. Memory T cells have greater *in vivo* anti-tumor effect due to increased proliferation and persistence ability thus holding promise to improve the treatment efficacy in the clinic (Cieri et al., 2013; Xu et al., 2014). Moreover, novel expansion protocols also employ IL-21 as a growth factor because IL-21-exposed CAR T cells have shown the greatest *in vivo* persistence in animal models (Singh et al., 2011; Xu et al., 2016). More recently, pharmacological immune modulators, that interfere with differentiation pathways of T cells, are under investigation, including inhibition of glycolysis (Sukumar et al., 2013) or AKT signaling (Crompton et al., 2015), induction of WNT/ $\beta$ -catenin signaling pathways (Gattinoni et al., 2009), and combinations thereof (Litterman et al., 2014). Independent of the growth stimulus used, most protocols aim at keeping CAR T cells less than 3 weeks in culture to limit aging and loss of proliferative potential.

Once the therapeutic cell dose is reached, the gene-modified T cells are reinfused back into the patient's circulation. As the CAR T cell manufacturing facility is usually separated from the

healthcare center, a cryopreservation step of the medicinal product often precedes shipment. However, such a freeze-thaw cycle is usually associated with a reduction in quality of the cellular product, which is why current endeavors are focusing on decentralizing the manufacturing procedure and bringing it closer to the bedside. In this context, the CliniMACS Prodigy® is gaining increased attention, a single device that accomplishes T cell preparation, enrichment, activation, transduction, and expansion in an automated and good manufacturing practice (GMP)-compliant fashion. Since all preparation steps are performed in a closed system, the clean room requirements are lower than for personnel-prepared cell products making them easier to realize in hospitals (Kaiser et al., 2015).

Prior to adoptive CAR T cell transfer, patients usually undergo preconditioning chemotherapy to both reduce the tumor burden and induce lymphopenia. In fact, it has been shown that lymphodepleting regimen greatly increase the therapeutic potential of CAR T cells by facilitating engraftment and expansion of the gene-modified immune cells (Brentjens et al., 2011; Heczey et al., 2017). The individual steps of CAR T cell generation with a cumulative consideration of the key variables in the protocols applied by different centers are summarized in Figure 6.

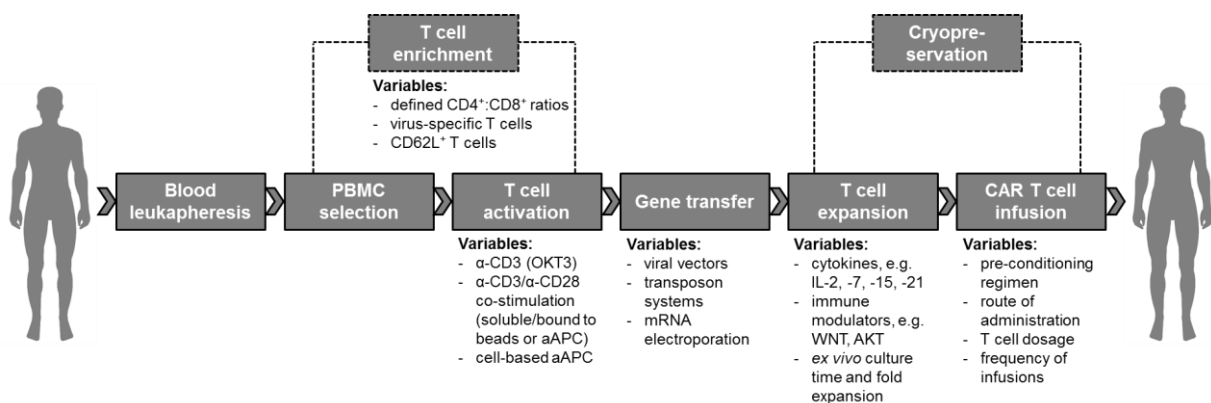


**Figure 6: A step-by-step breakdown of the CAR T cell manufacturing procedure.** For CAR T cell production, patients first undergo leukapheresis upon which the cellular product is further processed to obtain PBMCs. Prior to T cell activation and transgene integration, specific T cell subsets may be further enriched. Following T cell stimulation, the lymphocytes are genetically modified to express a transgene encoding a tumor antigen-directed CAR and expanded *ex vivo* under optimized T cell culture conditions. The cellular biomedical product can be cryopreserved for later administration or is infused directly into the patient. For better *in vivo* engraftment of the gene-modified T cells, patients are commonly preconditioned with lymphodepleting chemotherapy. Divergent variables in the protocols applied by different investigators are listed. Dashed lines represent optional steps in product preparation.

### 1.2.2 CAR T cell therapy in the solid tumor setting

Compared to hematological malignancies, the clinical experience of CAR T cell therapy for solid tumors has been less encouraging. Several challenges have hampered the therapeutic success with the lack of truly tumor-specific antigens being the predominant obstacle. In fact, the vast majority of CARs recognize tumor cells in a tumor-associated manner meaning that their targets are highly expressed by tumor cells, but are also present at low levels on healthy cells. Recognition of the non-malignant tissue by CAR T cells poses not only a potential concern, but has already occurred in the clinical setting – with partially lethal outcome (Morgan et al., 2010). Nevertheless, continuous optimization of the clinical protocols as well as in the CAR design led to the emergence of clinical incidences in which neuroblastoma, glioblastoma, prostate cancer, and sarcoma patients have benefitted from CAR T cell treatment (targets: GD2 (Louis et al., 2011), interleukin 13 receptor subunit  $\alpha$ -2 (IL13R $\alpha$ 2) (Brown et al., 2016), prostate-specific membrane antigen (PSMA) (Slovin et al., 2013), and HER2 (Ahmed et al., 2015)), suggesting that this strategy is still worthwhile pursuing. Presently, 29 solid tumor antigens are being evaluated preclinically and clinically for CAR T cell therapy against solid tumors (Table 1). Among them, only one, variant III mutation of EGFR (EGFRvIII), can be described as tumor-specific. The splice variant is the result of an in-frame deletion in the amplified EGFR gene, which lacks the antigen binding domain and constitutively delivers prosurvival signals (Villa and Mischel, 2016). Its expression has been strictly identified on tumorous cells (Wikstrand et al., 1995) and EGFRvIII-directed CAR T cell therapy for the treatment of glioblastoma is currently being evaluated by several centers (US: NCT02209376, NCT01454596, NCT02664363; China: NCT02844062). Preliminary phase I clinical data indicate tumor infiltration with both CAR-engineered and non-modified T cells as well as EGFRvIII target antigen loss suggesting CAR-mediated anti-tumor activity. No antigen recognition outside the tumorous tissue was reported so far (O'Rourke et al., 2017).

Despite the presence of targetable antigens in certain cancers, a high risk of therapeutic failure remains. Compared to hematological malignancies, solid tumors are characterized by stronger genetic heterogeneity with non-clonal antigen expression profiles (Sun and Yu, 2015) so that one-single-target therapy approaches may lead to selective expansion of target antigen-null tumor cells. To circumvent this hurdle, studies have reported the targeting of the immunosuppressive tumor microenvironment as a means to inhibit tumor growth and augment host immunity. In this context, fibroblast activating protein (FAP)-directed CAR T cell therapies have been controversially discussed in the literature. FAP is selectively expressed by cancer-associated stromal cells which form a significant component of the solid tumor stroma (Kakarla et al., 2013; Schuberth et al., 2013; Tran et al., 2013; Wang et al., 2014) and promote tumor growth, metastasis, and angiogenesis through secretion of growth factors, cytokines, and chemokines (Pure and Lo, 2016). By using a mouse specific scFv, Tran et al. tested a FAP-

directed CAR T cell therapy in several syngeneic mouse tumor models and described treatment-related lethal bone marrow toxicities with limited anti-tumor efficacy (Tran et al., 2013). By contrast, Kakarla et al. and Wang et al. developed FAP-directed CARs derived from human/mouse cross-reactive antibodies and demonstrated anti-tumor efficacy in the absence of toxicity symptoms of FAP-directed CAR T cell therapies in mice (Kakarla et al., 2013; Wang et al., 2014). The discrepancies in these findings are being attributed to the epitope specificity and affinity of the different scFvs which may confer the discrimination of highly FAP-expressing cancer-associated stromal cells and low level FAP-expressing normal tissue (Magee and Snook, 2014). One clinical trial is currently recruiting patients for the treatment of malignant pleural mesothelioma by FAP-directed CAR T cell therapy (NCT01722149).

Beyond FAP, targeting of vascular endothelial growth factor 2 (VEGFR-2) for the disruption of tumor blood vessels was investigated. In one completed phase I/II clinical study (NCT01218867), 24 patients received VEGFR-2-directed CAR T cell therapy, of which one patient achieved stable disease, one patient reached partial response and 22 showed progressive disease (Li and Zhao, 2017). This result was clearly disappointing but re-emphasized that additional factors are in play and their consideration is essential for a successful therapeutic outcome. One of these factors is the suboptimal trafficking of the T cells to the tumor site. Efficient tumor homing is a complex multi-step process which requires the appropriate expression of adhesion receptors on both T cells and tumor endothelium and a compatible expression profile of chemokine receptors on the CAR T cells and the chemokines secreted by the tumors. As this is rare in a biological setting, regional delivery of CAR T cells is being explored by several clinical trials (NCT00730613, NCT01373047, NCT01818323, NCT02208362, NCT02414269, NCT02498912) – primarily for the treatment of glioblastoma and metastatic colorectal cancer. While some studies are still ongoing, completed trials report good tolerance by this administration route and therapeutic efficacy in selected instances (Adusumilli et al., 2014; Brown et al., 2015; Brown et al., 2016; Katz et al., 2015; van Schalkwyk et al., 2013; Yaghoubi et al., 2009). Though very promising, it is unlikely that this approach will be universally applicable as some tumor sites are less well accessible for site-specific injections. Another potential limitation is that locally administered CAR T cells may not be able to traffic to other tumor sites in metastatic cancer patients. In such instances inefficient tumor homing may be overcome by CAR T cells engineered to co-express chemokine receptors that recognize tumor-secreted chemokines. Although this approach has only been tested preclinically as yet (Craddock et al., 2010; Moon et al., 2011; Peng et al., 2010), existing data is encouraging and clinical trials are awaited.

Additional factors that may hinder the therapeutic potential of CAR T cell therapy in solid tumors are the limited persistence of the gene-modified immune cells as well as the multiple immunosuppressive mechanisms of the tumor microenvironment, e.g. physical and

metabolical barriers, tumor-derived soluble factors and cytokines, and immunosuppressive immune cells. Their intervention points for improved therapeutic outcomes are still subject of preclinical research (Newick et al., 2016).

In summary, while the development of CAR T cell therapies for the treatment of solid tumors is still in its infancy and is facing several challenges at once, various approaches have been undertaken to circumvent these obstacles. Expanded clinical experience and therapeutic optimization will help maximizing clinical benefit and permit a widespread adoption of this treatment modality to the solid tumor setting.

**Table 1: Summary of solid tumor target antigens for CAR T cell therapy in clinical and preclinical evaluation.** Candidates for CAR T cell therapy and their distribution in malignant and healthy tissue are shown. For several clinical studies targeting one antigen, the most progressed phase is listed. Table amended from Gross and Eshhar (2016). CAIX, carbonic anhydrase IX; CEA, carcinoembryonic antigen; CNS, central nervous system; CSPG4, chondroitin sulfate proteoglycan 4; EGFR, epidermal growth factor receptor; EGFRvIII, variant III of the EGFR; EphA2, erythropoietin-producing hepatocellular carcinoma A2; FAP, fibroblast activation protein; FR- $\alpha$ , folate receptor- $\alpha$ ; GB, glioblastoma; GPC3, glypican 3; GPI, glycosylphosphatidylinositol; H&N, head and neck; Ig, immunoglobulin; L1-CAM, L1 cell adhesion molecule; MSLN, mesothelin; MUC-1, mucin 1; NB, neuroblastoma; PSCA, prostate stem cell antigen; PSMA, prostate-specific membrane antigen; RCC, renal cell carcinoma; ROR1, receptor tyrosine kinase-like orphan receptor 1; TNBC, triple negative breast cancer; TNF, tumor necrosis factor; TNFR, tumor necrosis factor receptor; VEGFR-2, vascular endothelial growth receptor 2.

Antigen	Key structural and functional features	Testing phase	Malignancy	Potential autoreactivity	Reference
CAIX	Transmembrane zinc metalloenzyme	Clinical phase I, completed	RCC, tumors under hypoxia	Pancreatobiliary epithelium, gastric mucosa, and small intestine crypt base	Lamers et al. (2006, 2007, 2013)
CD44v7/8	Alternatively spliced variant 7/8 of the hyaluronate receptor CD44	preclinical	Breast and cervical cancers	Normal epithelia	Dall et al. (2005)
CD54	Intercellular adhesion molecule 1 (ICAM-1); regulates interactions between immune cells	preclinical	Thyroid cancers	Endothelial cells, epithelial cells, immune cells	Min et al. (2017)
CD70	Member of the TNF superfamily; ligand for CD27	Clinical phase I/II, recruiting	H&N cancer, GBM, RCC	Activated T and B cells, mature dendritic cells	Park et al. (2018), Grewal (2008)
CD133	Prominin-1; pentaspan membrane glycoprotein with unknown function	Clinical phase I and I/II, recruiting	Pancreatic cancer	Epithelial and hematopoietic stem cells	Feng et al. (2017), Zhu et al., (2015)
CD171	neuronal cell adhesion molecule of the Ig superfamily	Clinical phase I, recruiting	NB	CNS, sympathetic ganglia, adrenal medulla	Künkele et al. (2017), Park et al. (2007), Hong et al. (2014)
CD326	transmembrane glycoprotein mediating epithelial-specific intercellular cell-adhesion	Clinical phase I, recruiting	Gastric, ovarian, and breast cancers	epithelium	Ang et al. (2017), Shirasu et al. (2012)
$\alpha\beta 6$	Epithelial specific integrin which mediates cell-cell interactions	preclinical	H&N, colon, ovarian, pancreatic and gastric cancers	epithelium	Whilding et al. (2017)
Axl	Tyrosine kinase receptor	Clinical phase I/II, recruiting	Colon, esophageal, thyroid, breast, lung, and liver cancers; RCC; GB	Brain, monocytes, macrophages, platelets, endothelial cells, heart, skeletal muscle, liver, kidney, and testis	Cho et al. (2018)

(continued)

Table 1: continued.

B7-H6	Ligand for Nkp30 expressed on NK cells	preclinical	Gastric cancer, melanoma, ovarian cancer	Not constitutively expressed on normal tissue	Wu et al. (2015), Hua et al. (2017)
CEA	Surface glycoprotein; member of the Ig superfamily and the CEA-related family of cell adhesion molecules	Clinical phase I/II, recruiting	Colorectal and breast cancers; solid tumors	Apical epithelial surface of colon, stomach, esophagus, and tongue	Hombach et al. (1999), Chmielewski et al. (2012), Parkhurst et al. (2011), Zhang et al. (2017)
c-MET	Hepatocyte growth factor receptor; disulfide-linked $\alpha$ -heterodimeric receptor tyrosine kinase	Clinical phase I, active	TNBC	Liver, gastrointestinal tract, thyroid, kidney, brain	Tchou et al. (2017)
CSPG4	High-molecular-weight melanoma-associated antigen; cell surface proteoglycan	preclinical	Melanoma, TNBC, GB, mesothelioma, H&N cancer, osteosarcoma	Epidermis basal cells, endothelial cells, activated pericytes	Beard et al. (2014), Wang et al. (2015)
EGFR	receptor tyrosine kinases signaling cell differentiation and proliferation upon ligand binding	Clinical phase I/II, recruiting	Solid tumors	Tissues of epithelial, mesenchymal, and neuronal origin	Zhou et al. (2013)
EGFRviii	Splice variant; in-frame deletion in the amplified EGFR gene encoding a truncated extracellular domain that constantly delivers pro-survival signals	Clinical phase I/II, recruiting	Brain, CNS, gliomas, GB	none	O'Rourke et al. (2017), Johnson et al. (2015)
EphA2	EphA2 receptor; a member of the Eph family of receptor tyrosine kinases	Clinical phase I/II, completed	Glioma; breast, colon, ovarian, prostate, lung and pancreatic cancers	Endothelia	Chow et al. (2013), Li et al. (2018)
FAP	Cell surface serine protease	Clinical phase I, recruiting	Mesothelioma, colon and ovarian cancers	Fibroblasts in chronic inflammation, wound healing, and tissue remodeling	Tran et al. (2013), Wang et al. (2014), Schuberth et al. (2013), Kakarla et al. (2013)
FR- $\alpha$	GPI-linked folate receptor; functions in the uptake of reduced folate cofactors	Clinical phase I, completed	Ovarian cancer	Apical surface in kidney, lung, thyroid, kidney, and breast epithelia	Kershaw et al. (2006)
GD2	Disialoganglioside	Clinical phase I/II, completed	NB and sarcomas	Skin, neurons	Louis et al. (2011), Pule et al. (2008), Heczey et al. (2017)
GPC3	cell surface proteoglycan involved in the control of cell division and growth regulation	Clinical phase I/II, completed	Liver and lung cancers	not available	Jiang et al. (2017), Li et al., (2015)

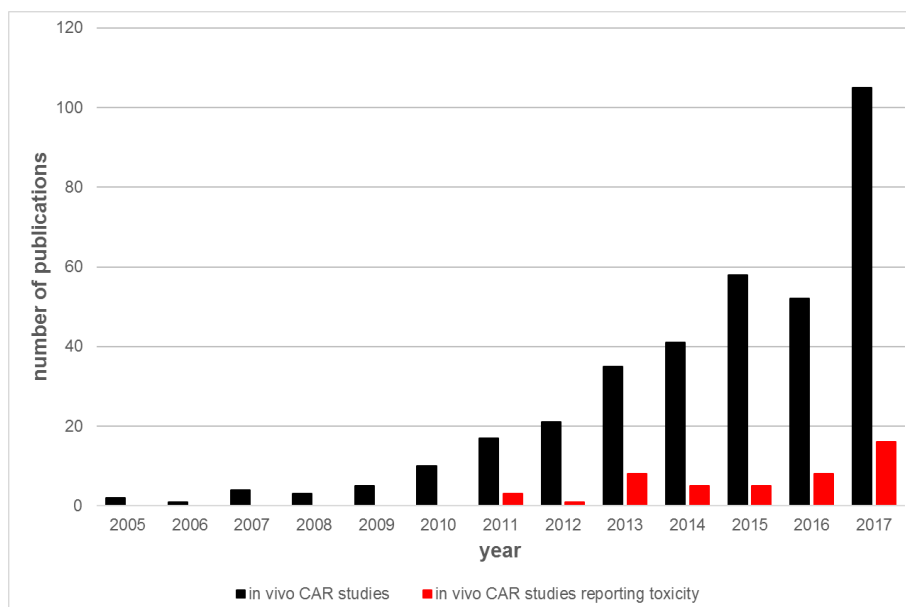
(continued)

Table 1: continued.

HER2	member of the EGFR family of receptor tyrosine-protein kinases	Clinical phase I/II, completed	GB, H&N, solid tumors	Gastrointestinal, respiratory, reproductive, and urinary tract epithelia; skin, breast, and placenta; hematopoietic cells	Feng et al. (2017), Morgan et al. (2010)
IL-11R $\alpha$	The $\alpha$ -subunit of the IL-11 receptor	preclinical	Colon, gastric, breast, and prostate cancers; osteosarcoma	Stromal tissues in the gastro-intestinal tract, endothelial cells, surface and gland epithelia, liver	Huang et al. (2012)
IL-13R $\alpha$	The $\alpha$ -chain of one of the two IL-13 receptors	Clinical phase I	GB	Astrocytes, brain, H&N tissue	Brown et al. (2015), Brown et al. (2016)
MSLN	40-kDa cell surface glycoprotein with unknown function	Clinical phase I, completed	Mesothelioma; pancreatic, and ovarian cancers	Peritoneal, pleural, and pericardial mesothelial surfaces	Adusumilli et al. (2014), Beatty et al. (2018)
MUC-1	Densely glycosylated member of the mucin family of glycoproteins	Clinical phase I/II, recruiting	Colon, lung, pancreatic, breast, ovarian, prostate, kidney, stomach, and H&N cancers	Apical surface of most glandular epithelia	Posey et al. (2016), You et al. (2016)
PSCA	GPI-anchored membrane glycoprotein of the Thy-1/ly-6 family	Clinical phase I, recruiting	Prostate, bladder, and pancreatic cancers	Normal prostate	Morgenroth et al. (2007), Priceman et al. (2018)
PSMA	Type II membrane glycoprotein possessing N-acetylated $\alpha$ -linked acidic dipeptidase and folate hydrolase activity	Clinical phase I/II, recruiting	Prostate cancer	Apical surface of normal prostate, intestinal epithelium and renal proximal tubular cells	Junghans et al. (2016), Zuccolotto et al. (2014)
ROR1	Type I orphan-receptor tyrosine-kinase-like receptor mediating survival-signaling in tumors	Clinical phase I, recruiting	Breast and lung cancers	Pancreas, adipose cells	Huang et al. (2015)
VEGFR-2	Type III transmembrane kinase receptor of the Ig superfamily; regulates vascular endothelial function	Clinical phase I/II, completed	Solid tumors	Vascular and lymphatic endothelia	Chinnasamy et al. (2010, 2012)

### **1.2.3 CAR T cell therapy-mediated toxicity**

To date, the majority of preclinical CAR T cell research has primarily focused on establishing target specificity and anti-tumor potency of the gene-modified cells. Potential side effects associated with this treatment modality have not been addressed in the therapeutic evaluation. This is largely due to the incompatibility of the mouse models that are used for therapy assessment. Regulatory authorities generally require information on the *in vivo* effectivity of the CAR T cell product to approve clinical translation and standard laboratory practice has become to use immunocompromised mice for these purposes as they allow engraftment of human T cells. The experimental design of these studies involves systemically administered human CAR T cells targeting human antigens whose expression is restricted to the xenografted tumor cells. Consequently, the interplay of the transgenic cells with other immune cells as well as the on target/off tumor reactivity remain unassessable. As illustrated in Figure 7, despite a rising interest in CAR research with more and more therapies being evaluated in animal models, there are very few studies that document toxicity – even where toxicity has been observed in the clinic. This highlights the poor predictive nature of current models for a complete therapeutic evaluation. As an inevitable consequence of this trend, most CAR T cell-based clinical trials have been initiated without proper toxicity profiling and many adverse events associated with this therapy were primarily learnt “the hard way” in the clinical setting. In some instances, the unpredictability and intensity of the side-effects led to patient mortality. With increasing clinical experience, the mechanisms of regularly occurring adverse events are starting to be better understood and allow for better preparation and toxicity management. It is now widely established, that there are several potential routes to be considered by which CAR T cells may contribute to toxicity.



**Figure 7: *In vivo* application of CARs.** Timeline shows the number of publications citing chimeric antigen receptors analyzed in animal models as well as the proportion that reports therapy-associated toxicity between 2005 and 2017. For *in vivo* CAR studies, search terms “chimeric antigen receptor”[TIAB] AND mice’ and “chimeric antigen receptor”[TIAB] AND “in vivo” were applied. To select *in vivo* CAR studies that report toxicities the search terms “chimeric antigen receptor”[TIAB] AND mice AND toxicity’ and “chimeric antigen receptor”[TIAB] AND “in vivo” AND toxicity’ were used.

### 1.2.3.1 Anaphylaxis

The vast majority of CARs used in clinical trials incorporate a murine scFv which renders the receptors immunogenic. Both cellular and humoral anti-scFv responses have been described that not only lead to rejection of CAR T cells (Jensen et al., 2010; Kershaw et al., 2006; Turtle et al., 2016), but can also induce acute anaphylaxis in patients receiving multiple rounds of CAR T cell infusions. In a phase I clinical trial aimed to evaluate the on target/off tumor toxicity of mesothelin-directed CAR T cells, mesothelioma and pancreatic cancer patients received repetitive doses of T cells transiently expressing mesothelin-directed CAR. The transgene was introduced temporarily into T cells by mRNA electroporation to limit potential adverse effects due to low level mesothelin expression by a variety of normal tissue. One minute following the completion of the third CAR T cell infusion, one patient experienced an anaphylactic shock and cardiac arrest as a result of a human anti-mouse antibody (HAMA) response directed against the mouse scFv. He received cardiopulmonary resuscitation and recovered (Maus et al., 2013). To avoid such drastic immune reactions against the therapeutic drug, humanized scFvs or scFvs derived from fully human antibodies should be used in the future.

### 1.2.3.2 Cytokine release syndrome

CRS is the most commonly observed toxicity in CAR T cell treated patients and occurs within 1-14 days of CAR T cell infusion. It is a systemic inflammatory response that results from a strong antigen-specific activation of CAR T cells which in turn activates other immune cells. Patients with CRS show elevated circulating levels of C-reactive protein (CRP), ferritin, GM-CSF, IL-1 $\beta$ , IL-2, IL-8, IFN $\gamma$ , TNF $\alpha$ , but also IL-6 and IL-10, the latter two cytokines traditionally associated with macrophage activation syndrome. As a rule of thumb, the amount of inflammation produced correlates with disease burden and the input CAR T cell dose. Of note, CRS induced by CAR T cells is usually more severe than that by tumor-infiltrating lymphocytes (TILs) or TCR-based therapies (Kalos et al., 2011) and its resolution typically takes 2-3 weeks (Frey and Porter, 2016).

Clinical signs of CRS are initially fever and malaise but can progress to life-threatening vasodilatory shock and capillary leakage with hypoxic respiratory failure. Intervention occurs when patients develop severe signs of CRS as early immunosuppression bears the possibility to limit the therapeutic efficacy. Front-line treatment of CRS is the blockade of the IL-6/IL-6 receptor axis by the monoclonal antibody (mAb) tocilizumab alone or in combination with corticosteroids. Where possible, corticosteroids are excluded as their prolonged treatment leads to ablation of the therapeutic cells (Davila et al., 2014; Frey and Porter, 2016).

### 1.2.3.3 Insertional mutagenesis

To facilitate the stable expression of CARs on T cell surface, integrating vectors of retroviral and lentiviral background are commonly used. In this context, malignant transformation of T cells, caused by the integration of vector DNA into host cells near an oncogene, is a potential concern. In practice, no cases of T cell transformation have been reported – despite a decade-long experience. Although insertional oncogenesis has been reported in gene therapy of hematopoietic stem cells for X-linked severe combined immunodeficiency (SCID) due to retroviral insertion near the LIM domain only 2 (LMO-2) oncogene (Hacein-Bey-Abina et al., 2003; Howe et al., 2008; Kohn et al., 2003), in T cells LMO-2 is silent making it an unlikely target for retroviral integration (Scholler et al., 2012). Nevertheless, as CAR T cells are able to persist in treated patients for months or years, insertional mutagenesis is an important consideration in the future.

### 1.2.3.4 Neurological toxicity

Neurological complications – mainly observed in CD19-directed CAR T cell therapies – were largely unforeseen adverse events and manifest as confusion, delirium, tremor, aphasia, and

ataxia. They may occur at different time points than CRS with incidences ranging between 0-50% of affected patients (Brudno and Kochenderfer, 2016; Davila et al., 2014; Kochenderfer et al., 2015; Maude et al., 2014; Porter et al., 2015; Turtle et al., 2016). Although in the majority of cases neurological toxicities are reversible, treatment-related mortalities due to cerebral edema have been reported in two clinical trials (one sponsored by Juno Therapeutics, Inc.; another one by Kite Pharma, Inc.). In one of these trials, 133 adults with refractory B-ALL, NHL, or CLL were treated with CD19-directed CAR T cells upon which five patients experienced lethal cerebral swelling. Autopsies of two of the deceased patients revealed that elevated blood cytokine levels induced endothelial cell activation leading to bleeding disorder, capillary leakage, and blood-brain-barrier disruption. The latter allowed CAR T cells and high concentrations of systemic cytokines to enter the cerebrospinal fluid inducing continuous activation of endothelial cells and pericytes in the central nervous system (CNS) which ultimately led to deadly brain edema. A more detailed pathophysiology of these neurologic side effects is necessary to allow intervention or prophylaxis in future CAR T cell treatments (Gust et al., 2017).

#### **1.2.3.5 On target/off tumor recognition**

Due to a lack of truly tumor-specific antigens, on target/off tumor toxicity is inevitable and occurs through recognition of the target antigen on healthy tissue. In B cell malignancies, CD19 is co-expressed by malignant B cells and normal cells of the B cell lineage from pro-B cells to mature B cells. Therefore, therapeutic intervention with CD19-directed CAR T cells leads not only to tumor eradication but also to on target/off tumor aplasia of healthy B cells – a side effect that is clinically managed by repetitive infusions of immunoglobulins to avoid susceptibility to infections.

In the solid tumor setting, the target antigen is generally overexpressed by tumor cells but may be present at low levels on healthy tissue. If such tissue resides in an essential organ, life-threatening consequences may occur. In fact, in the past, on target/off tumor recognition was the main cause hampering the application of CAR T cell therapies to solid tumors (as illustrated by several clinical examples in preceding chapters). Consequently, target antigen selection is probably the most critical factor for a successful CAR therapy.

### 1.3 Aims of the study

TNBC is a particularly aggressive form of breast cancer with high propensity for metastatic spread and poor survival rates. Currently, cytotoxic chemotherapy is the only treatment available for TNBC patients, but its efficacy is often challenged by the chemoresistant nature of the disease. Therefore, there is an unmet clinical need for a second-line therapy for patients with refractory or relapsed TNBC. Due to the immunogenic properties of this cancer type, immunotherapeutic approaches are particularly promising as an alternative treatment modality. In this context, targeting SSEA-4, a recently identified plasma membrane epitope of a TNBC subpopulation that survives chemotherapy and has high metastatic potential, represents a complementary therapeutic strategy that can be applied to chemotherapy-pretreated patients. It allows to specifically target those tumor cells that escape chemotherapy this way giving hope to accomplish improved therapeutic efficacy and increased overall survival of TNBC patients. The objective of this study was therefore to develop and evaluate a CAR T cell-based targeting approach to SSEA-4. As CARs are synthetic receptors whose efficacy can vary tremendously depending on the spatial topologic structure of their epitope as well as on the CAR architecture itself, an array of different chimeric receptors was to be empirically designed, tested, and compared using different *in vitro* functionality assays. The most bioactive receptors were then to be evaluated in an *in vivo* mouse model for both anti-tumor efficacy and toxic potential to identify the CAR variant with the best efficacy-to-toxicity profile. In the presence of on target/off tumor reactivity, the collaterally damaged non-cancerous cells were to be identified to assess the risks and side effects of an SSEA-4 CAR T cell therapy in the clinical setting.

## 2 Material and Methods

### 2.1 Materials

#### 2.1.1 Animals and animal facility products

NOD.Cg- <i>Prkdc</i> <sup>scid</sup> <i>Il2rg</i> <sup>tm1Wjl</sup> /SzJ	Charles River, Ecully, France
SmartFlow	Tecniplast, Buggugiate, Italy
Single use mouse cage (SUMC) composed of	Tecniplast, Buggugiate, Italy
<ul style="list-style-type: none"> <li>- IVC rack adaptor</li> <li>- card holder</li> <li>- food hopper</li> <li>- cage body</li> <li>- static filter top</li> <li>- top adaptor</li> </ul>	
SUM water bottle pre-filled irradiated	Tecniplast, Buggugiate, Italy
2919 Teklad 19% protein extruded rodent diets	Envigo, Madison, USA

#### 2.1.2 Antibodies

##### 2.1.2.1 Biotinylated antibodies

Table 2: Biotin-conjugated primary antibodies used within the scope of this study.

Specificity	Clone	Species (Isotype)	Dilution factor	source
anti-mouse IgG (Fab-specific)	polyclonal	goat (n/a)	1:100	Sigma Aldrich
LNGFR, h	ME20.4-1.H4	mouse (IgG1κ)	1:10	Miltenyi Biotec GmbH

### 2.1.2.2 Fluorescence-labeled antibodies

Table 3: Fluorochrome-conjugated antibodies used within the scope of this study.

Specificity	Coupled fluorophore	Clone	Species (Isotype)	Dilution factor	source
CD3, h	FITC	BW264/56	mouse (IgG2aκ)	1:10	Miltenyi Biotec GmbH
CD4, h	APC, VioBlue, VioGreen	VIT4	mouse (IgG2aκ)	1:10	Miltenyi Biotec GmbH
CD8, h	FITC, VioBlue, VioGreen	BW135/80	mouse (IgG2aκ)	1:10	Miltenyi Biotec GmbH
CD24, m	FITC	M1/69	rat (IgG2bκ)	1:10	Miltenyi Biotec GmbH
CD31, m	FITC	390	rat (IgG2aκ)	1:10	Miltenyi Biotec GmbH
CD34, m	FITC	REA383	rec. human (IgG1)	1:10	Miltenyi Biotec GmbH
CD34, h	APC	AC136	mouse (IgG2aκ)	1:10	Miltenyi Biotec GmbH
CD38, h	FITC	IB6	mouse (IgG2aκ)	1:10	Miltenyi Biotec GmbH
CD38, m	APC	90.4	rat (IgG2aκ)	1:10	Miltenyi Biotec GmbH
CD41, m	FITC	MWReg30	rat (IgG1κ)	1:10	Miltenyi Biotec GmbH
CD43 Glyco	APC	REA364	rec. human (IgG1)	1:10	Miltenyi Biotec GmbH
CD44, m	FITC	IM7.8.1	rat (IgG2bκ)	1:10	Miltenyi Biotec GmbH
CD45, h	FITC	5B1	mouse (IgG2aκ)	1:10	Miltenyi Biotec GmbH
CD45, m	FITC	30F11	rat (IgG2bκ)	1:10	Miltenyi Biotec GmbH

(continued)

Figure 3: continued.

CD48, m	FITC, PE	HM48-1	hamster IgG1 $\lambda$	1:10	Miltenyi Biotec GmbH
CD49a, m&r	PE	REA493	rec. human (IgG1)	1:10	Miltenyi Biotec GmbH
CD49f, h&m	PE	REA518	rec. human (IgG1)	1:10	Miltenyi Biotec GmbH
CD68, m	FITC	FA-11	rat (IgG2a)	1:10	Miltenyi Biotec GmbH
CD71, m	APC	REA627	rec. human (IgG1)	1:10	Miltenyi Biotec GmbH
CD81, m&r	FITC	EAT2	hamster IgG $\kappa$	1:10	Miltenyi Biotec GmbH
CD98, m	FITC	REA861	rec. human (IgG1)	1:10	Miltenyi Biotec GmbH
CD102, m	APC	REA745	rec. human (IgG1)	1:10	Miltenyi Biotec GmbH
CD105, m	FITC	MJ7/18	rat (IgG2a $\kappa$ )	1:10	Miltenyi Biotec GmbH
CD106, m	APC	429	rat (IgG2a $\kappa$ )	1:10	Miltenyi Biotec GmbH
CD107a, h	VioBlue	H4A3	mouse (IgG1 $\kappa$ )	1:10	Miltenyi Biotec GmbH
CD115, m	PE	AFS98	rat (IgG2a $\kappa$ )	1:10	Miltenyi Biotec GmbH
CD117, m	PE	3C11	rat (IgG2b $\kappa$ )	1:10	Miltenyi Biotec GmbH
CD119, m	APC	REA189	rec. human (IgG1)	1:10	Miltenyi Biotec GmbH
CD135, m	APC	A2F10	rat (IgG2a $\kappa$ )	1:10	Miltenyi Biotec GmbH
CD138, m	PE	REA104	rec. human (IgG1)	1:10	Miltenyi Biotec GmbH
CD140b, m	APC	APB5	rat (IgG2a $\kappa$ )	1:10	Miltenyi Biotec GmbH

(continued)

Figure 3: continued.

CD146, m	FITC	ME-9F1	rat (IgG2ak)	1:10	Miltenyi Biotec GmbH
CD150, m	APC	REA299	rec. human (IgG1)	1:10	Miltenyi Biotec GmbH
$\alpha$ -Biotin	APC	Bio3-18E7	mouse (IgG1)	1:10	Miltenyi Biotec GmbH
Embigin, m	PE	REA501	rec. human (IgG1)	1:10	Miltenyi Biotec GmbH
ESAM, m	PE	REA722	rec. human (IgG1)	1:10	Miltenyi Biotec GmbH
Gr-1, m	FITC	RB6-8C5	rat (IgG2bk)	1:10	Miltenyi Biotec GmbH
Hapten NP acetyl (isotype ctrl)	APC, FITC, VioBlue, VioGreen	S43.10	mouse (IgG2ak)	1:10	Miltenyi Biotec GmbH
IFN $\gamma$	APC-Vio770	45-15	mouse (IgG1k)	1:10	Miltenyi Biotec GmbH
Keyhole limpet hemocyanin (isotype ctrl)	APC, FITC, PE, VioBlue	IS5-21F5	mouse (IgG1k)	1:10	Miltenyi Biotec GmbH
Keyhole limpet hemocyanin (isotype ctrl)	PE-Vio770	IS6-11E5.11	mouse (IgG2bk)	1:10	Miltenyi Biotec GmbH
Keyhole limpet hemocyanin (isotype ctrl)	APC, FITC, PE, PE- Vio770, VioBlue	REA293	rec. human (IgG1k)	1:10	Miltenyi Biotec GmbH
LNGFR, h	APC, FITC, PE	ME20.4- 1.H4	mouse (IgG1k)	1:10	Miltenyi Biotec GmbH
PD-1, h	PE-Vio770	PD1.3.1.3	mouse (IgG2bk)	1:10	Miltenyi Biotec GmbH
PD-L1, h	APC	MIH1	mouse (IgG1k)	1:10	Miltenyi Biotec GmbH

(continued)

Figure 3: continued.

PD-L2, h	APC	MIH18	mouse (IgG1κ)	1:10	Miltenyi Biotec GmbH
Prominin-1, m	APC	MB9-3G8	rat (IgG1)	1:10	Miltenyi Biotec GmbH
RAMP-2	APC	REA703	rec. human (IgG1)	1:10	Miltenyi Biotec GmbH
Sca-1, m	APC, PE-Vio770	REA422	rec. human (IgG1)	1:10	Miltenyi Biotec GmbH
SSEA-4, h&m	APC, PE, VioBlue	REA101	rec. human (IgG1)	1:10	Miltenyi Biotec GmbH
TNFα	PE-Vio770	cA2	human (IgG1κ)	1:10	Miltenyi Biotec GmbH

### 2.1.3 Buffer and solutions

#### 2.1.3.1 Ready-to-use buffers and solutions

CliniMACS® PBS/EDTA Buffer, pH7.2	Miltenyi Biotec GmbH, Bergisch Gladbach, Germany
InsideFix	Miltenyi Biotec GmbH, Bergisch Gladbach, Germany
InsidePerm	Miltenyi Biotec GmbH, Bergisch Gladbach, Germany
MACS® Bleach Solution	Miltenyi Biotec GmbH, Bergisch Gladbach, Germany
MACS® BSA Stock Solution	Miltenyi Biotec GmbH, Bergisch Gladbach, Germany
MACS® Tissue Dissociation Solution	Miltenyi Biotec GmbH, Bergisch Gladbach, Germany
MACS® Tissue Storage Solution	Miltenyi Biotec GmbH, Bergisch Gladbach, Germany
MACSQuant® Running Buffer	Miltenyi Biotec GmbH, Bergisch Gladbach, Germany

---

MACSQuant® Storage Solution	Miltenyi Biotec GmbH, Bergisch Gladbach, Germany
MACSQuant® Washing Solution	Miltenyi Biotec GmbH, Bergisch Gladbach, Germany
Gibco™ PBS, pH7.2	Thermo Fisher Scientific, Schwerte, Germany

### 2.1.3.2 Self-prepared buffers and solutions

PEB buffer	CliniMACS® PBS/EDTA Buffer 0.5% MACS® BSA Stock Solution
TAE running buffer (50x), pH8.4	242 g Tris base 57,1 mL acetic acid 100 mL 0.5 M EDTA ad 1 L ddH <sub>2</sub> O
Sodium butyrate stock solution, 500 mM	5.5 g sodium butyrate ad 100 mL ddH <sub>2</sub> O
D-luciferin solution, 30 mg/mL	1 g D-luciferin ad 33 mL ddH <sub>2</sub> O

## 2.1.4 Cell lines

### 2.1.4.1 Prokaryotic cells

Table 4: Prokaryotic cells used for cloning.

Denotation	Description	Source
DH5-alpha	Chemically competent cells that can be transformed with high efficiency	New England BioLabs GmbH, Frankfurt am Main, Germany

### 2.1.4.2 Eukaryotic cells

Table 5: Eukaryotic cell lines used within the scope of this study.

Cell line	Characterization	source
HEK293T	Human embryonic kidney cell line genetically engineered to express the large T antigen	ATCC, Wesel, Germany
HT1080	Human fibrosarcoma cell line	ATCC, Wesel, Germany
MCF-7	Human breast cancer cell line that is oestrogen and progesterone receptor positive	ATCC, Wesel, Germany
MCF-7_eGFP_Luc	MCF-7 cell line engineered in-house to stably express eGFP and luciferase	-
MDA-MB-231	Human breast cancer cell line that lacks oestrogen receptor and progesterone receptor expression, as well as HER2 amplification	ATCC, Wesel, Germany
MDA-MB-231_eGFP_Luc	MDA-MB-231 cell line engineered in-house to stably express eGFP and luciferase	-
SK_BR_3	Human breast cancer cell line that over-expresses the Her2 (Neu/ErbB-2) gene product	ATCC, Wesel, Germany
BT-474	Human breast cancer cell line that over-expresses the Her2 (Neu/ErbB-2) gene product	ATCC, Wesel, Germany

## 2.1.5 Cell culture media and supplements

### 2.1.5.1 Media and supplements for prokaryotic cell cultures

LB agar	Carl Roth, Karlsruhe, Germany
LB medium	Carl Roth, Karlsruhe, Germany
SOC medium	New England BioLabs GmbH, Frankfurt am Main, Germany

### 2.1.5.2 Media and supplements for eukaryotic cell cultures

DMEM high glucose w/ L-glutamine w/o sodium pyruvate	Biowest, Nuaille, France
Fetal calf serum (FCS)	Biochrom GmbH, Berlin, Germany
L-Glutamine, 200 mM	Lonza, Basel, Switzerland
TexMACS™ medium, research grade	Miltenyi Biotec GmbH, Bergisch Gladbach, Germany
T cell TransAct™, research grade	Miltenyi Biotec GmbH, Bergisch Gladbach, Germany
IL-2, improved sequence (IS), research grade	Miltenyi Biotec GmbH, Bergisch Gladbach, Germany

## 2.1.6 Enzymes and enzyme reaction buffers

### 2.1.6.1 Enzymes

<i>Bam</i> HI	New England BioLabs GmbH, Frankfurt am Main, Germany
<i>Nhe</i> I	New England BioLabs GmbH, Frankfurt am Main, Germany
<i>Nde</i> I	New England BioLabs GmbH, Frankfurt am Main, Germany
<i>Not</i> I	New England BioLabs GmbH, Frankfurt am Main, Germany

<i>SacI</i>	New England BioLabs GmbH, Frankfurt am Main, Germany
<i>SalI</i>	New England BioLabs GmbH, Frankfurt am Main, Germany
<i>XmaI</i>	New England BioLabs GmbH, Frankfurt am Main, Germany

### 2.1.6.2 Enzyme reaction buffers

CutSmart® Buffer, 10x	New England BioLabs GmbH, Frankfurt am Main, Germany
NEBuffer 3.1, 10x	New England BioLabs GmbH, Frankfurt am Main, Germany
NEBuffer 1.1, 10x	New England BioLabs GmbH, Frankfurt am Main, Germany

### 2.1.7 Disposables

Blood lancets Solofix®	B. Braun Melsungen AG, Melsungen, Germany
Cell culture flasks (T25, T75, T175)	Corning Inc., Durham, USA
Cell culture plates (6 well, 24 well, 48 well, 96 well)	Corning Inc., Durham, USA
C-Chip Neubauer counting chamber	Science Services GmbH, München, Germany
Nalgene® system 100™ cryogenic vials (1 mL, 2 mL)	Thermo Fisher Scientific, New York, USA
Falcon® tubes (15, 50 mL)	Corning Inc., Durham, USA
Filter tips (10 µL, 100 µL, 200 µL, 1000 µL)	Kisker Biotech GmbH & Co. KG, Steinfurt, Germany
Flat cap microcentrifuge tubes (0.5, 1.5, 2.0 mL)	StarLab, Hamburg, Germany

gentleMACS® C tubes	Miltenyi Biotec GmbH, Bergisch Gladbach, Germany
MACS® Columns (MS, LS)	Miltenyi Biotec GmbH, Bergisch Gladbach, Germany
MACS® SmartStrainer (30 µm, 70 µm)	Miltenyi Biotec GmbH, Bergisch Gladbach, Germany
Needles (Microlance: 23G, 26G, 27G)	BD Biosciences, New Jersey, USA
Reagent reservoir (25 mL)	VWR, Darmstadt, Germany
Serological pipettes (5, 10, 25, 50 mL)	Sarsted AG & Co. KG, Nümbrecht, Germany
Surgical disposabel scalpels	B. Braun Melsungen AG, Melsungen, Germany
Storage Bottle (250 mL, 500 mL, 500 mL)	Corning Inc., Durham, USA
Syringes (1, 2, 5, 10 mL)	B. Braun Melsungen AG, Melsungen, Germany
Microtube K3 EDTA (1.3 mL)	Sarsted AG & Co. KG, Nümbrecht, Germany

### 2.1.8 Laboratory equipment

Table 6: Laboratory equipment used within the scope of this study.

Denotation	Type	Supplier
Agarose gel electrophoresis chamber	Wide Mini-Sub Cell GT cell	Bio-Rad Laboratories, Inc., Hercules, USA
Agarose gel electrophoresis imaging system	cool SamBa HR-830	LTF Labortechnik GmbH, Wasserburg, Germany
Autoclave	VX-150	Systeme GmbH, Linden, Germany
Centrifuge	Centrifuge 4515R	Eppendorf AG, Hamburg, Germany

(continued)

Table 6: continued.

	Multifuge 4KR	Thermo Fisher Scientific, Waltham, USA
	Eppendorf 5415D	Eppendorf AG, Hamburg, Germany
	Multifuge X3R	Heraeus Instruments, Hanau, Germany
Digital Electronic Caliper		Fine Science Tools GmbH, Heidelberg, Germany
Gas anesthesia system	XGI-8	Perkin Elmer, Inc., Waltham, USA
gentleMACS <sup>®</sup> Dissociator	Octo	Miltenyi Biotec GmbH, Bergisch Gladbach, Germany
In vivo Bioluminescent imaging system	Lumina Series III	Perkin Elmer, Inc., Waltham, USA
Incubation shaker (bacteria)	CERTOMAT <sup>®</sup> BS-1	B. Braun Biotech International GmbH, Melsungen, Germany
CO <sub>2</sub> Incubator (eukaryotic cells)	HERAcell <sup>™</sup> 240i	Thermo Fisher Scientific, New York, USA
Cryobox	Mr. Frosty	Thermo Fisher Scientific, New York, USA
Incubator (bacteria)	ED 53	Binder GmbH, Tuttlingen, Germany
Live cell imaging system	IncuCyte <sup>®</sup> S3	Essen BioScience, Inc., Ann Arbor, USA
Light microscope	Axiovert 25	Zeiss, Oberkochen, Germany
Multi pipette	Transferpette <sup>®</sup> S-12	BRAND GmbH & CO KG, Wertheim, Germany
Spectrophotometer	NanoDrop <sup>™</sup> 1000	Thermo Fisher Scientific, New York, USA
pipetting aid	Thermo Scientific <sup>™</sup> S1 Pipet Filler	Thermo Fisher Scientific, New York, USA
pH meter	InLab730	Mettler Toledo AG, Schwerzenbach, Switzerland

(continued)

Table 6: continued.

pipets	Research Plus (10 µL, 100 µL, 1,000 µL)	Eppendorf AG, Hamburg, Germany
refrigerator	LKV3910 MediLine	Liebherr, Bulle, Switzerland
scale	Kern ABT 220-4M  Kern PES 2200-2M	KERN & SOHN GmbH, Barlingen, Germany  KERN & SOHN GmbH, Barlingen, Germany
tabletop centrifuge	Biofuge Pico	Kendro Laboratory Products GmbH, Hanau, Germany
Thermo shaker/mixer	ThermoMixer C	Eppendorf AG, Hamburg, Germany
Flow cytometer	MACSQuant™ Analyzer 10	Miltenyi Biotec GmbH, Bergisch Gladbach, Germany
Laminar airflow workstation	HERAsafe™ K12	Thermo Fisher Scientific, New York, USA
Freezer (-20°C)	G4013 Comfort	Liebherr, Bulle, Switzerland
Freezer (-80°C)	HERAfreeze HCF286	Thermo Fisher Scientific, New York, USA
UV transilluminator	SM-20 Single	LTF Labortechnik GmbH, Wasserburg, Germany
Vortex mixer	Vortex-Genie 2	Scientific Industries, Inc., New York, USA
Water bath	GFL-1083	GFL GmbH, Burgwedel, Germany
Water purification system	Professional G7895	Miele & Cie. KG, Gütersloh, Germany

### 2.1.9 Plasmids

pMDG2 (VSV-G)	generated in-house (R&D version)
pCMVdR8.74 (gag/pol)	generated in-house (R&D version)
pSEW-GFP	generated in-house (R&D version)
various CAR transfer plasmids	generated in-house (R&D version)

### 2.1.10 Ready-to-use kits

Lineage cell depletion kit, mouse	Miltenyi Biotec GmbH, Bergisch Gladbach, Germany
Pan T cell isolation kit, human	Miltenyi Biotec GmbH, Bergisch Gladbach, Germany
NucleoSpin	Machery-Nagel GmbH & Co. KG, Düren; Germany
EndoFree® Plasmid Maxi Kit	Qiagen, Hilden, Germany
MACSPlex Cytokine 12 Kit, human	Miltenyi Biotec GmbH, Bergisch Gladbach, Germany
QIAquick Gel Extraction Kit	Qiagen, Hilden, Germany
Rapid DNA Ligation Kit	Roche Diagnostics GmbH, Mannheim, Germany

### 2.1.11 Reagents and chemicals

1 kb Plus DNA Ladder	ThermoFisher Scientific, Schwerte, Germany
17 $\beta$ -estradiol powder	Sigma-Aldrich, Schnelldorf, Germany
17 $\beta$ -estradiol pellet, 0.18 mg/pellet	Innovative Research of America, Sarasota, USA
Acetic acid	Merck KGaA, Darmstadt, Germany
Baytril™ 10%	Bayer Vital GmbH, Leverkusen, Germany
BD GolgiPlug™ (Brefeldin A)	BD Biosciences, New Jersey, USA
BD GolgiStop™ (Monensin)	BD Biosciences, New Jersey, USA
Capillary tubes	Roche Diagnostics GmbH, Mannheim, Germany

---

Cell Stimulation Cocktail (500x)	Thermo Fisher Scientific, Schwerte, Germany
COBAS® capillary tubes	Roche Diagnostics GmbH, Mannheim, Germany
D-luciferin, potassium salt	Gold Biotechnology, Inc., Missouri, USA
Dimethyl sulfoxide (DMSO)	Sigma-Aldrich, Schnelldorf, Germany
Ethanol	Merck KGaA, Darmstadt, Germany
Ethidium bromide	Miltenyi Biotec GmbH, Bergisch Gladbach, Germany
Erythrosine B	Merck KGaA, Darmstadt, Germany
FcR blocking reagent, human	Miltenyi Biotec GmbH, Bergisch Gladbach, Germany
FcR blocking reagent, mouse	Miltenyi Biotec GmbH, Bergisch Gladbach, Germany
Gel loading dye (DNA), 6x	New England BioLabs GmbH, Frankfurt am Main, Germany
Isoflurane	Zoetis Schweiz GmbH, Zurich, Switzerland
Isopropanol	Carl Roth, Karlsruhe, Germany
Kanamycin sulfate	Carl Roth, Karlsruhe, Germany
LB Agar (Luria/Miller)	Carl Roth, Karlsruhe, Germany
LB medium (Luria/Miller)	Carl Roth, Karlsruhe, Germany
MACSfectin™ reagent	Miltenyi Biotec GmbH, Bergisch Gladbach, Germany
MACSQuant® calibration beads	Miltenyi Biotec GmbH, Bergisch Gladbach, Germany

MACSelect LNGFR MicroBeads	Miltenyi Biotec GmbH, Bergisch Gladbach, Germany
Pancoll	Pan-Biotech GmbH, Aidenbach, Germany
Propidium iodide	Miltenyi Biotec GmbH, Bergisch Gladbach, Germany
Protein L-biotin	GenScript, New Jersey, USA
Red blood cell lysis buffer, 10x	Miltenyi Biotec GmbH, Bergisch Gladbach, Germany
Sodium butyrate	Merck KGaA, Darmstadt, Germany
Tris base	Sigma-Aldrich, Schnellendorf, Germany
UltraPure™ Agarose	Thermo Fisher Scientific, Schwerte, Germany

### 2.1.12 Software

Table 7: Softwares used within the scope of this study.

Software	Application	Source
MACSQuantify™ 2.11	Analysis of flow cytometric data	Miltenyi Biotec GmbH, Bergisch Gladbach, Germany
Microsoft Office Professional 2016	Word, Excel, PowerPoint, Outlook	Microsoft Corporation, Redmond, USA
Mendeley Desktop 1.16.3	Reference management	Elsevier, Amsterdam, Netherlands
GraphPad Prism 7.03	Graphical data evaluation	GraphPad Software Inc, La Jolla (USA)
Living Image 4.5.2	Analysis of <i>in vivo</i> imaging data	Perkin Elmer, Inc., Waltham, USA

(continued)

**Table 7: continued.**

Clone Manager 9 Professional Edition	<i>In silico</i> cloning tool	Scientific & Educational Software, Denver; USA
IncuCyte <sup>®</sup> S3 Control Software	Data analysis of cellular growth assays	Essen BioScience, Inc., Ann Arbor, USA
Image Lab <sup>™</sup>	Analysis of agarose gels and Western blots	Bio-Rad Laboratories, Inc., Hercules, USA
NanoDrop <sup>™</sup> 1000 Software	DNA quantification	Thermo Fisher Scientific, New York, USA

---

## 2.2 Methods

### 2.2.1 Molecular biology methods

#### 2.2.1.1 Plasmid transformation and amplification

To amplify plasmid DNA via bacterial cellular replication, chemically competent NEB5-alpha were transformed with the plasmid of interest according to manufacturer's instructions. A certain proportion of the mixture was then plated on LB plates containing the desired antibiotic for selection and incubated at 37°C overnight. Subsequently, single colonies were picked and inoculated into 5 mL LB medium containing the appropriate antibiotic. Upon overnight culture at 37°C and vigorous agitation (200 rpm), the samples were either processed using the NucleoSpin® Plasmid Kit (small scale plasmid preparation) or the culture was diluted in 200 mL LB medium and bacteria were grown further at 37°C and 200 rpm overnight. DNA was then purified in large scale using the EndoFree® Plasmid Maxi Kit (2.2.1.2).

#### 2.2.1.2 Plasmid preparation

Preparation of plasmid DNA from transformed NEB5-alpha was performed in small-scale using the NucleoSpin® Plasmid Kit or in large-scale using the EndoFree® Plasmid Maxi Kit following manufacturers' instructions. The principle of both kits is based on alkaline lysis of the bacterial membrane after which the extracted plasmids are bound to silica membranes in the presence of high concentrations of chaotropic salts (NucleoSpin® Plasmid Kit) or to anion exchange columns (EndoFree® Plasmid Maxi Kit). Cellular contaminations such as proteins and metabolites are then washed away, while the DNA is retained within the columns. Eventually, pure and concentrated plasmid DNA is eluted using water or appropriate buffers.

Small scale plasmid preparations were performed after amplification of newly received plasmid gene sequences (all ordered from ATUM; <https://www.atum.bio/>) or from colonies containing recombinant plasmids for subsequent confirmation of proper cloning. The DNA yield was typically in the range of 10-20 µg. For DNA applications in transfection experiments, large scale plasmid purification was conducted. The utilized kit contained an endotoxin removal step thus minimizing agonists in the final DNA product that may decrease viability of mammalian cell cultures and inhibit transfection efficiencies. Generally, a total of 400-700 µg DNA was obtained using the EndoFree® Plasmid Maxi Kit. After quantitation (2.2.1.5), the DNA was aliquoted and stored at -20°C.

#### 2.2.1.3 Restriction of plasmid DNA

To verify sequence integrity of recombinant plasmids or to isolate a subfragment of interest, plasmid DNA was subjected to enzymatic restriction reactions. Restriction enzymes are

bacterial endonucleases that catalyze the cleavage of duplex DNA at specific palindromic sequences generating characteristic fragments. These DNA fragments are then electrophoretically separated and – when necessary – extracted from the gel (2.2.1.4). Generally, a restriction reaction was set up as listed in Table . For restriction reaction with two enzymes, the buffer ensuring the maximal activity for both nucleases was selected using the NEB double digest finder (<https://nebcloner.neb.com/#!/redigest>). In an analytical setting, the reaction mixture was incubated for 1 hour at the temperature recommended by the manufacturer. Preparative restrictions were performed for 3 hours at the temperature optimum of the utilized restriction enzymes.

**Table 8: Composition of analytical and preparative restriction reactions**

<b>Chemical</b>	<b>Analytical restriction enzyme reaction</b>	<b>Preparative restriction enzyme reaction</b>
DNA	1 µg	20 µg
10x buffer	2 µL	5 µL
Enzymes (each in case of a double digest)	5 U	10 U
ddH <sub>2</sub> O	ad 20 µL	ad 50 µL

#### **2.2.1.4 Agarose gel electrophoresis and isolation of DNA**

For the separation and analysis of DNA fragments exclusively on the basis of their size, agarose gel electrophoresis was used as the method of choice. Agarose is a seaweed-derived polysaccharide that, once hydrated and polymerized, functions as a sieve through which DNA molecules can migrate. When an electric field is applied across it, DNA fragments travel to the anode due to their negatively charged phosphate backbone. Shorter strands move through the gel more quickly than larger strands whereby the gel pore size affects the migration rate and the separation resolution. For the separation of DNA fragments >1,000 bp, 0.8-1% (w/v) agarose gels were used, whereas 1.5-2% (w/v) agarose gels were prepared for smaller fragments. For this purpose, the appropriate amount of agarose was emulsified in 250 mL TBE buffer and then dissolved by heating the suspension in a microwave oven. After cooling down to 60°C, the solution was supplied with ethidium bromide (EtBr) to a final concentration of 50 µg/mL and subsequently transferred into a cartridge for polymerization. Before the gel solidified, a well-forming comb was inserted to generate pockets for subsequent sample loading. DNA samples and 1 kb Plus DNA ladder as a size standard were mixed with 6x DNA loading dye and applied into the wells of the polymerized agarose gel. Following

electrophoresis at 100 V for 45 min in TBE buffer, the DNA was visualized by fluorescence of DNA-intercalating EtBr excited by UV light. Analytical gels performed to verify correct cloning were investigated at 254 nm whereas preparative gels were analyzed at a longer wavelength (302 nm) to reduce the induction of double strand breaks in the DNA molecules. In the latter instances, the desired DNA was subsequently isolated by excising the respective gel fragments with a scalpel and extracting the DNA using the Gel Extraction Kit following manufacturer's instructions.

#### **2.2.1.5 Quantitation of DNA**

DNA was quantitated spectrophotometrically by measuring the absorbance at 260 nm ( $A_{260}$ ) using the NanoDrop™ 1000. The absorbance maximum of nucleic acids at 260 nm originates from the delocalized  $\pi$ -electron system of purine and pyrimidine rings in nucleotides and thus correlates with the DNA or RNA concentration of a given solution. Thereby, an  $A_{260}$  of one equals 50  $\mu\text{g/ml}$  double-stranded DNA or 40  $\mu\text{g/ml}$  RNA, respectively. To assess the purity of the DNA,  $A_{280}$  was additionally determined as aromatic amino acids derived from protein contaminations have an absorbance maximum at 280 nm. A ratio of the absorbance at 260 nm and 280 nm ( $A_{260/280}$ ) of 1.8 is indicative for pure DNA, while  $A_{260/280} < 1.8$  corresponds to protein impurities and  $A_{260/280} > 1.8$  points to RNA contamination.

#### **2.2.1.6 Ligation**

The ligation of vector and insert fragments derived from gel extractions of preparative restrictions was performed using the Rapid DNA Ligation Kit from Roche Diagnostics GmbH as instructed by the manufacturer. The linearized insert was added in a molar ratio of 5:1 to the vector backbone and ligation was performed for 5-10 min at room temperature. To assess the frequency of backbone religation, a ligation reaction containing only the vector but no insert was set up as a control. Finally, 2  $\mu\text{l}$  of the ligation reaction or the religation control were used to transform chemically competent NEB5-alpha (2.2.1.1).

#### **2.2.1.7 Sequencing of DNA**

DNA sequencing was performed at GATC Biotech GmbH. For this purpose, plasmid DNA from large scale preparations was diluted with ddH<sub>2</sub>O to a concentration of 50-100 ng/ $\mu\text{L}$  and a total volume of 50  $\mu\text{L}$  and sent to the company. Suitable primers were designed using the Clone Manager software and ordered along with sequencing orders. The obtained sequences were analyzed by comparison with an *in silico* reference sequence.

## 2.2.2 Cell biology methods

Cell preparation and handling was exclusively performed under laminar flow and strict aseptic conditions. All cell cultures and assays were conducted in appropriate culture medium (for adherent cells see 2.2.2.1; for T cells 2.2.2.11) at 37°C in a 5% CO<sub>2</sub> atmosphere and 95% humidity. Functionality assays with T cells were performed in TexMACS™ medium without additives.

### 2.2.2.1 Cultivation of adherent cell lines

All cell lines utilized in this study were maintained in DMEM supplemented with 2 mM glutamine and 10% FCS. To further support the growth of MCF-7, 17β-estradiol was supplied to the culture medium at a final concentration of 10 nmol/L. Cell confluency ranged typically between 20-80% during the culture maintenance phase.

### 2.2.2.2 Passaging of adherent cells

Adherent cells were subcultured or used for downstream applications when they had reached a confluency of 70-80%. For detachment, the medium was aspirated and the cultures were washed briefly with pre-warmed PBS (5 mL for T75 flask; 8 mL for T175 flask). Following a 2 min incubation with Trypsin/EDTA (1.5 mL for T75 flask; 3 mL for T175 flask), 5-7 mL culture medium containing 10% FCS was added and the cells were gently dissociated from the plastic culture surface using light pipetting. The detached cells were pelleted by centrifugation at 300xg for 5 min at 21°C, resuspended in 10 mL culture medium, and then seeded into T75 or T175 flasks at the desired density. Alternatively, the cells were used as antigen expressing target cells for *in vitro* or *in vivo* CAR T cell functionality studies.

### 2.2.2.3 Cryopreservation of cells

PBMCs and T cells were cryopreserved at a maximal cell concentration of  $2 \cdot 10^7$  cells/mL while adherent cancer cell lines were frozen at a density of  $3 \cdot 10^6$  cells/mL. For this, the cell sediment was resuspended in an appropriate volume of freezing medium composed of 9 parts FCS and 1 part DMSO and transferred to cryovials placed in a cryocontainer. The isopropanol within the cryocontainer allowed the cooling of cells by approximately 1°C per minute when put at -80°C. After a 24 hour storage period at -80°C, the cell aliquots were transferred to liquid nitrogen for long-term storage at -196°C.

#### 2.2.2.4 Thawing of cells

Cryovials containing the cells of interest were thawed at 37°C for a few minutes until only a small amount of ice remained, after which the cells were transferred into an appropriate, 37°C prewarmed culture medium. After centrifugation at 21°C and 300xg for 5 min, the cells were resuspended in fresh culture medium, counted (2.2.2.5) and seeded at the desired density.

#### 2.2.2.5 Cell quantitation

Cell number determination was performed either automatically via MACSQuant<sup>®</sup> Analyzer or manually using the Neubauer chamber. For MACSQuant<sup>®</sup>-based cell quantitation, the cell suspension was supplied with propidiumiodide (PI) at a dilution factor of 100 and immediately thereafter, a volume of at least 50 µL of the cell suspension was measured. PI is a membrane impermeable dye that only penetrates into dead cells with compromised plasma membrane. Due to its DNA intercalating properties and an emission peak shift upon DNA binding, PI allows for exclusion of dead cells in a flow cytometric setting and was therefore also applied to assess the viability of the cell suspensions.

For cell density determination via the Neubauer chamber, 30 µL of the cell suspension were diluted with erythrosine B, which selectively stains dead cells with compromised membrane integrity. Routinely, a dilution ratio of 1:2 was used. Upon transfer of the cell solution into the Neubauer chamber, the non-stained cells in all four major quadrants were counted, including those placed on two of the four borderlines. The cell number was calculated according to the formula:

$$\frac{\sum \text{cell count in 4 quadrants}}{4} \cdot \text{dilution factor} \cdot \frac{10^4}{\text{mL}} = \frac{\text{cell number}}{\text{mL}}$$

#### 2.2.2.6 Transfection of HEK293T cells for CAR expression

The expression of generated chimeric receptors was first assessed in HEK293T cells by transient transfection of the transgene-encoding transfer vectors. To introduce the plasmid DNA into cells, MACSfectin<sup>™</sup> reagent was used, a composition of cationic lipopolyamines that facilitates nucleic acid condensation and cellular uptake. One day prior to transfection, 3·10<sup>5</sup> HEK293T cells were plated per cavity of a 6 well-plate and were allowed to adhere overnight in standard culture medium. The next day, the transfection solution was prepared with a DNA:MACSfectin<sup>™</sup> ratio of 1:2. For this, 3 µg of plasmid DNA were diluted in additive-free DMEM to give a final volume of 100 µL. In a second tube, another 100 µL were prepared containing 6 µL MACSfectin<sup>™</sup> reagent in additive-free DMEM. After transfer of the

MACSfectin™ solution to the DNA mix and careful mixing by inversion 3-4 times, the mixture was incubated for 20 min at room temperature to allow complex formation between the plasmids and MACSfectin™. Eventually, the transfection solution was added dropwise to the cells and the plate was rocked gently for uniform distribution. Transfection efficiency was assessed by transfecting a separate well with a plasmid encoding GFP, e.g. pSEW-GFP. Transgene expression was analyzed flow cytometrically 48 hours after transfection when peak expression was expected. For this purpose, cells were detached with 1 mL of pre-warmed PBS/EDTA per well and careful trituration followed by fluorescent labeling of the CAR as described in 2.2.2.16.

### **2.2.2.7 Transfection of HEK293T cells for lentiviral vector production**

To achieve stable and efficient gene transfer into primary T cells, lentiviral transduction was the method of choice. Lentiviral vectors are a subgroup of retroviral vectors that display two key advantages over other retroviral systems: (1) they are able to integrate their genetic cargo into chromosomes of both dividing and non-dividing cells, thus improving transduction efficiencies and (2) they are less likely to integrate in proto-oncogenic regions of the genome, which may lead to insertional mutagenesis (Biffi et al., 2013). Hence, lentiviral-based gene delivery offers a superior safety profile in the gene therapeutic setting compared to other retroviral vectors.

Second generation self-inactivating VSV-G-pseudotyped lentiviral vectors were produced by transient transfection into adherent HEK293T cells. One day before transfection,  $1.6 \cdot 10^7$  HEK293T cells were seeded per T175 flask to reach a confluency of 70-90% on the following day. Each T175 flask was then transfected with a total of 35 µg plasmid DNA composed of 3.14 µg pMDG2 (encoding VSV-G), 19.34 µg pCMVdR8.74 (encoding gag/pol), and 12.52 µg transfer vector (encoding the transgene) using MACSfectin™ reagent. When titer analyses of different transfer vectors were performed, the transfer vectors were used in equimolar amounts. All transfection reactions were performed with a DNA:MACSfectin™ ratio of 1:2. In a first step, the different DNA plasmids were mixed with additive-free DMEM to yield a final volume of 3.5 mL while in another reaction tube, MACSfectin™ reagent was diluted in additive-free DMEM to 3.5 mL. Both tubes were mixed by inverting 3-4 times and afterwards the MACSfectin™ solution was transferred to the DNA mix. Upon careful mixing by inverting 3-4 times, the transfection solution was incubated for 20 min at room temperature. In the meantime, the culture medium of the cells was replaced by 18 mL of fresh additive-free DMEM and then, the transfection solution was added to the cells. Following an incubation period of 6 hours, the cells were supplied with 2.5 mL FCS and after an additional 10 hours, sodium butyrate was given at a final concentration of 10 mM. Sodium butyrate is an inhibitor of histone deacetylases

and has been shown to prevent DNA compaction. In this way, promoter regions remain accessible which in turn improves RNA transcription and consequently vector production (Jaalouk et al., 2006). At 48 hours after DNA introduction into the cells, the medium was collected, cleared by centrifugation at 300xg and 4°C for 5 min and filtered through 0.45 µm-pore-size PVDF filters. Concentration of the viral stock was performed by centrifugation at 4°C and 4,000xg for 24 hours. Pellets containing lentivirus were air-dried and resuspended at a 100-fold concentration with 4°C cold PBS by trituration. Storage of the lentiviral aliquots occurred at -80°C.

### 2.2.2.8 Titration of lentiviral vectors

Lentiviral titers were determined by transduction of HT1080 cells with serially diluted viral vector preparations and subsequent flow cytometric analysis for transgene expression. One day prior to titration, HT1080 cells were plated at a concentration of  $1.1 \cdot 10^5$  cells/well of a 48-well plate and incubated overnight. The following day, the culture medium was removed and each well was washed with 1 mL DMEM without additives. To determine the number of adherent cells at the time point of transduction, the cells of one well were detached with CliniMACS® buffer and quantitated. Subsequent transduction was performed by covering the cells with 250 µL of the serially diluted vector preparations in the presence of 8 µg/mL polybrene. The highest vector concentration used for titration was 2.5 µL per 250 µL DMEM and was diluted 2-fold in 4 steps yielding 0.156 µL per 250 µL DMEM as the lowest vector concentration. Addition of polybrene to the transduction mix helped to enhance transduction efficiency by neutralizing the charge repulsion between the vector particles and the cell surface (Davis et al., 2004).

After an incubation period of 3 hours at 37°C, the transduction reaction mix was replaced by 1 mL of fresh DMEM supplemented with 10% FCS and the cells were allowed to express the transgene for 3 days. Then, the transduction efficiency was analyzed flow cytometrically and the amount of transducing units (TU) per mL was calculated according to the formula below. Only dilutions that resulted in 1-20% of transduced cells were considered for titer determination as these most likely represent only one viral integration per cell.

$$\frac{TU}{mL} = \frac{\text{cell number at time of viral vector addition} \cdot \left(\frac{\% \text{ fluorescent cells}}{100}\right) \cdot 1000}{x \mu\text{L of viral vector concentrate}}$$

### 2.2.2.9 Isolation of human PBMCs

Peripheral blood mononuclear cells (PBMCs) were isolated either from erythrocyte-depleted, heparinized peripheral blood, so-called *buffy coats*, or from leukapheresis obtained from the University Hospitals in Cologne and Dortmund. All cellular products were derived from healthy donors after informed consent.

Isolation of PBMCs was conducted by density gradient centrifugation. Therefore, the blood products were diluted with CliniMACS<sup>®</sup> buffer in a ratio of 1:2 and 30 mL were carefully layered onto a 15 mL cushion of Pancoll. Generally, between 4 (*buffy coats*) and 12 (leukapheresis) 50 mL Falcon tubes were prepared per donor. The tubes were then centrifuged for 30 min at 21°C and 450xg in swing-out buckets with the brake switched off. During this procedure, erythrocytes and granulocytes penetrate the 1.077 g/mL dense Pancoll medium due to their higher density, while the low density mononuclear cells and platelets are retained at the interface between Pancoll and the sample layer. After centrifugation, the cells at the interface were carefully sucked off, pooled, and washed three times with 50 mL CliniMACS<sup>®</sup> buffer each in order to remove platelets and residual Pancoll. The washing steps were performed for 5 min at 21°C and descending g-force (400xg, 300xg, 200xg). Finally, the PBMCs were either directly processed for Pan T cell isolation (2.2.2.10) or cryopreserved for long-term storage (2.2.2.3).

#### 2.2.2.10 Pan T cell isolation

Pan T cells were negatively selected from PBMCs by magnetic cell sorting (MACS<sup>®</sup>) using the Pan T Cell Isolation Kit from Miltenyi Biotec GmbH. In a first step, PBMCs were pelleted for 5 min at 4°C and 300xg and the sediment was resuspended in 40 µL PEB buffer per 10<sup>7</sup> total cells. Subsequently, 10 µL of Pan T Cell Biotin-Conjugated Antibody Cocktail against non-target cells (specifically against CD14, CD15, CD16, CD19, CD34, CD36, CD56, CD123, and CD235a) were added for each 10<sup>7</sup> cells. Following a 5 min incubation at 4°C, 30 µL of PEB buffer as well as 20 µL of Naïve Pan T cell MicroBead Cocktail per 10<sup>7</sup> total cells were given to the cell suspension, mixed and anti-biotin-directed MicroBead labelling was allowed for 10 min at 4°C. The volume was adjusted to a minimum of 500 µL using PEB buffer and the cell suspension was allowed to pass through a PEB-equilibrated separation column placed in a magnetic field bead separator. During this step, the magnetically labeled non-target cells are depleted by being retained within the separation column in the magnetic field, while the unlabeled cells run through the column. The column was then washed twice with PEB buffer and the flow-through cell population representing the enriched pan T cell fraction was collected.

### 2.2.2.11 T cell activation, transduction and expansion

Enriched pan T cells were resuspended at a density of  $1 \cdot 10^6$  cells/mL in TexMACS medium containing IL-2 at 40 IU/mL and T cell TransAct™ at a dilution of 1:17.5. As a colloidal polymeric nanomatrix incorporating CD3- and CD28-directed antibodies, TransAct™ allows efficient activation of resting T cells which in turn results in upregulated surface expression of the low density lipoprotein receptor (LDL-R). Since LDL-R serves as the major entry port for VSV-G-pseudotyped lentiviral vectors, transduction efficiencies of T cells can thus be dramatically increased (Finkelshtein et al., 2013; Amirache et al., 2017).

The applied T cell seeding conditions for each culture vessel type are summarized in Table . Twenty-four hours after TransAct™ activation, lentiviral gene transfer into T cells was induced by adding the viral vector concentrate to the cell cultures at a multiplicity of infection (MOI) of 1.5. Following proper resuspension, the cells were incubated for an additional 2 days, after which excessive TransAct™ was removed by replacing the culture supernatant with fresh T cell expansion medium (TexMACS™ medium supplemented with 40 IU/mL IL-2). By this day, the lymphocytes had usually reached a density of  $\geq 2.5 \cdot 10^6$  cells/mL and the cells were transferred to a T25, T75 or T175 flask in order to adjust the cell density to  $1 \cdot 10^6$  cells/mL. From this day onward, cell numbers were determined every 2-3 days and fresh T cell expansion media was added to maintain a cell concentration of  $1 \cdot 10^6$  cells/mL until enrichment for  $\Delta$ LNFR-positive cells (2.2.2.12) or day 12. Flow cytometric analysis for CD4, CD8,  $\Delta$ LNFR and CAR expression was performed before activation, on day 6 and day 11 of expansion.

**Table 9: Cell numbers and volumes for different cell culture vessels**

	area/well [cm <sup>2</sup> ]	Seeded T cells/well	Volume of medium/well [mL]
96 well plate	0,32	$2 \cdot 3 \cdot 10^5$	0.2
48 well plate	1	$1 \cdot 10^6$	1
24 well plate	2	$2 \cdot 10^6$	2
12 well plate	4	$4 \cdot 10^6$	3
6 well plate	10	$10 \cdot 10^6$	5

### 2.2.2.12 Selection of $\Delta$ LNGFR-expressing cells

Transgene-encoded expression of  $\Delta$ LNGFR was employed as a selection marker for the enrichment of transduced T cells by positive MACS<sup>®</sup> sorting. Using LNGFR MicroBeads, MACS<sup>®</sup> selection was performed in accordance with manufacturer's instructions on day 6 of T cell culture and day 5 after transduction, respectively. Afterwards, cells were resuspended to a cell density of  $1 \cdot 10^6$  cells/mL in TexMACS<sup>™</sup> medium containing 40 IU/mL IL-2 and expanded until downstream processing. In 2-3 day intervals, fresh TexMACS<sup>™</sup> medium with 40 IU/mL IL-2 was supplied to adjust the cell concentration to  $1 \cdot 10^6$  cells/mL.

### 2.2.2.13 Bead-based cytokine detection

Quantitative analysis of cytokine secretion by CAR T cells upon antigen recognition was performed using the MACSPlex Cytokine 12 Kit for human analytes. MACSPlex is a bead-based assay technology that relies on the same principle as a sandwich ELISA with the minor modification that the capture antibody is bound to soluble beads instead of being immobilized on a plate. The colloidal beads distribute evenly in solution thus enabling a more efficient antigen capturing than the static surface of ELISA well bottoms. To allow determination of multiple cytokines simultaneously, the MACSPlex assay consists of a mixture of 12 bead populations, each coupled to a different capture antibody directed against one of the following cytokines: GM-CSF, IFN $\alpha$ , IFN $\gamma$ , IL-2, IL-4,

IL-5, IL-6, IL-9, IL-10, IL-12p70, IL-17A, and TNF $\alpha$ . For identification and discrimination purposes using flow cytometry, each bead population is color-coded with a unique mixture of two fluorochromes that emit in the FITC and PE channels (Figure 8). Upon binding to the beads-bound detection antibodies, the cytokines are detected by use of antibodies labeled with APC. The fluorescence intensity measured with APC is proportional to the cytokine concentration in the sample and is quantified from a calibration curve.

For quantitative cytokine release analysis, CAR T cells were stimulated with target cells at a ratio 1:2 and incubated for 24 hours. Routinely, co-cultures were set up in U-bottomed 96 well plates with  $5 \cdot 10^4$  CAR-positive effector cells and a total volume of 200  $\mu$ L. Harvested supernatants were either stored at  $-20^\circ\text{C}$  until further processing or analyzed directly using the

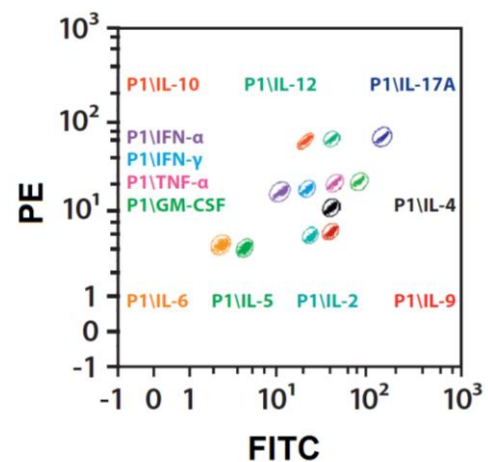


**Figure 8: Detection of MACSPlex cytokine capture bead populations.** Depicted FITC-PE scatter plot shows the fluorescence distribution of the 12 bead populations in samples. Each population is defined in an elliptic gate region. Figure modified from <https://www.miltenyibiotec.com/~media/Images/Products/Import/0009700/IM0009780.ashx>

protocol provided with the kit. Flow cytometric measurements and subsequent data analysis were performed automatically using the MACSQuant<sup>®</sup> Express Mode for MACSPlex.

#### **2.2.2.14 Live cell imaging-based kinetic cell lysis assay**

Measurement of CAR T cell-mediated cytotoxicity by target cell death was performed by real-time monitoring using the IncuCyte<sup>®</sup> S3 system. IncuCyte<sup>®</sup> is a live-cell imaging platform that enables automated analysis of cell behavior over time by automatically gathering and processing images in defined time intervals. This way, it provides information about cell behavior over an extended period of time, thus enabling more insight into the biological processes than standard end-point killing assays such as the chromium release assay (CRA).

Cytotoxicity assays were set up by seeding 15,000 GFP-transgenic target cells per well of flat bottomed 96 well plates and – following overnight incubation – adding equivalent numbers of CAR T cells to the cultures. A ratio of 1 between target and effector cells was used as it reflects the physiological conditions within a tumor. Cultures of target cells only and target cells with mock-transduced T cells were taken along as controls. Phase contrast and green fluorescence images were captured with 10x magnification every hour for 3-6 days. Analysis of images was performed using the software provided by the manufacturer and the following settings for GFP: Top-hat (100  $\mu\text{m}$  and 2.0 GCU) with edge sensitivity of -38 and filters of 2,000  $\mu\text{m}^2$  area, 70.0 mean intensity and 2E5 integrated intensity.

#### **2.2.2.15 Concurrent detection of degranulation and production of IFN $\gamma$ and TNF $\alpha$**

To assess the degranulative capacity of CAR T cells in a quantitative manner, the surface expression of lysosome associated membrane protein 1 (LAMP-1, also known as CD107a) was analyzed following antigen engagement. In resting T cells, CD107a is predominantly located intracellularly in the membrane of secretory granules. Upon activation, when lytic granules are exocytosed, their lipid layer fuses with the T cell plasma membrane thus exposing CD107a to the cell surface. Consequently, labeling responding T cells with an antibody to CD107a and measuring its surface expression by flow cytometry can directly identify degranulating CAR T cells. In this work, the measurement of CD107a expression on the cell surface was combined with intracellular cytokine staining for IFN $\gamma$  and TNF $\alpha$  in order to provide a more complete assessment of the functionality of CAR T cells and identify polyfunctional T cells.

For stimulation,  $2 \cdot 10^5$  CAR T cells were co-cultured with an equal number of target cells per well of a round bottomed 96 well plate. As CD107a is only transiently expressed on the cell surface and rapidly re-internalized via the endocytic pathway, VioBlue-labeled mAb directed

against CD107a was added directly after setting up the co-cultures. Following an incubation period of 1 hour, the cultures were further supplemented with 10 µg/mL monensin to prevent acidification and subsequent degradation of endocytosed CD107a antibody complexes. Moreover, to improve the readout of cytokine expression, Brefeldin A was given to the cultures at a final concentration of 10 µg/mL. The chemical inhibits the cytokine transport between the endoplasmic reticulum and the Golgi, in this way enabling accumulation of cytokines within the cell and increasing the sensitivity of cytokine detection. After an additional 4 hours of incubation, the cultivation was stopped and surface staining for CD4, CD8, and ΔLNGFR was performed. Therefore, the culture supernatant was removed after a centrifugation step at 300xg and 4°C for 5 min and the cells were resuspended in 110 µL per well of the respective antibody cocktail. Following incubation at 4°C for 10 min, the cultures were washed twice with cold PBS and the cells were fixed for intracellular staining by resuspending the pellet of each well in 100 µL PBS and 100 µL InsideFix. Cells were then incubated for 20 min at 4°C in the dark, after which they were washed with 200 µL InsidePerm per well. Antibodies directed against IFN $\gamma$  and TNF $\alpha$  were diluted in InsidePerm and following cell sedimentation at 500xg and 4°C for 5 min, the cells were resuspended in 110 µL antibody mix per well. Upon incubation for 15 min at 4°C in the dark, cells were washed twice with PEB buffer (400xg, 4°C, 5 min), resuspended in 200 µL PEB buffer and analyzed flow cytometrically.

#### **2.2.2.16 Flow Cytometry**

Analyses of cellular properties on single cell level were performed by multicolor flow cytometry with the MACSQuant<sup>®</sup> Analyzer 10. The flow cytometer is equipped with a violet (405 nm), a blue (488 nm) and a red (638 nm) laser and allows the detection of 8 different fluorochromes simultaneously. Before each multi-parametric measurement, channel voltage settings were optimized using MACSQuant<sup>®</sup> calibration beads and compensation was performed with single fluorochrome stained cells in combination with the MACSQuant<sup>®</sup> multicolor compensation modus. For cell immuno-phenotyping, antibodies were applied according to manufacturers' recommendations and appropriate isotype-matched antibodies were used as controls. Surface expression of CARs was analyzed either by Protein L or by polyclonal antibody-based anti-mouse IgG (Fab-specific) staining. To exclude dead cells from the analysis, PI was added to each sample right before the measurement using the MACSQuant<sup>®</sup> auto-labeling modus.

Analysis of acquired flow cytometry data was carried out using the MACSQuantify<sup>™</sup> software. The general gating strategy for each FACS experiment was based on the following three parameters: identification of target cells by appropriate forward scatter (FSC) and side scatter (SSC) setting, exclusion of cell aggregates by FSC-A and FSC-H blot and of dead cells by

gating on PI negative cells. Only these pre-gated cells were finally analyzed for expression of specific antigens.

### Protein L labeling

Protein L is a bacterial protein that interacts with the framework regions in the variable domain of immunoglobulin  $\kappa$  light chains, in particular those of  $\kappa 1$ ,  $\kappa 3$ , and  $\kappa 4$  (Graille et al., 2001). Its ability to also bind mammalian scFvs of CARs has recently been described by Zheng et al. suggesting its application as a general CAR detection reagent (Zheng et al., 2012). In initial validation experiments, in which the cells were processed according to the published protocol, strong unspecific staining was regularly observed. Therefore, the labeling procedure was optimized and

from this point on, cells were stained adhering to the following protocol: On day 6 or 11 after TransAct™ activation, T cells were harvested and subjected to efficient washing. Generally,  $1 \cdot 10^6$  cells were washed twice with 5 mL CliniMACS® buffer each (300xg, 5 min, 4°C) to remove possible carry-over immunoglobulins in culture media. Subsequent cell labeling was performed in 200  $\mu$ L CliniMACS® buffer containing 0.5  $\mu$ g/ $\mu$ L of biotinylated Protein L for 45 min at 4°C. Afterwards, cells were washed 3x with 5 mL CliniMACS® buffer (300xg, 5 min, 4°C) and then incubated with APC-conjugated  $\alpha$ -biotin monoclonal antibody (mAb) following manufacturer's recommendations. Following a washing step with 200  $\mu$ L PEB buffer (300xg, 5 min, 4°C), cells were resuspended in 200  $\mu$ L of fresh PEB buffer and analyzed by flow cytometry. Importantly, no combinatorial labeling with immunophenotypic antibodies was possible as one Protein L molecule contains two antigen binding sites that can concurrently interact with two  $\kappa$  light chains (Graille et al., 2001; Figure 9B). Simultaneous interactions of Protein L with a CAR molecule on the one hand and a  $\kappa$  light chain-containing antibody on the other hand, raise the possibility of false-positive signals and data misinterpretation. To exclude this, CAR expression analyses by Protein L labeling were strictly performed as single-stainings.

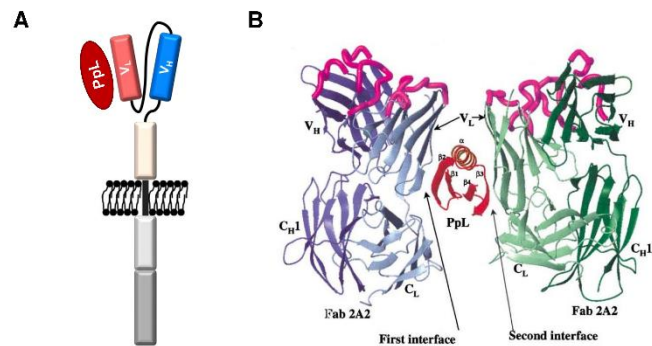


**Figure 9: Illustration of the binding sites of Protein L.** (A) Schematic representation of Protein L binding to the  $\kappa$  light chain of a single chain variable fragment of a CAR. V<sub>L</sub>, variable light chain; V<sub>H</sub>, variable heavy chain; PpL, *Peptostreptococcus magnus*-derived Protein L. (B) Ribbon representation of a 2 Fab:1 Protein L complex. The two Fab molecules sandwich a single Protein L molecule which contacts similar V<sub>L</sub> framework regions of two light chains via independent interfaces. Light colors represent the light chain, while dark colors the heavy chain. Magenta highlights the complementarity determining regions (CDR). C<sub>H</sub>, constant heavy chain; C<sub>L</sub>, constant light chain. Figure adopted from Graille et al. (2001).

### **Anti-mouse IgG (Fab-specific) labeling**

Polyclonal antibody stainings directed against the scFv region of the CAR molecule are currently most widely used to determine the surface expression of CARs by flow cytometry. The limitation here is that the polyclonal nature of the antibodies does not provide information on whether the detected CARs are properly folded as some antibodies can recognize linear epitopes of the CAR amino acid sequence that reaches the cell surface. The ease of the staining procedure, however, makes it a quick and thus convenient detection method for artificial chimeric receptors. To evaluate the cell surface expression of CARs by anti-mouse IgG (Fab-specific) labeling, harvested cells were resuspended in 200  $\mu$ L PEB buffer containing the biotinylated goat anti-mouse IgG (Fab-specific) antibody at a dilution of 1:100. Following an incubation period of 10 min at 4°C, cells were washed once with 200  $\mu$ L of PEB (300xg, 5 min, 4°C) and then subjected to  $\alpha$ -biotin labeling using an APC-conjugated mAb as instructed by the manufacturer. Afterwards, cells were washed once with 200  $\mu$ L PEB buffer (300xg, 5 min, 4°C) and resuspended in fresh 200  $\mu$ L of PEB buffer for subsequent flow cytometric analysis.

### **2.2.3 *In vivo* study methods**

#### **2.2.3.1 Animal model and housing conditions**

To study the *in vivo* activity of human SSEA-4-directed CAR T cells, the NOD/scid/IL2 $\gamma$ <sup>-/-</sup> (NSG<sup>TM</sup>) mouse model was selected. The NOD genetic background of this mouse strain confers an intrinsic reduction of innate immunity due to an absent complement system, defective dendritic cells and macrophages as well as lowered NK cell activity. On the other hand, the loss-of-function mutation in the *PRKDC* gene, which is commonly known as SCID, eliminates the adaptive immune system. The underlying mechanism here is that the mutational silencing of *PRKDC* abrogates the expression of the catalytic subunit of a protein kinase complex that is crucial for the repair of DNA double-strand breaks during V(D)J recombination. In the absence of V(D)J recombination, B and T cells fail to express their cell specific receptors and cannot mature. Moreover, the knockout of the IL-2-receptor common  $\gamma$  chain gene (IL2 $\gamma$ ) further abolishes the adaptive and innate immune system by eliminating high affinity signaling through IL-2, IL-4, IL-7, IL-9, IL-15, and IL-21 receptors. The major consequence of this genetic deletion is the prevention of NK cell differentiation, because its development is strongly dependent on IL-15 signaling. As an ultimate result, neutrophils and monocytes constitute most of the remaining mouse immune cells which renders the NSG<sup>TM</sup> strain highly immunodeficient and this way amendable to engraftment of human cells (Shultz et al., 2005; Shultz et al., 2014).

All experimental procedures conducted within this study were in compliance with European and German guidelines for the care and use of laboratory animals and were approved by the ethical committee on animal care and use in Nordrhein-Westfalen (approval number: 84-02.04.2016.A177). Mice were purchased at an age of six weeks and were allowed to adapt to the housing conditions for at least two weeks before starting the experiments. Maximum occupancy was 5 animals per cage. At all times, the animals were maintained under specific pathogen-free (SPF) conditions using individually ventilated cages (IVC), sterile chow and antibiotic-supplemented drinking water provided *ad libitum*. A 12 hour day and night cycle was sustained.

### 2.2.3.2 Tumor inoculation

To establish subcutaneous (s.c.) tumors from cancer cell lines, female NSG<sup>TM</sup> mice of 8 to 10 weeks of age were injected subcutaneously with  $5 \cdot 10^6$  cells resuspended in 150  $\mu$ L PBS in the flank. Mice were shaved at site of injection beforehand and injections were performed using a 1 mL syringe equipped with 27G needle. In the context of the MCF-7 tumor model, mice were additionally supplied with slow-release 17 $\beta$ -estradiol pellets directly before tumor cell injection. Through s.c. implantation of the pellets in the neck region, a continuous release of the hormone was ensured over 60 days, which was meant to support the growth of the estrogen-dependent tumor cell line (Dall et al., 2015).

After tumor inoculation, the growth rate of the tumors was monitored by both measuring the size using a caliper and by bioluminescent imaging.

### 2.2.3.3 T cell injections

Adoptive transfer of CAR or mock T cells into NSG<sup>TM</sup> mice occurred via the intravenous route and was kindly performed by Janina Brauner and Dr. Wa'el Al Rawashdeh. Doses between  $2 \cdot 10^6$  CAR T cells in 100  $\mu$ L PBS per mouse were administered while the untransduced T cell control was adjusted to the total T cell number injected in the CAR T cell groups.

### 2.2.3.4 Physical tumor measurements

Measurements of tumor size were performed 2–3 times weekly by determining the greatest longitudinal diameter (*length*) and the greatest transverse diameter (*width*) using an electronic caliper. Tumor volume was then calculated using the formula (Euhus et al., 1986; Tomayko and Reynolds, 1989):

$$Tumor\ volume = \frac{1}{2}(length \cdot width^2)$$

### **2.2.3.5 Bioluminescent imaging of mice**

For bioluminescent imaging of luciferase-expressing tumor or T cells, mice received intraperitoneal (i.p.) injections of 3 mg D-luciferin dissolved in 100  $\mu$ L PBS and 10 min after injection, anesthetized mice were imaged using an IVIS Lumina III imaging system. General anesthesia was induced by inhalation of 1.5% (v/v) isoflurane in oxygen and continued during the measurement procedures with 0.5% (v/v) introduced via a nose cone (flow rate: 1 L/min). Image acquisition was conducted in auto-exposure mode, binning 8, field of view E, and F-stop 1.2. Using Living Image software, regions of interest (ROIs) were manually drawn around the luminescent signal and luciferase activity for each mouse was quantitatively analyzed as total flux.

### **2.2.3.6 Preparation of blood plasma**

Blood samples were collected by puncture of *vena facialis* using a lancet and immediately transferred to EDTA-coated microtubes to avoid agglutination. After centrifugation at 4,000 rpm for 20 min at 4°C the supernatant blood plasma was harvested and stored at -20°C until further processing. Routinely, 80  $\mu$ L of whole blood were used for blood plasma preparation.

### **2.2.3.7 Preparation of single cell suspensions for flow cytometry**

For organ harvest, mice were euthanized by cervical dislocation and rinsed with 80% ethanol prior to excision of the respective organs. The organs were stored in MACS<sup>®</sup> tissue storage solution until downstream processing.

#### **2.2.3.7.1 Blood**

Peripheral blood with a maximum volume of 80  $\mu$ L was collected from *vena facialis* after puncturing it with a lancet. To prevent agglutination, sample takes were directly transferred to EDTA-coated tubes, after which equal blood volumes of each mouse were withdrawn and red blood cell lysed. Routinely, 50  $\mu$ L of whole blood were lysed in 1 mL 1x RBC lysis buffer for 5 min at room temperature. After centrifugation at 300xg and room temperature for 5 min, the specimens were processed for flow cytometric analysis as described in 2.2.3.8.

#### **2.2.3.7.2 Bone marrow**

Bone marrow was extracted from the femurs and tibias of mice by cutting off the heads of the bones and rinsing the inner fragments with RPMI 1640 using a 21G needle. Upon thorough

trituration to break up the tissue, the cell suspension was passed through a MACS® SmartStrainer with 70 µm pore size and centrifuged at 300xg for 5 min at 21°C. Subsequent RBC lysis was performed by resuspending the cell pellet in 1 mL of 1x RBC lysis buffer and incubating the cells at room temperature for 2 min. Addition of 5 mL PBS then stopped the reaction, after which the cells were pelleted at 300xg for 5 min at 21°C. Following resuspension of the cell sediment in 2 mL of PBS, the cell number per mL was determined using MACSQuant® Analyzer and  $2 \cdot 10^6$  cells were extracted for flow cytometric analysis (2.2.3.8).

#### **2.2.3.7.3 Liver and lung**

Liver and lung were mechanically disaggregated with scalpels and transferred to 37°C pre-warmed gentleMACS™ C Tubes containing MACS® tissue dissociation solution. For lung 2.5 mL and for liver 5 mL of dissociation solution per organ were used. Upon manual disaggregation, automated tissue homogenization was started by transferring the gentleMACS™ C Tubes onto a gentleMACS™ Octo Dissociator and selecting the appropriate program settings (program for lung: m\_LDK\_37; program for liver: m\_LIDK\_37). Routinely, the viability of the dissociated specimens was in the range of 80-90% for lung and 85-95% for liver. After dissociation, the homogenized tissues were filtered through MACS® SmartStrainers with 70 µm pore size and sedimented at 300xg and 4°C for 5 min. To lyse red blood cells, the pellet was resuspended in 2 mL of 1x RBC lysis buffer and after a 2 min incubation at room temperature, 5 mL PEB buffer were added. Upon centrifugation at 300xg and 4°C for 5 min, the cellular sediment was resuspended in 3-5 mL of PEB buffer and cell numbers per mL were determined by MACSQuant® Analyzer. Two million cells of each specimen were then used for flow cytometric phenotyping as detailed in 2.2.3.8.

#### **2.2.3.7.4 Spleen**

Spleen cell suspensions were prepared by gently mashing the organs with the plunger end of a 5 mL syringe in a Petri dish. Following transfer of the splenocyte suspensions through a 70 µm pore-size MACS® SmartStrainer, the cells were centrifuged at 300xg and 21°C for 5 min and subsequently depleted from red blood cells by resuspending the sediment in 2 mL of 1x RBC lysis buffer. After an incubation period of 2 min at room temperature, the reaction was stopped by addition of 5 mL PEB and the cells were re-pelleted at 300xg and 21°C for 5 min before being resuspended in 1 mL PBS. Ensuing cell counting was performed with MACSQuant® Analyzer and  $2 \cdot 10^6$  cells were routinely used for downstream flow cytometric application (2.2.3.8).

### 2.2.3.8 Flow cytometric analysis of *ex vivo* organ preparations

To minimize non-specific binding of fluorochrome-conjugated antibodies during labeling procedures, all specimens obtained from *ex vivo* organ preparations were first pre-incubated with anti-human and anti-mouse FcR blocking reagent following manufacturer's instructions. Labeling of cells was then performed by adding the respective antibody or antibody cocktail to the cell suspension as recommended by the supplier. Following an incubation period of 15 min at 4°C, unbound antibodies were removed by washing the cells twice with PEB buffer, after which the cell pellets were resuspended in 300 µL PEB buffer and subjected to flow cytometric analysis. An effort was made to acquire a total of  $1 \cdot 10^6$  viable cells per specimen at rates not exceeding 3,000 events per second.

### 2.2.4 Statistics

Unless otherwise specified, all graphical error bars represent standard deviation of the mean. Statistical comparisons between two groups were conducted by paired two-tailed Student's t-tests using GraphPad Prism 7.03. To facilitate overview, the significance analyses were organized in a pairwise significance matrix where each box represents a comparison between two groups. The order, in which the groups were compared, is illustrated in Figure 1. Significant differences between two comparing groups are defined by a white box, while insignificant differences by a black box. Moreover, asterisks within a white box denote the degree of significance where \*,  $p < 0.05$ ; \*\*,  $p < 0.01$ ; \*\*\*,  $p < 0.001$ .

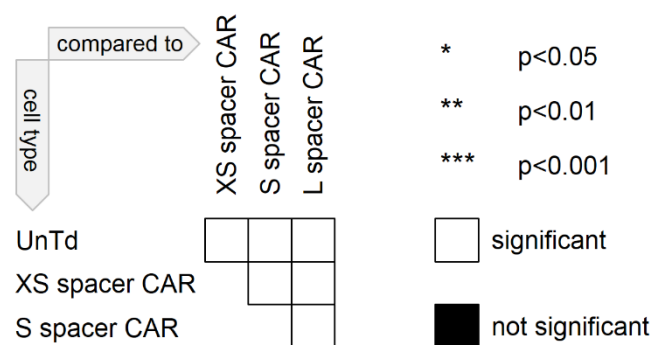


**Figure 10: Organization of the pairwise significant matrix for group comparison.**

### 3 Results

#### 3.1 Construction of SSEA-4-specific chimeric antigen receptors

Several studies have demonstrated that the spacer region can have a significant impact on CAR T cell function and needs to be customized for each epitope (Guest et al., 2005; Hudecek et al., 2016; Haso et al., 2013). Hence, a panel of SSEA-4-reactive second generation CARs was generated by using an in-house generated CAR spacer library. Within this library, each CAR-encoding transfer vector contained the following active transgene elements (Figure 11A):

- Phosphoglycerate kinase (PGK) promoter to drive the expression of the transgene
- 5'-3' CAR open reading frame (ORF) consisting of
  - $\beta$ -galactosidase (lacZ) reporter gene for blue/white selection
  - spacer region
  - CD8 $\alpha$  transmembrane domain
  - CD137 (4-1BB) endodomain
  - CD3 $\zeta$  endodomain
- Porcine teschovirus-1 2A (P2A) ribosome skip sequence
- A truncated low affinity nerve growth factor receptor ( $\Delta$ LNGFR) that lacks the cytoplasmic signaling endodomain and serves both as a transduction marker as well as for enrichment purposes of transduced cells

Depending on the transfer vector, the spacer region encompassed either the domain for IgG4 CH1-hinge-CH2CH3 (extra large (XL) spacer), IgG4 hinge-CH2CH3 (large (L) spacer), IgG4 hinge-CH3 (medium (M) spacer), CD8 $\alpha$  hinge (small (S) spacer) or IgG4 hinge (extra small (XS) spacer) (Figure 11B). To abrogate potential interactions of the L and XL spacer CARs with FcR-expressing cells, the first six amino acids of the CH2 domain (APEFLG) were replaced with the corresponding five amino acids of IgG2 (APPVA) and an N $\rightarrow$ Q mutation at the glycosylation site at position 297 was introduced (Hudecek et al., 2016).

The backbone of the transfer vectors consisted of bacterial plasmid portions to allow selective plasmid amplification in bacteria, and standard lentiviral vector elements to enable the production of transgene-encoding lentiviral vectors in mammalian cells based on a three plasmid system (2.2.2.7).

Specificity for SSEA-4 was introduced into the chimeric receptors by replacing the LacZ reporter gene with a codon-optimized V<sub>L</sub>-(G<sub>4</sub>S)<sub>3</sub>-V<sub>H</sub>-oriented scFv derived from the SSEA-4-reactive monoclonal antibody REA101 into each CAR plasmid. To facilitate receptor trafficking to the plasma membrane, a mouse  $\kappa$  light chain leader sequence was added N-terminally to the scFv sequence (Figure 11C).

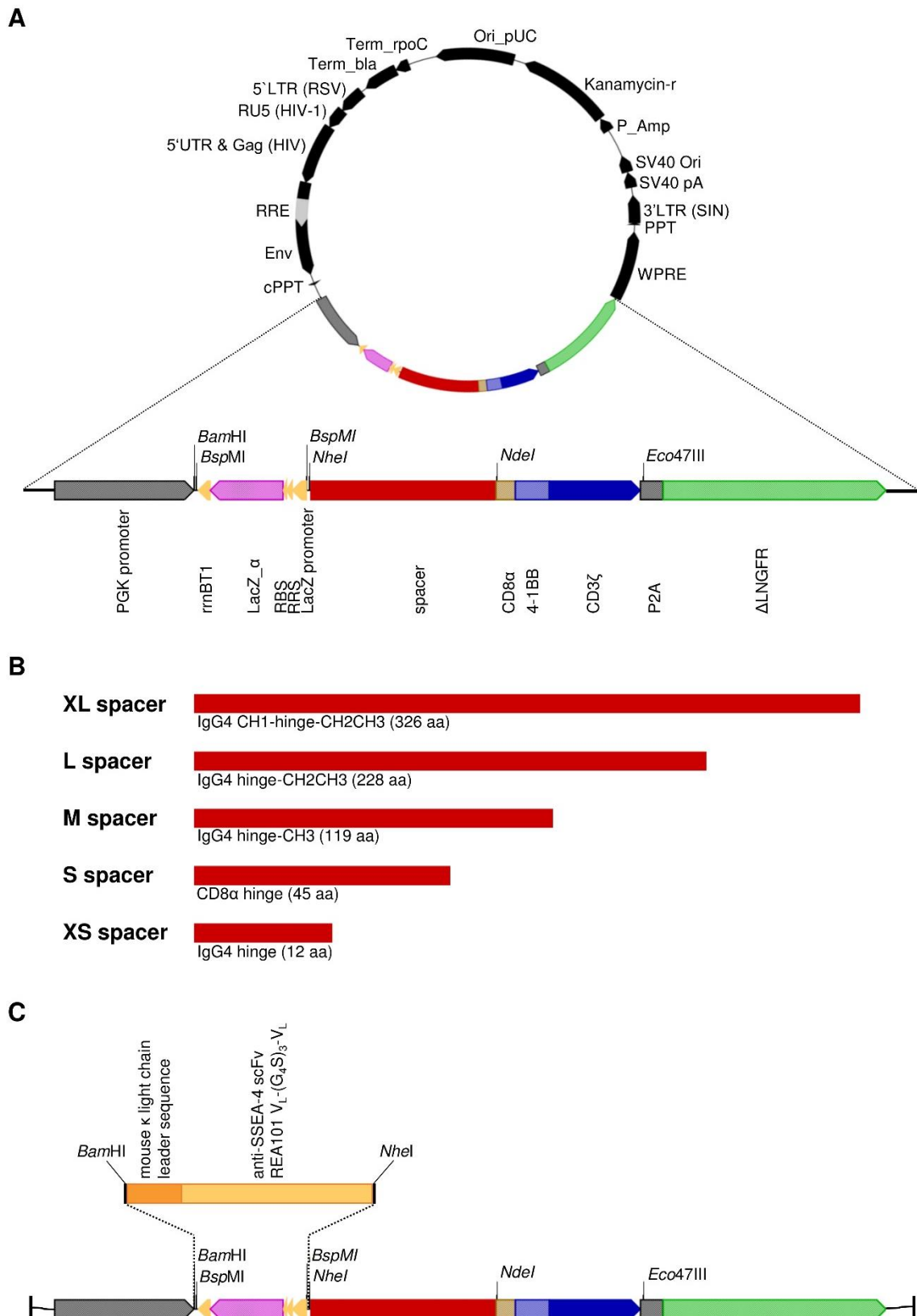


**Figure 11: Schematic representation of the lentiviral transfer vectors used in this study and construction of SSEA-4-specific CARs.** (A) Organization of the CAR expression vectors. (B) Overview of the spacer members comprised in the CAR spacer library. (C) Cloning strategy for introducing SSEA-4 specificity into a CAR backbone. aa, amino acid; cPPT, central polypurine tract; env, envelope protein;  $\Delta$ LNGFR, truncated low affinity growth factor receptor; HIV, human immunodeficiency virus; Kanamycin-r, Kanamycin resistance gene; LacZ $_{\alpha}$ ,  $\alpha$  monomer of  $\beta$ -galactosidase; LTR, long terminal repeats; Ori\_pUC, origin of replication derived from *Escherichia coli* plasmid pBR322; P2A, porcine teschovirus-1 2A peptide; pAmp, promoter of the Ampicillin resistance gene; PGK, human

phosphoglycerate kinase; RBS, ribosome binding site; RRE, rev responsive element; rrnBT1, transcriptional terminator T1 of ribosomal RNA operon B (rrnB); RSV, Rous sarcoma virus promoter; RU5 (HIV1), R and U5 components of HIV-1 LTR; SV40 pA, simian virus 40 polyadenylation sequence; SV40 Ori, simian virus 40 origin of replication; Term\_bla, terminator operon of  $\beta$ -lactamase; Term\_rpoC, terminator operon of RNA polymerase  $\beta'$  subunit; 5'UTR, 5' untranslated region; V<sub>H</sub>, variable heavy chain; V<sub>L</sub>, variable light chain; WPRE, woodchuck hepatitis virus regulatory element. *Italic typefaces indicate restriction sites for the respective endonucleases.*

## 3.2 Expression analysis of SSEA-4-directed CAR variants in HEK293T cells

Before characterizing the generated CAR constructs in-depth in primary T cells, their cell surface expression along with proper folding was first assessed in HEK293T cells. Contrary to suspension cells, HEK293T cells can be easily transfected by most transfection reagents thus enabling quick and efficient delivery of exogenous DNA and uncomplicated expression analyses.

Equimolar amounts of CAR-encoding transfer vectors were introduced into HEK293T cells by lipofection (2.2.2.6) and surface expression was evaluated 48 hours later, when the level of transiently expressed proteins is expected to peak. For the determination of the transfection efficiency of each set-up, cells were labeled with a mAb directed against  $\Delta$ LNGFR, which is encoded downstream of the CAR-P2A sequence in the transfer vectors (Figure 11A). In this configuration, CAR and  $\Delta$ LNGFR are transcribed as a single mRNA, but translated into two separate proteins allowing a direct measurement of CAR expression efficiency when compared to the marker protein. No irregularities in  $\Delta$ LNGFR expression were expected as the marker protein is (1) a naturally occurring protein with an evolutionary established amino acid sequence and (2) its efficient expression has already been verified in various mammalian systems within Miltenyi Biotec GmbH, among others in HEK293T cells and in connection with a P2A element (data not shown). To probe directly the expression of CARs, Protein L was employed – a bacterial agent that binds to variable  $\kappa$  light chains present in immunoglobulins, Fab, scFvs and consequently also CARs (2.2.2.16). An overview of the resultant expression data is illustrated in Figure 12. For all transfer vectors tested, the frequency of  $\Delta$ LNGFR-positive cells was higher than that of Protein L-positive cells. In general, 95-99% of cells expressed the reporter protein, indicating a uniform and high degree of transfection had occurred. By contrast, strong variabilities in CAR surface expression were observed depending on the nature of the spacer region. The following expression hierarchy was determined in descending order: L spacer CAR > S spacer CAR > XS spacer CAR > XL spacer CAR > M spacer CAR.

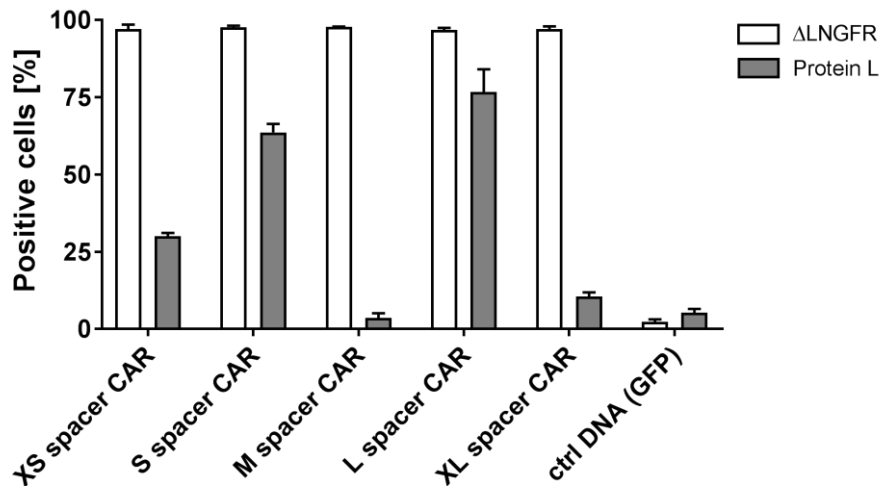


**Figure 12: Expression of  $\Delta$ LNGFR and second generation XS, S, M, L, and XL spacer CAR variants on HEK293T cell surface.** Transfer vector DNA was introduced transiently into HEK293T cells by lipofection and flow cytometric analysis was performed 48 hours later. Expression of  $\Delta$ LNGFR was detected by mAb staining, while that of CARs by Protein L staining. Both detection reagents were used in biotinylated form and fluorescence tagging was performed by secondary  $\alpha$ -Biotin-APC mAb labeling. A GFP-encoding vector served as control. Results are the average of 3 independent experiments.

### 3.3 Generation of lentiviral vectors encoding SSEA-4 CAR variants and T cell engineering

Self-inactivating (SIN) HIV-1-based lentiviral vectors encoding the CAR of interest were produced based on the three plasmid system and an effort was made to transduce T cells under standardized conditions for a maximum degree of reproducibility. The rationale was based on the assumption that strong differences in the transgene copy number in the T cell genome can lead to differential intensity of transgene expression on the cell surface in this way impacting the amplitude and kinetics of CAR T cell responses. On the other hand, as indicated by the CAR surface expression data on HEK293T cells in Figure 12, the inequality of surface expression of the CAR variants had to be taken into consideration. Therefore, for comparison purposes, a congruent surface expression of  $\Delta$ LNGFR intra- and interexperimentally was aimed for, so that each lentiviral batch was first titrated on HT1080 and the amount of transduction-competent virions was determined based on surface  $\Delta$ LNGFR expression. As exemplified in Table and in accordance with published literature, functional viral titers decreased as the size of the cargo increased. In fact, the rough tendency was observed that addition of 100 bp to the transgenic cargo reduced the vector concentration of approximately 10%.

**Table 10: Overview of cargo length and obtained titers for lentiviral vectors encoding XS, S, M, L, and XL spacer CAR variants.** Transduction experiments were performed with lentiviral vector suspensions received after 100-fold concentration. Each vector batch was subjected to serial dilution and then used to transduce HT1080 cells in the presence of polybrene (8 µg/mL). Following 72 hours of incubation, ΔLNGFR expression was assayed flow cytometrically. Only samples displaying transduction efficiencies ≤20% were considered for concentration calculations of transduction-competent virions. Data represents the average of 3 independently produced batches for each construct.

	CAR payload [bp]	CAR-P2A-ΔLNGFR payload [bp]	Average titer [TU <sub>HT1080</sub> /mL]
<b>XS spacer CAR</b>	1,358	2,267	7.2·10 <sup>8</sup>
<b>S spacer CAR</b>	1,457	2,366	6.6·10 <sup>8</sup>
<b>M spacer CAR</b>	1,679	2,588	5.4·10 <sup>8</sup>
<b>L spacer CAR</b>	2,006	2,915	3.0·10 <sup>8</sup>
<b>XL spacer CAR</b>	2,294	3,203	1.4·10 <sup>8</sup>

In a first T cell transduction experiment, all spacer CAR variants were tested for surface expression on the immune cells. T cells were transduced with a MOI<sub>HT1080</sub> of 1.5 of the respective lentiviral vector and transgene surface expression was assayed 5 days later. As depicted in Figure 13, the rates of surface ΔLNGFR ranged between 40 and 55%, whereas surface CAR expression was in general lower than that of the reporter protein and ranged between 13 and 38% as determined by Protein L staining.

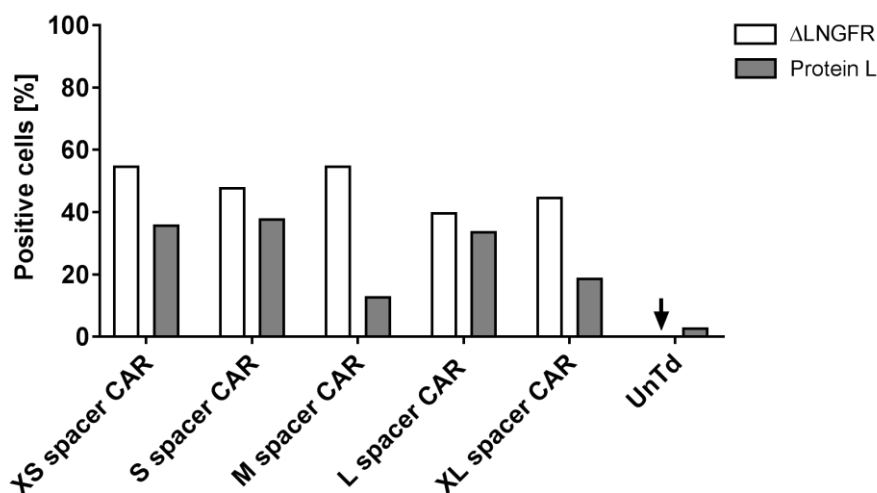


**Figure 13: Expression of ΔLNGFR and second generation XS, S, M, L, and XL spacer CAR variants on T cell surface.** Naïve Pan T cells were isolated from PBMCs and cultured in the presence of IL-2 and the T cell stimulating matrix TransAct™. For permanent receptor expression, the lymphocytes were transduced lentivirally with an MOI of 1.5 and expanded in IL-2. Surface transgene expression was determined by flow cytometry 5 days after transduction and 4 days after TransAct™ removal, respectively. Expression of ΔLNGFR was analyzed by mAb-based staining, while Protein L staining was applied to analyze CAR expression. Both detection reagents were used as biotin-conjugates and fluorescence marking was achieved by secondary labeling with α-biotin-APC mAb. The results of one experiment are displayed. UnTd, untransduced.

Notably, normalization of CAR expression based on  $\Delta$ LNGFR-positive cells revealed that the immune cells displayed an equivalent efficiency trend in expressing the individual chimeric receptors when compared with HEK293T expression data (Table 11). In both cell types, the highest frequency of CAR-positive cells was observed in cell populations that received the genetic element for the L spacer CAR, followed by the S and then XS spacer CAR. The lowest frequency of CAR-positive cells was detected in the M spacer CAR-engineered populations and the second lowest in the XL spacer CAR groups. At this stage, a percentual CAR: $\Delta$ LNGFR ratio below 50% was defined as an inefficient CAR expression and the M and XL spacer CAR constructs were eliminated from progression into the next series of experiments.

**Table 11: Expression efficiency of XS, S, M, L, and XL spacer CAR on the T cell surface normalized to  $\Delta$ LNGFR.** Calculations are based on the assumption that Protein L<sup>+</sup> cells are within the  $\Delta$ LNGFR<sup>+</sup> population.

	XS spacer CAR	S spacer CAR	M spacer CAR	L spacer CAR	XL spacer CAR
<b>Protein L<sup>+</sup> cells/ <math>\Delta</math>LNGFR<sup>+</sup> cells</b>	65%	79%	23%	85%	42%

Extended T cell transduction experiments with the three lead CAR candidates reproducibly confirmed the similar transduction efficiencies for each transfer vector by  $\Delta$ LNGFR-specific staining. Frequencies of transgenic cells routinely ranged between 35-60% for XS and S spacer CAR encoding vectors and between 20-55% for L spacer CAR encoding vectors. Notably, for all donors and viral vectors, CD4<sup>+</sup> T cells demonstrated a slight but significantly higher percent transduction than the CD8<sup>+</sup> population (Figure 14).

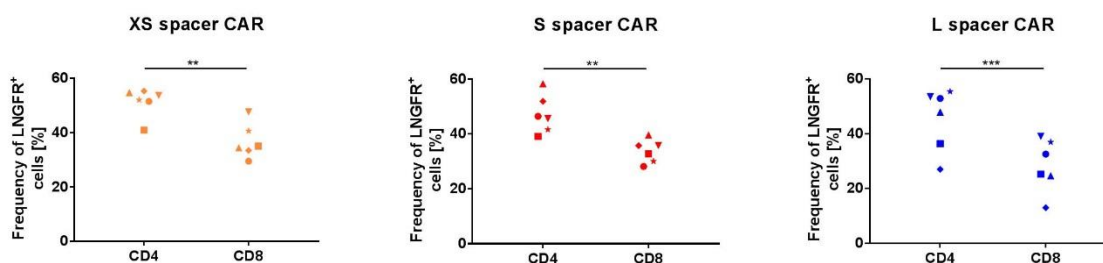


**Figure 14: Expression of  $\Delta$ LNGFR on CD4<sup>+</sup> and CD8<sup>+</sup> T cells after transduction of Pan T cells with XS, S, and L spacer CAR encoding lentiviral vectors.** Pan T cells isolated from PBMCs were stimulated for 24 hours with TransAct™ and IL-2 and subsequently exposed to the respective vector at an MOI<sub>HT1080</sub> of 1.5. One day after transduction, the medium was replaced and the cells were expanded in the presence of IL-2. Expression of  $\Delta$ LNGFR was analyzed by flow cytometry 5 days after transgene transfer. The results are a summary of 4 independent experiments.

### 3.4 Comparison of different flow cytometric CAR detection methods before and after $\Delta$ LNGFR enrichment

Due to the unavailability of fluorochrome-conjugated SSEA-4, up to this point of the study, Protein L staining was employed for the direct identification of surface expressed CARs. This detection method, however, suffers from the disadvantages that it often gives high background in stainings and – more importantly – cannot be combined with antibodies to achieve multifactorial characterization of CAR T cells. The two binding sites per Protein L molecule can bind concurrently to a CAR receptor and an antibody resulting in false-positive double or multi labeling of cells. Sequential staining approaches of CAR T cells with Protein L labeling followed by a blocking step with fluorochrome-free antibodies and subsequent cell phenotyping by fluorochrome-conjugated antibodies were hindered by the low antigen affinity of Protein L which induced the protein to “fall off” of the cells (data not shown). For these reasons, a second direct CAR detection method was tested by staining the mouse-derived scFv domain of the receptors. Pan T cells transduced with lentiviral vectors that direct the co-expression of either XS, S, or L spacer CAR and  $\Delta$ LNGFR were expanded for 5 days following transgene integration and one fraction of cells was subjected to transgene surface expression analysis. CAR expression was validated by both Protein L and anti-mouse IgG (Fab-specific) polyclonal antibody staining and compared to the expression of  $\Delta$ LNGFR as determined by mAb labeling. All stainings were performed separately, but in parallel. Using the remaining cell fraction, the applicability of these staining methods after positive MACS<sup>®</sup> sorting was verified. In the setting of positive selection, target cells are labelled by antibody-bead conjugates which remain on the cell surface following the enrichment procedure. Subsequent CAR staining approaches bear the risk to result in false-positive signals due to binding of the detection reagents to the  $\alpha$ -LNGFR mAb. To exclude this possibility, an expansion period of 6 days between  $\Delta$ LNGFR enrichment and CAR expression analysis was introduced, in this way allowing the antibody-bead conjugates to be degraded and/or diluted on the T cell surface. A representation of repeatedly obtained staining patterns for the different spacer CARs is shown in Figure 15. Based on  $\Delta$ LNGFR expression, less than 50% of the T cells showed genetic modification before enrichment. With a regular compromise of roughly 3-5%, the frequency for transgene-positive cells corresponded to that obtained by  $\Delta$ LNGFR staining when the anti-mouse IgG Fab-directed antibody was used for CAR expression identification. This was indicative that a correlated expression of both transgenes was taking place. Strikingly, for the XS spacer CAR, a peak-shift towards lower MFI was observed, indicating that the receptor is either present in lower numbers on the cell surface than the marker protein or the antibody binding is affected by inefficient epitope accessibility due to the very short spacer region (12 amino acids in length). When using Protein L staining, a CAR spacer-dependent staining pattern was observed: with decreasing spacer length the discrepancy in the staining efficiencies of transgene-positive cells

with  $\Delta$ LNGFR and Protein L reagents increased. Consequently, there was no compatibility in the staining pattern of the S and XS spacer CARs among the two CAR detection methods. This became more apparent when working with enriched populations. Reproducibly, MACS<sup>®</sup> sorting for  $\Delta$ LNGFR yielded enriched transgene-positive cell populations with purities ranging between 78-96% and homogeneous levels of  $\Delta$ LNGFR expression as determined by flow cytometry. In the context of the anti-mouse IgG Fab-staining approach, the staining patterns of  $\Delta$ LNGFR were again reproducible for the L and S spacer CAR. However, similar to the non-enriched population, for the XS spacer CAR a left-shift of the histogram's peak was observed compared to the flow cytometric data of the marker protein. Nevertheless, the percentage of CAR-positive cells remained comparable. In strong disagreement with this, Protein L staining for the detection of XS spacer CAR displayed a reduction of > 50% in the frequency of transgene-positive cells when compared to the  $\Delta$ LNGFR signal. In addition, the staining pattern adopted a shoulder type shape. A similar, although less drastic, trend was observed for the S spacer CAR staining. In comparison to the  $\Delta$ LNGFR staining, labeling of the same population with Protein L showed a 20% lower frequency of transgene-positive cells and a broader peak with lower MFI. In contrast to these observations, staining of the L spacer CAR corresponded to that of  $\Delta$ LNGFR. In summary, these data demonstrate that although the identification of transgene expression is not hampered after positive MACS<sup>®</sup> sorting, for some CAR variants, different CAR detection methods can give rise to contradictory results and have to be interpreted with caution.

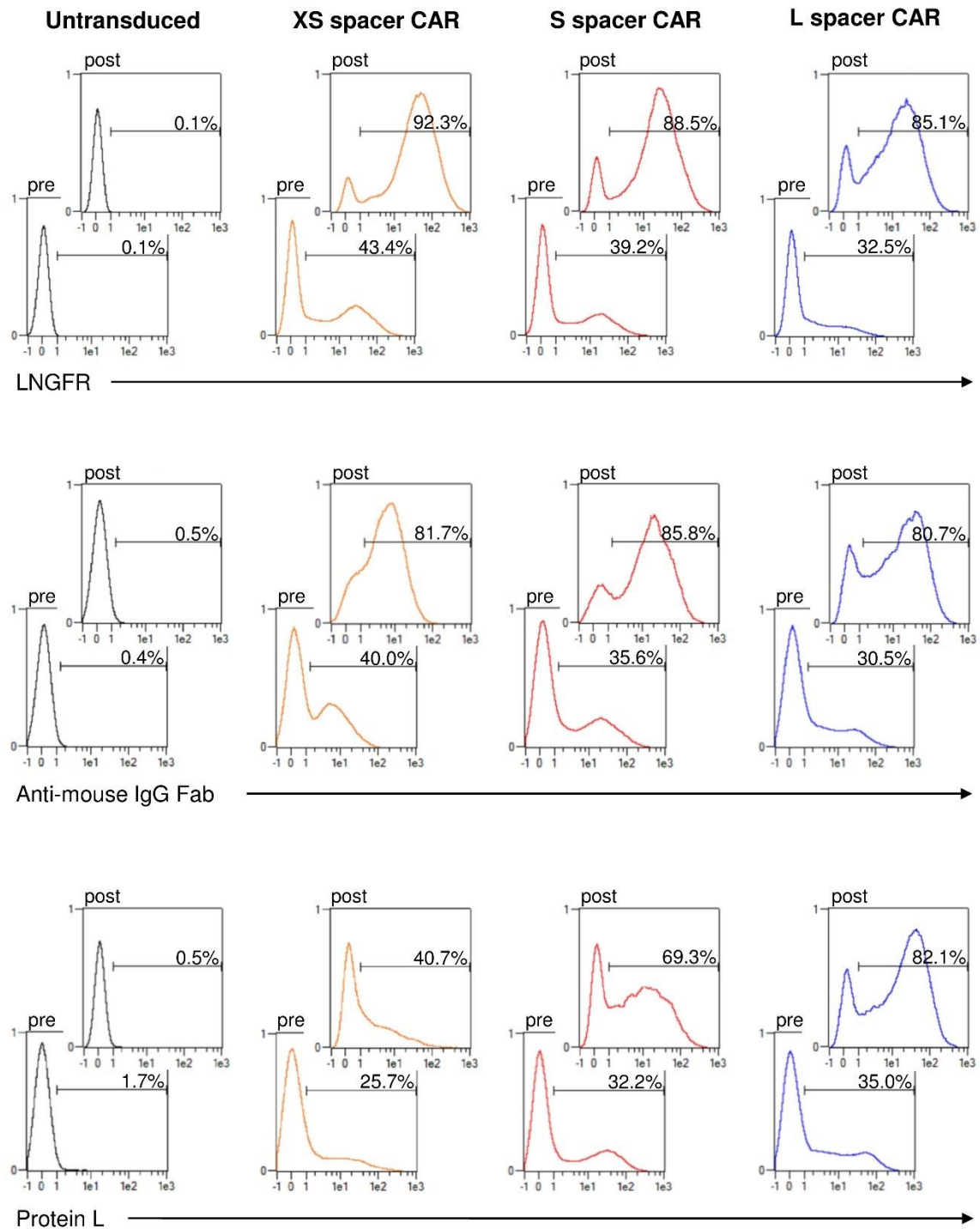


**Figure 15: Comparison of different flow cytometric methods for the detection of CAR expression on the T cell surface before  $\Delta$ LNGFR enrichment (pre) and after  $\Delta$ LNGFR enrichment and expansion (post).** Five days after transduction of pan T cells with lentiviral vectors encoding the XS, S, or L spacer CAR variant, engineered T cells were enriched for  $\Delta$ LNGFR by positive MACS<sup>®</sup> selection and expanded for an additional 6 days in the presence of IL-2. Transgene expression was analyzed directly before and 6 days after enrichment using different labeling methods. To detect the frequency of genetically modified T lymphocytes, cells were stained for  $\Delta$ LNGFR using antigen-specific biotin-coupled mAb, while CAR expression was analyzed either by a biotinylated polyclonal goat anti-mouse IgG Fab-specific antibody or by staining with biotinylated Protein L. Detection of the biotin conjugates was performed using  $\alpha$ -biotin-APC secondary mAb labeling. Percentage of positive staining is indicated in each histogram. Results are representative for 4 independent experiments. Fab, fragment antigen binding.

### 3.5 Surface expression of SSEA-4 on breast cancer cell lines

As a prerequisite for the evaluation of CAR functionality, the surface expression of SSEA-4 by established breast cancer cell lines was first investigated. Flow cytometric analysis was performed on MCF-7, MDA-MB-231, SK\_BR\_3, and BT-474, as their use has already been described in *in vivo* models, thus confirming their engraftment ability in mice and their suitability for potential upcoming animal experiments. For SSEA-4 expression screening, fluorochrome-labeled REA101 was used, the clone from which the scFv sequence of the CARs was derived, and controls were treated with an irrelevant isotype matched antibody. While no SSEA-4 signal was detectable for the two HER2-overexpressing cell lines SK\_BR\_3 and BT-474, a high percentage of MCF-7 and MDA-MB-231 cells displayed expression of the glycolipid (Figure 16). In case of MDA-MB-231, which is known as a highly aggressive triple negative breast cancer cell line, 95±4% of the cells were SSEA-4-positive and surface antigen density was relatively high with a median fluorescence intensity for FITC (MFI<sub>FITC</sub>) of 24.9±0.8. Moreover, the intercellular surface expression of the antigen was rather homogeneous as indicated by the narrow width of the histogram's peak. Contrary to that, the luminal A breast cancer cell line MCF-7, which is characterized by a low aggressive phenotype, showed antigen-positivity in 80±3.2% of the cells with a low overall antigen density represented by a MFI<sub>FITC</sub> of 7.6±0.5. However, as suggested by the histogram's broad peak width the intercellular antigen variation was broad. In summary, two breast cancer cell lines with differential SSEA-4 expression characteristics were identified and selected for following functionality screenings of SSEA-4-redirected CAR T cells.

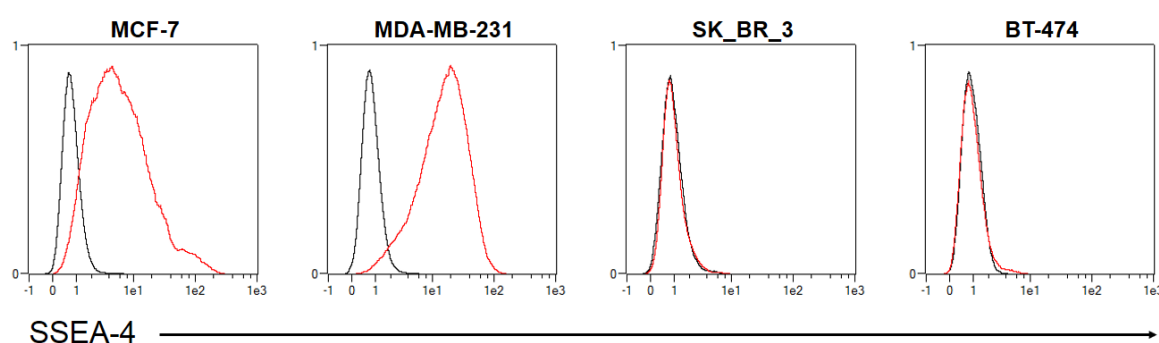


**Figure 16: Surface expression of SSEA-4 on the breast cancer cell lines MCF-7, MDA-MB-231, SK\_BR\_3, and BT-474.** Antigen expression was determined by flow cytometry using FITC-labeled SSEA-4 specific mAb REA101. Black line is isotype control and red line points out SSEA-4 labeling. Data is representative for 3 independent experiments.

### 3.6 Functional *in vitro* characterization of SSEA-4-directed XS, S, and L spacer CAR T cells

To assess the bioactivity of the XS, S and L spacer CARs, T cells incorporating the respective receptors were analyzed for their effector function following antigen stimulation. All functionality assays were performed with  $\Delta$ LNGFR-enriched populations and on day 12-14 following TransAct™ activation. Cytotoxicity was evaluated based on CD107a expression on the T cells surface and target cell death, whilst the ability for cytokine production and secretion was investigated using intracellular cytokine staining and MACSPlex. To exclude potentially confounding effects imparted by different levels of transduction, it was strived to achieve comparable  $\Delta$ LNGFR expression levels in all T cell groups intra- and interexperimentally. The frequency of CAR-expressing T cells was equalized before all functional assays and untransduced T cells served as a control for allogeneic reactivity. Following activation with MDA-MB-231 and MCF-7, T cells engineered to express SSEA-4-directed CARs showed degranulation but not untransduced control T cells (Figure 17), demonstrating that the genetically modified T cells acquired specific lytic activity against SSEA-4-positive tumor cells. Intriguingly, despite the difference in the antigenic load between MDA-MB-231 and MCF-7, the frequency of degranulating T cells incorporating the same CAR variant was comparable. Also, T cell groups incorporating the S and L spacer CARs showed near-identical degranulative capacity, although the spacer of both receptors vary by 183 amino acids in length (for comparison: an Immunoglobulin domain is ~70-110 amino acids in length). The XS spacer CAR, however, which is 216 amino acids shorter than the L spacer receptor and 33 amino acids shorter than the S spacer receptor, induced a significantly lower degree of degranulation in T cells compared to the other CAR variants. Consequently, while all 3 chimeric receptors were able to activate degranulation of T cells following SSEA-4 engagement, no direct correlation of receptor potency and spacer length was detectable.

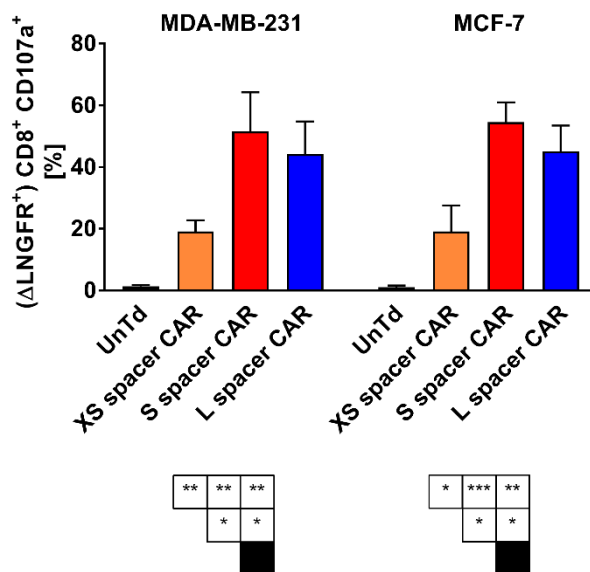


**Figure 17: Degranulation of T cells after stimulation with MDA-MB-231 and MCF-7.** SSEA-4-specific CAR T cells and non-transduced control T cells were co-cultured with the indicated breast cancer cell lines at a ratio of 1:1 and in the presence of fluorochrome-conjugated CD107a mAb. After a 5 hours incubation, CD107a externalization was measured by flow cytometry. Analysis was performed on the CD8<sup>+</sup> population for non-modified control T cells and on the  $\Delta$ LINGFR<sup>+</sup>CD8<sup>+</sup> subset for transgenic T cells. Data represent the average of 4 donors and 3 similar independent experiments.

Since degranulation assays investigate intrinsic T cell properties and allow only analysis of the initial events after T cell stimulation, a live cell imaging-based cell lysis assay was performed to study the cytolytic activity of CAR T cells based on target cell death and for an extended period of time. Dynamic monitoring of CAR T cell cytotoxicity was performed using the IncuCyte<sup>®</sup> S3, an automated imaging system that quantifies cell behavior over time by automatically gathering and analyzing images of cell cultures. As illustrated in Figure 18, all CAR T cell groups showed reactivity against tumor cells, but different SSEA-4 CARs induced different tumor elimination kinetics. In case of MDA-MB-231 as target cell line, XS spacer CAR-expressing T cells only controlled the tumor growth throughout the detection period, but did not eliminate the tumor cells. The most rapid tumor eradication was observed when target cells were treated with S spacer CAR-expressing T cells, while the L spacer CAR T cell group required longer time intervals to reach comparable MDA-MB-231 cell killing. In control groups, the tumor cells remained in an exponential growth phase throughout the experimental period. When MCF-7 were used as target tumor cells, similar functional efficacies were seen. Again, T cells expressing the S spacer CAR were most potent in inducing tumor cell death, followed by L spacer CAR T cells. In contrast to co-cultures with MDA-MB-231, however, the XS spacer CAR T cell group also induced MCF-7 regression although the kinetics were the slowest

among all receptor constructs tested. Noticeably, in the control groups the growth of MCF-7 cells stagnated in the last third of the test period although confluency was not reached. This emphasizes the slow growth kinetics of this cell line upon estrogen removal (assay was performed in TexMACS™ medium without additives).

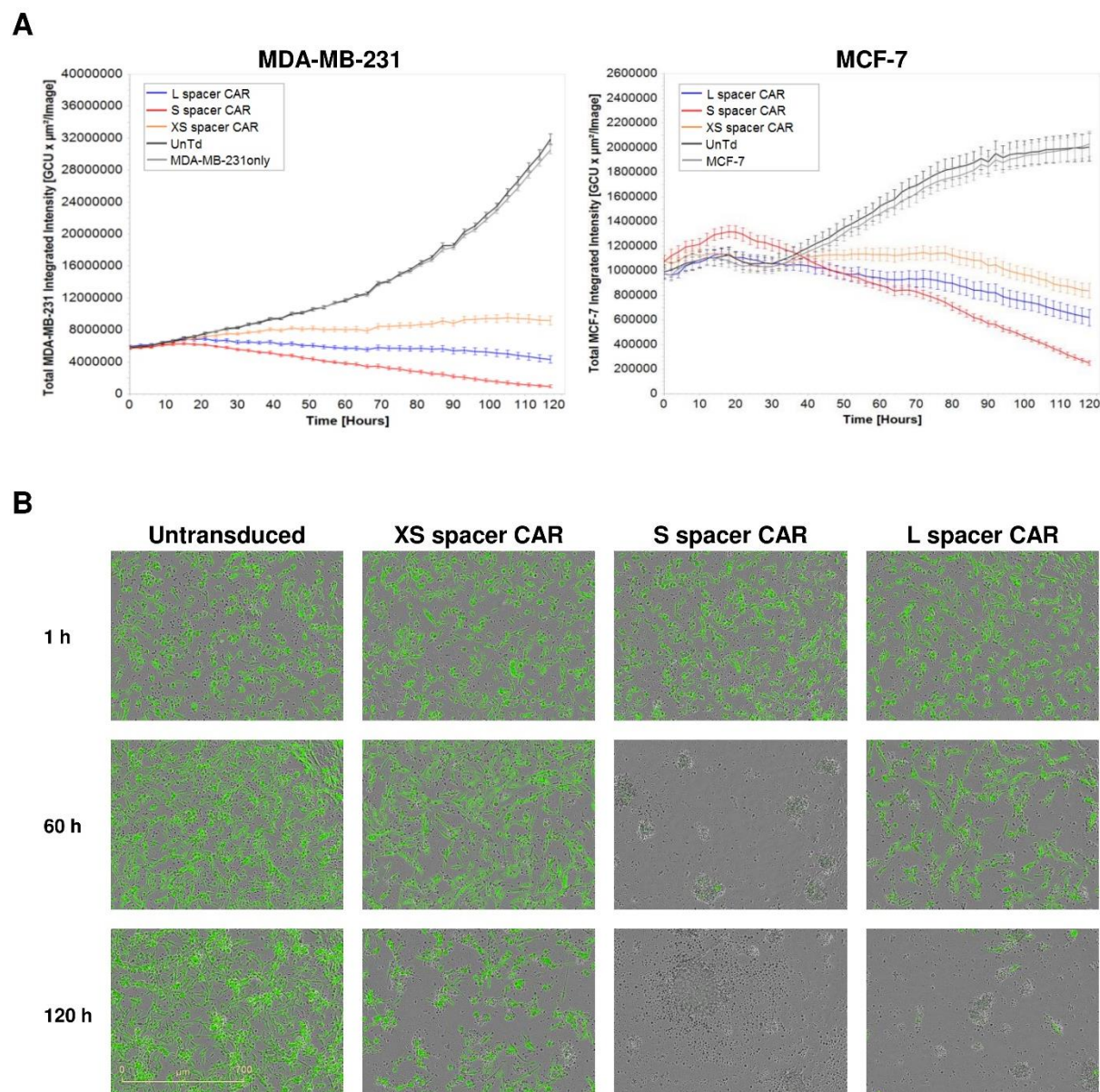


**Figure 18: Dynamic monitoring of CAR T cell-mediated cytotoxicity.** (A) On day 11 after T cell transduction, MDA-MB-231 and MCF-7 cells stably expressing eGFP were co-cultured with different CAR T cell groups at a ratio of 1:1 and fluorescence emission was measured in the IncuCyte® imaging platform for 5 days with 2 hours interval. Untransduced T cells and target cells only served as negative controls. Shown is one representative experiment from 3 separate experiments and 5 donors in total. (B) Sequential images of co-cultured MDA-MB-231 and CAR or control T cells. Green fluorescence represents target cells, while immune cells are not labeled.

In addition to their cytotoxic potential, tumor-activated CAR T cells were tested for their cytokine production and secretion ability. Using the MACSPlex technique, supernatants of

24 hour co-cultures were analyzed for secreted levels of GM-CSF, IFN $\alpha$ , IFN $\gamma$ , IL-2, IL-4, IL-5, IL-6, IL-9, IL-10, IL-12p70, IL-17A, and TNF $\alpha$ . While IL-4, IL-5, IL-6, IL-9, IL-10, IL-12p70, and IL-17A were not detected at significant levels (data not shown), all CAR T cell groups showed increases in GM-CSF, IFN $\gamma$ , IL-2, and TNF $\alpha$  in comparison to non-transduced T cells. Essentially, for both target cell lines a similar efficacy pattern was observed as in the kinetic cell lysis assay with the S spacer CAR being consistently the strongest inducer of T cell effector function. Cytokine levels induced by the L spacer CAR were either comparable or slightly higher to those induced by the S spacer CAR.

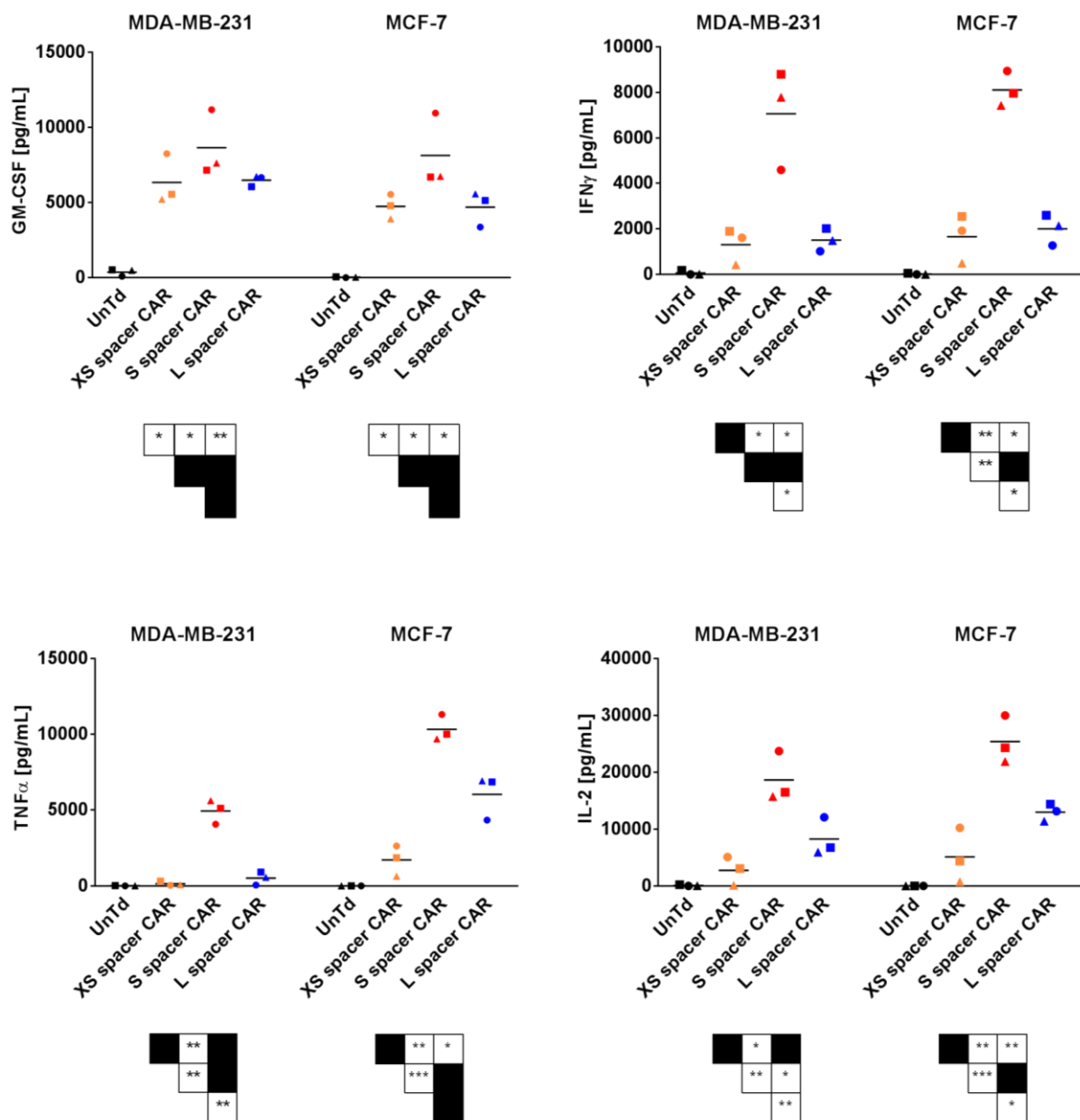


**Figure 19: Cytokine secretion by CAR transduced T cells following antigen stimulation.** On day 11 following transduction, XS, S, and L spacer CAR expressing T cells were cocultured with the indicated cell lines at a ratio of 1:2 for 24 hours and culture supernatants were analyzed for cytokine release using the MACSPlex technique. Cultures of non-modified T cells with tumor cells served to assess the specificity of CAR-mediated lymphocyte response. Results are a summary of 3 independently tested donors.

Of note, when CAR T cells were co-cultured with MCF-7 cells, higher levels of IL-2 and TNF $\alpha$  were detected than for the cohort co-incubated with MDA-MB-231. This is likely due to the fact that the production of these cytokines is most sensitive to PD-1 signaling (Wei et al., 2013) and MDA-MB-231 expresses higher levels of its ligands PD-L1 and PD-L2 than MCF-7 (Figure 20).

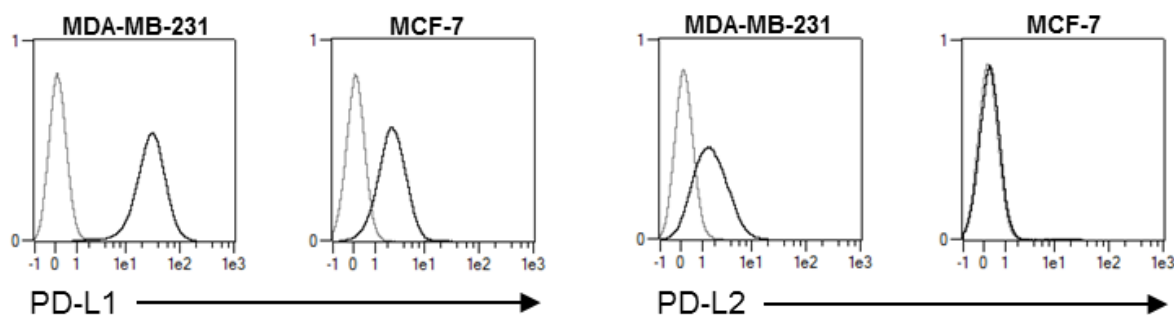


**Figure 20: Expression of PD-L1 and PD-L2 on MDA-MB-231 and MCF-7.** Surface expression was analyzed by flow cytometry when cells reached a confluency of 80%. APC conjugated mAbs were used for antigen detection. Grey line is isotype control and black line is SSEA-4 stain.

It is well established, that T cells which are able to execute several effector functions at the single cell level, called “polyfunctional” T cells, are the key mediators contributing to the development of potent and durable immunity against viral infections or cancer (Almeida et al., 2007; Baitsch et al., 2011; Seder et al., 2008). To evaluate whether the generated SSEA-4-directed CAR variants are able to induce polyfunctionality in modified T cells, analyses on single cell level by intracellular cytokine staining combined with concurrent detection of degranulation was performed following antigen stimulation. SSEA-4-specific CAR T cells were co-incubated with either MDA-MB-231 or MCF-7 and gene-modified degranulating T cells were then analyzed for their ability to simultaneously produce the effector cytokines IFN $\gamma$  and TNF $\alpha$ . The gating strategy applied for analysis is depicted in Figure 21A. As expected, the response of activated CAR T cells was in all groups heterogeneous. Overall, the frequency of cytokine producing cells within the CD107a-positive compartment ranged between 14-40% with TNF $\alpha$  being the predominant cytokine. In the context of this work, polyfunctionality was defined as the ability to degranulate and concurrently produce both IFN $\gamma$  and TNF $\alpha$ . When CAR T cells were stimulated with MDA-MB-231, the lymphocyte group incorporating the S spacer CAR showed the highest frequency of polyfunctional effector cells for both the CD4 $^+$  as well as the CD8 $^+$  subset, while the XS spacer CAR T cell group displayed the lowest frequency. Stimulation with MCF-7, on the other hand, resulted in the XS spacer CAR group showing the highest percentage of CD107a $^+$ TNF $\alpha$  $^+$ IFN $\gamma$  $^+$  T cells, followed by the S spacer CAR followed by the L spacer CAR T cells. However, the data for the XS spacer CAR T cell group needs to be

considered with caution, as the overall frequency of degranulating T cells was comparably low, in this way reducing the statistical power.

Taken together, all 3 CAR spacer variants tested were able to induce cytotoxicity and cytokine production in T cells following SSEA-4 stimulation. The extent of T cell reactivity differed among the different receptor constructs, although no direct correlation of receptor potency and spacer length was observable. The following functional hierarchy from most reactive to least reactive was seen: S spacer CAR > L spacer CAR > XS spacer CAR.

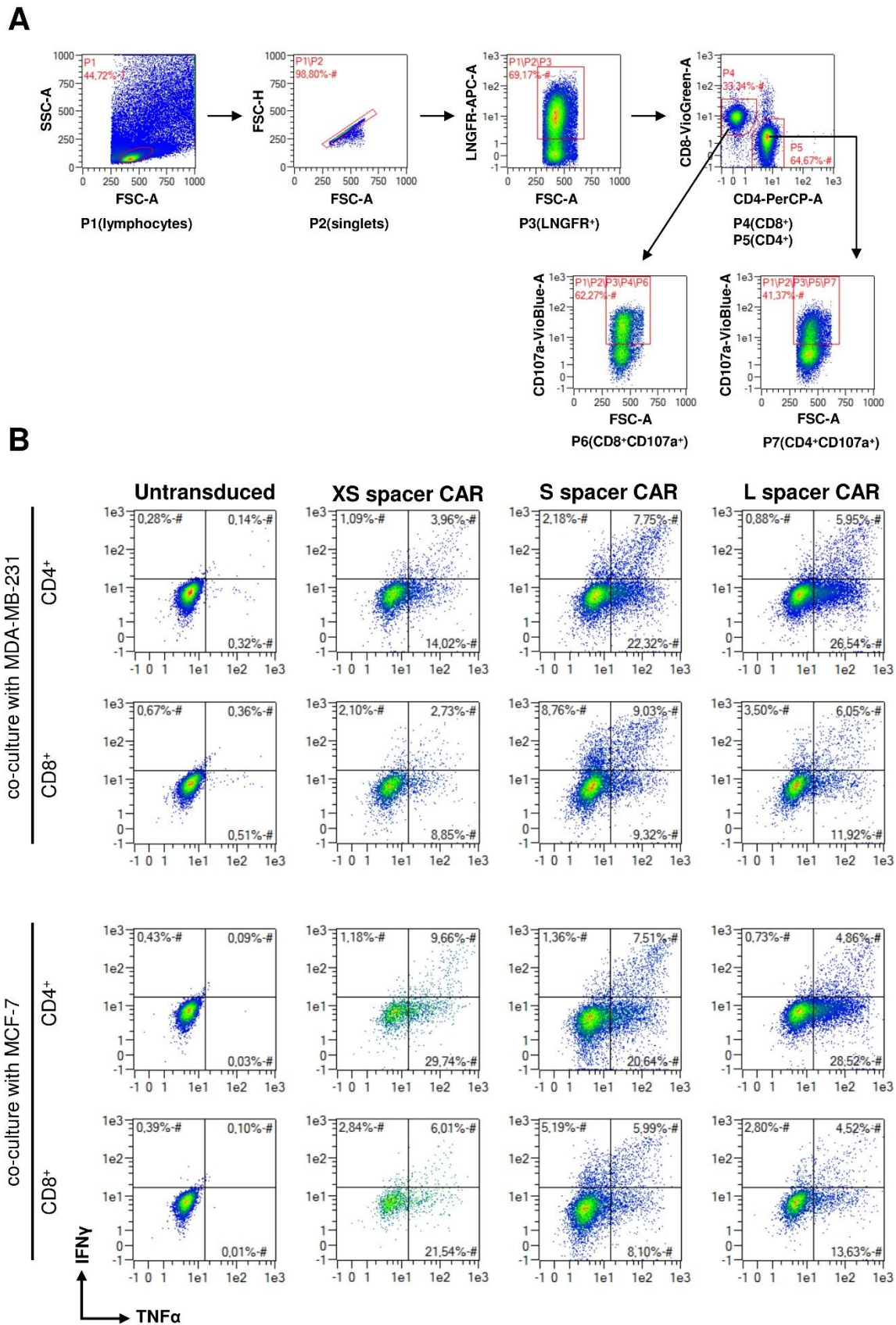


**Figure 21: Heterogeneity of IFN $\gamma$  and TNF $\alpha$  production by cytolytic CAR T cells.** (A) Gating strategy applied to analyze the cytokine production within the CD107a<sup>+</sup> compartment of gene-modified CD4<sup>+</sup> and CD8<sup>+</sup> T cells. (B) IFN $\gamma$  and TNF $\alpha$  production of CD107a<sup>+</sup>CD4<sup>+</sup> and CD107a<sup>+</sup>CD8<sup>+</sup> CAR T cells stimulated with MDA-MB-231 or MCF-7 at a ratio of 1:1. Analysis for non-modified control T cells was performed on the entire CD8<sup>+</sup> and CD4<sup>+</sup> subsets. Representative data for 4 donors and after 5 h of stimulation is shown.

### 3.7 Establishment of *in vivo* tumor xenograft models with MDA-MB-231 and MCF-7

Having confirmed the *in vitro* function of SSEA-4-directed CAR T cells, the next step was to evaluate the *in vivo* activity of these cells in a xenograft model. To determine the appropriate time point for CAR T cell therapeutic intervention, a tumor growth kinetic analysis was first performed. For this purpose, female NSG<sup>TM</sup> mice were inoculated with  $5 \cdot 10^6$  or  $10 \cdot 10^6$  cells of luciferase-GFP-expressing MDA-MB-231 or MCF-7 and from day 7 on, tumor progression was followed 2-3 times weekly for a period of 40 days. Measurements of tumor load were performed by both serial BLI and physical caliper measurements of which a summary is shown in Figure 22A. In general, imaging data correlated to standard external caliper measurements of tumor growth, but BLI permitted earlier detection of tumor progression. This observation was most pronounced for MCF-7. While physical measurements did not show any tumor growth throughout the measurement period, BLI indicated, that in the initial phase, cell proliferation had taken place, but reached a plateau after approximately 28 days. Consequently, optical imaging was considered accurate and therefore appropriate to assess tumor burden in upcoming therapeutic studies. A tumor dose of  $10 \cdot 10^6$  cells was selected for tumor inoculation and day 14 post tumor implantation was chosen as the starting point for CAR T cell therapy, as from this day on the slope of the growth curve remained constant (MCF-7) or kept increasing (MDA-MB-231). *Ex vivo* analysis of two tumor samples per group on day 14 confirmed that no antigen loss occurred during *in vivo* propagation. Indeed, both cell lines retained antigen positivity at levels comparable to their *in vitro* cultured counterparts – irrespective of whether  $5 \cdot 10^6$  or  $10 \cdot 10^6$  cells were injected (Figure 22B, data not shown for  $5 \cdot 10^6$  injected cells). Additionally, histological examination of these tumors for mouse CD31 expression, a marker for blood vessels, showed that extensive vascularization had taken place in MDA-MB-231 but not in MCF-7 tumors. Indeed, while in the first xenograft model, mature blood vessels were already identifiable, the MCF-7 tumor model failed to induce pronounced angiogenesis as indicated by the relatively small puncta-like staining of CD31 in these tumors. This is likely the cause for the observed arrest in MCF-7 tumor growth. Since proper tumor vascularization is a prerequisite to allow systemically administered CAR T cells to efficiently traffic to the tumor sites, the MCF-7 tumor xenograft model was deselected from upcoming *in vivo* CAR T cell functionality studies. Consequently, only the MDA-MB-231 tumor model was used as a target for the therapeutic evaluation of SSEA-4-redirected T cells *in vivo*.

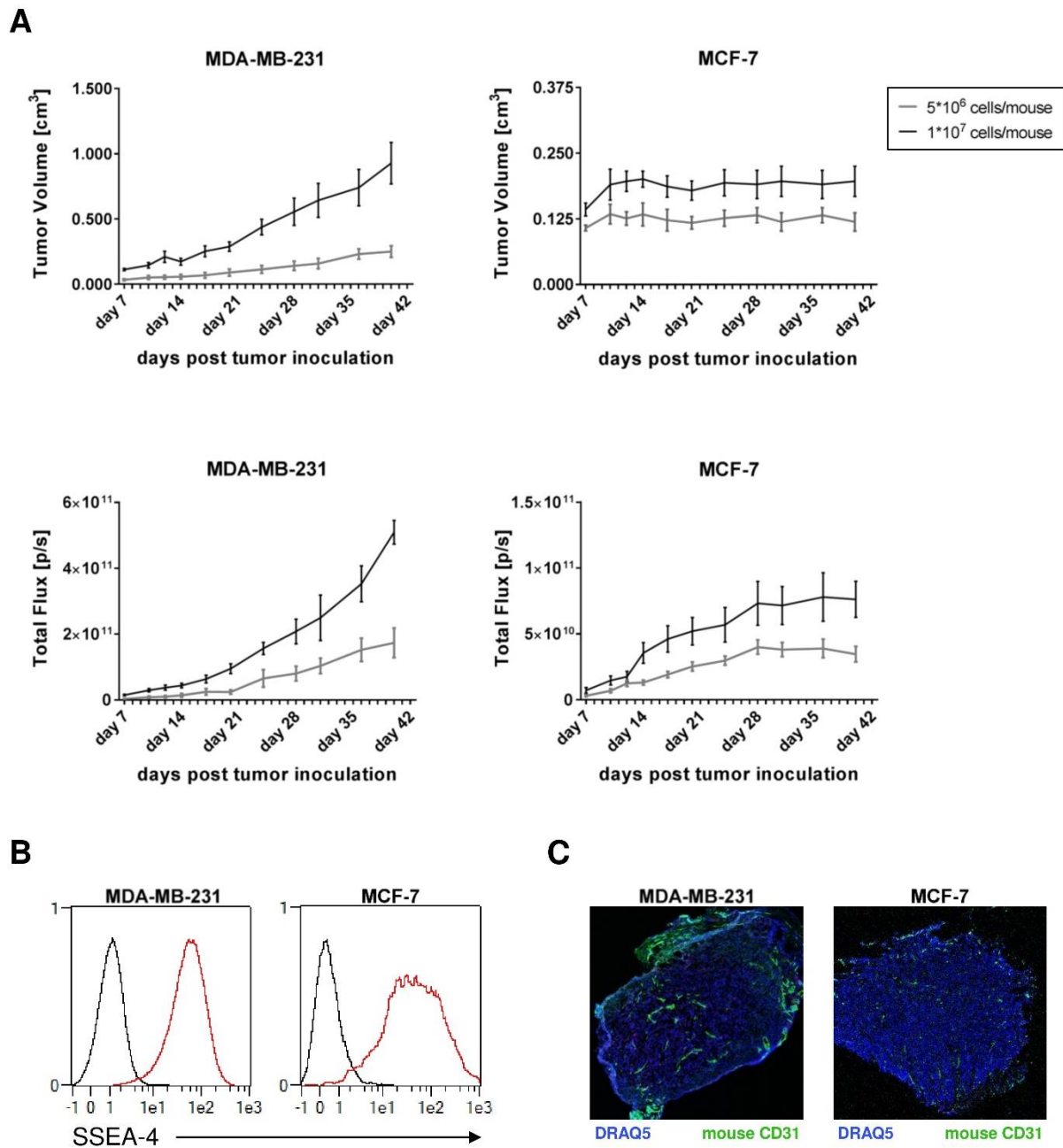


**Figure 22: Characterization of MDA-MB-231 and MCF-7 tumor growth in subcutaneous xenograft models.** (A) *In vivo* tumor growth curves of MDA-MB-231 and MCF-7. Female NSG<sup>TM</sup> mice were injected s.c. with either 5·10<sup>6</sup> or 10·10<sup>6</sup> tumor cells stably expressing luciferase and progression of tumor growth was monitored in 2-4 day intervals by physical caliper measurements and BLI (n=5-6 for each MDA-MB-231 group and n=12-13 for each MCF-7 group). On the day of tumor inoculation, MCF-7 injected mice were additionally supplemented s.c. with estrogen pellets to support tumor growth. Data are presented as means ± SEM. (B) SSEA-4 expression by MDA-MB-231 and MCF-7 after *in vivo* propagation. Following 14 days of *in vivo* expansion, tumors were removed, dissociated and single cell suspensions were analyzed for SSEA-4 expression by flow cytometry. Red line points out SSEA-4 labeling by APC-conjugated mAb, while black line represents staining with isotype-matched control antibody. Data shown is from the cohorts injected with 10<sup>7</sup> tumor cells and representative for two tumors analyzed per group. (C) Immunofluorescent analysis of tumor angiogenesis by pan endothelial marker CD31 (green). DRAQ5 (blue) was used to visualize cell nuclei. Images are derived from tumors initiated with 10<sup>7</sup> cells and representative for two tumors analyzed per group.

### 3.8 Functional *in vivo* characterization of SSEA-4 directed XS, S, and L spacer CAR T cells

To assess the *in vivo* therapeutic potential of SSEA-4-redirected XS, S, and L spacer CAR T cells, NSG™ mice were implanted s.c. with  $1 \cdot 10^7$  luciferase-GFP-expressing MDA-MB-231 tumors and 14 days later a single dose of  $2 \cdot 10^6$  of the respective CAR T cells was administered systemically. All T cell products had been previously enriched for  $\Delta$ LNFR as described in 2.2.2.12. For the control group receiving untransduced immune cells, T cell doses were adjusted to the highest total cell number administered among the different CAR T cell cohorts. During the therapeutic treatment, tumor burden and CAR T cell frequency in peripheral blood were analyzed weekly by BLI and flow cytometry, respectively (Figure 23A). As evident in Figure 23B, XS and L spacer CAR T cell therapy mediated no anti-tumor effect and only mice that had received S spacer CAR T cells experienced a reduction in tumor growth as compared with the control group treated with untransduced lymphocytes ( $p=0.079$ ). However, on day 16 following therapy start, the latter cohort required euthanasia due to severe morbidity symptoms such as ruffled fur, hunched body posture, lack of motility, and weight loss (Figure 23C). Notably, the pattern of body weight loss observed in the S spacer CAR-treated group (Figure 23C) inversely correlated with the pattern of CAR T cell infiltration in peripheral blood (Figure 24) suggesting that proliferation of the cellular product had been occurring and further promoted toxicity.

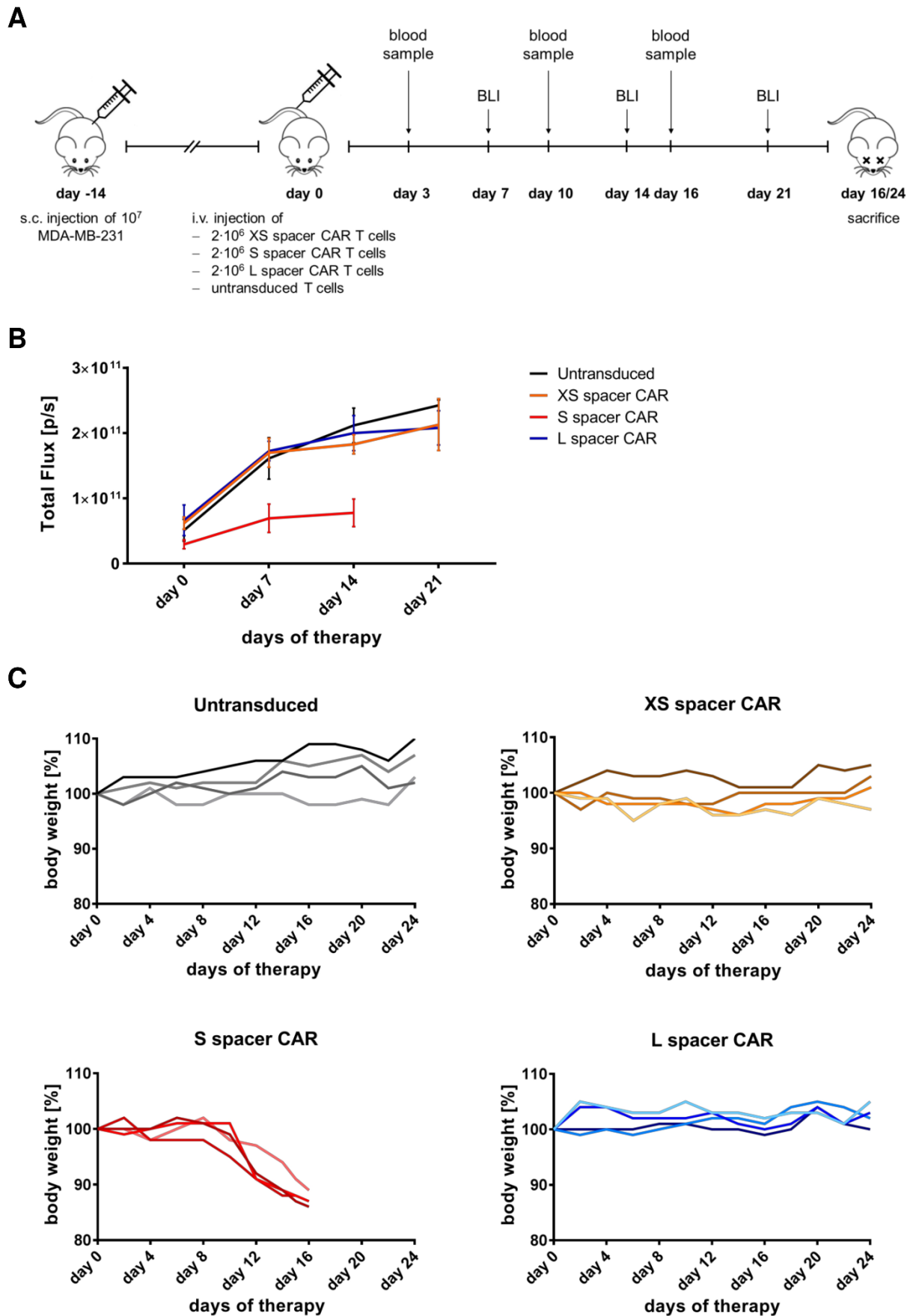


**Figure 23: In vivo activity of SSEA-4-directed CAR T cells.** (A) Outline of the experimental design to study the therapeutic potential of XS, S, and L spacer CAR T cells in a subcutaneous xenograft model. Female NSG<sup>TM</sup> mice injected s.c. with MDA-MD-231 tumors on day -14 were therapeutically treated with untransduced or XS, S, or L

spacer CAR T cells on day 0 and subsequently subjected to blood analysis and BLI according to the schedule shown. Study endpoint for each group was defined by tumor reaching 1 cm in any direction, more than 20% weight loss, lack of motility or a combination thereof. For the S spacer CAR T cell-treated group, humane endpoint criteria were generally reached on day 16 and for the remaining cohorts on day 24. (B) Mean growth of s.c. MDA-MB-231 tumors in the 4 cohorts as determined by BLI over time. Error bars represent SEM. (C) Body weight development of mice treated with untransduced or XS, S, or L spacer CAR T cells throughout the therapeutic period (4 mice per group; each line represents one mouse). Similar results were seen in mice treated with  $1 \cdot 10^7$  SSEA-4 CAR T cells.

By contrast, XS and L spacer CAR T cell-treated mouse cohorts did not display body weight reduction during therapeutic treatment (Figure 23C) and an increase of peripheral blood infiltration by transgenic T cells was observed only for the L spacer CAR group – although the proliferative capacity was less pronounced than for S spacer CAR-expressing T cells (Figure 24). Collectively, targeting SSEA-4 *in vivo* by CAR T cells generally mediated weak anti-tumor effects at best and efficacy was associated with CAR T cell proliferation, but also with adverse events.

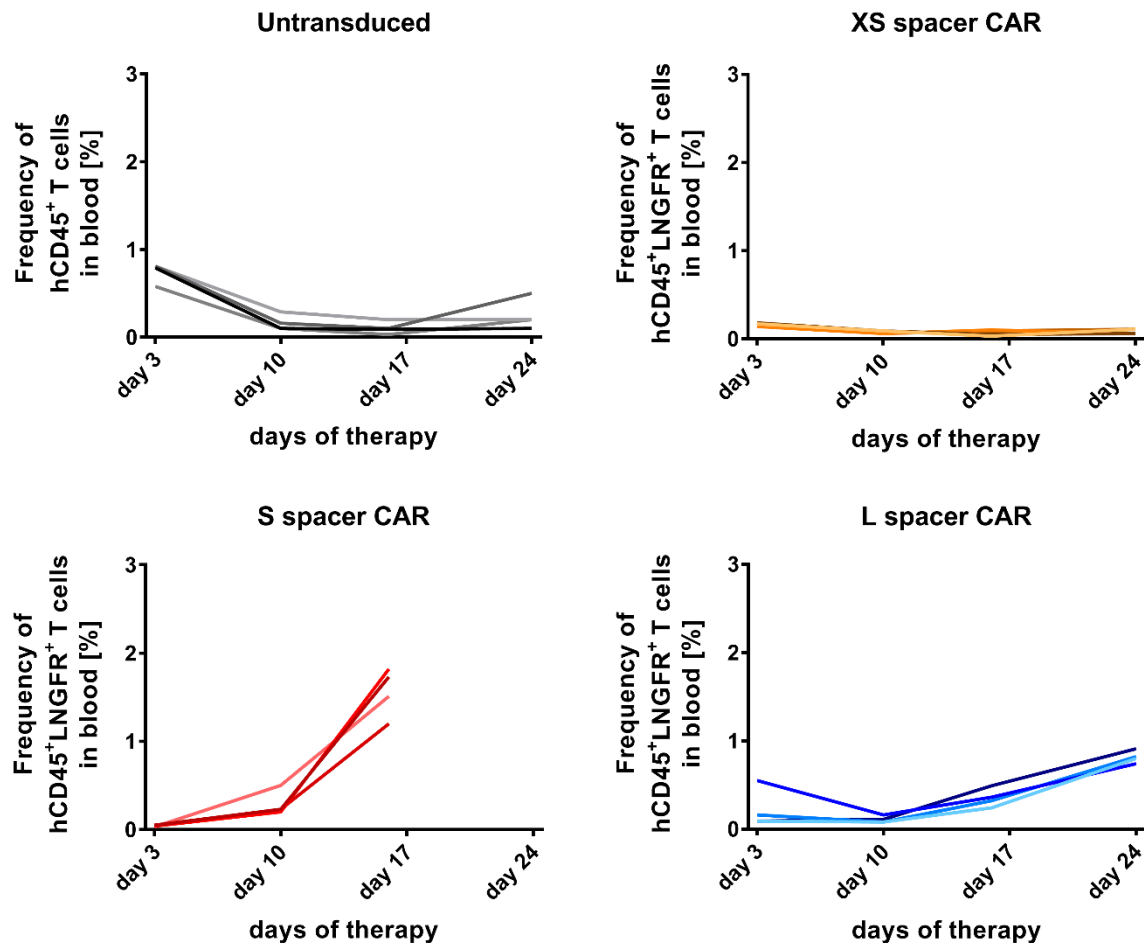


**Figure 24: Frequency of CAR (human CD45 $\Delta$ LNGFR $^+$ ) and untransduced (human CD45 $^+$ ) control T cells in mouse peripheral blood over the course of therapy.** Female NSG<sup>TM</sup> mice with established s.c. MDA-MB-231 tumors were injected i.v. with  $2 \cdot 10^6$  XS, S, and L spacer CAR T cells and starting day 3 post adoptive transfer their frequency in peripheral blood was monitored by flow cytometry. For injection of untransduced control T cells, cell number was adjusted to the highest total T cell number injected in the CAR T cell groups. Each line represents one mouse.

When mice cohorts reached the humane experimental endpoint, in addition to blood, bone marrow, spleen, lung, and liver were subjected to flow cytometric analysis for CAR T cell infiltration. Initially, tumor samples were included in analysis, but the low cell viability upon dissociation (~25-33%) as well as the strong GFP signal spreading in all flow cytometric channels yielded unreliable data for interpretation (data not shown).

As illustrated in Figure 25, a significant and large increase in transgenic cells was found in blood and all four organs of mice treated with S spacer CAR T cells compared to the cohort receiving untransduced control T cells. The pronounced bioactivity of these cells was in strong contrast to XS spacer CAR T cells, for which no significant *in vivo* proliferation was seen in any of the organs. Altogether, it appeared that XS spacer CAR T cells were inert to activation. Intriguingly, for the L spacer CAR T cell group, a significant expansion was observed only in the lung, indicating that the cells are either partially retained and activated for proliferation or retraffic to the pulmonary organ from the system.

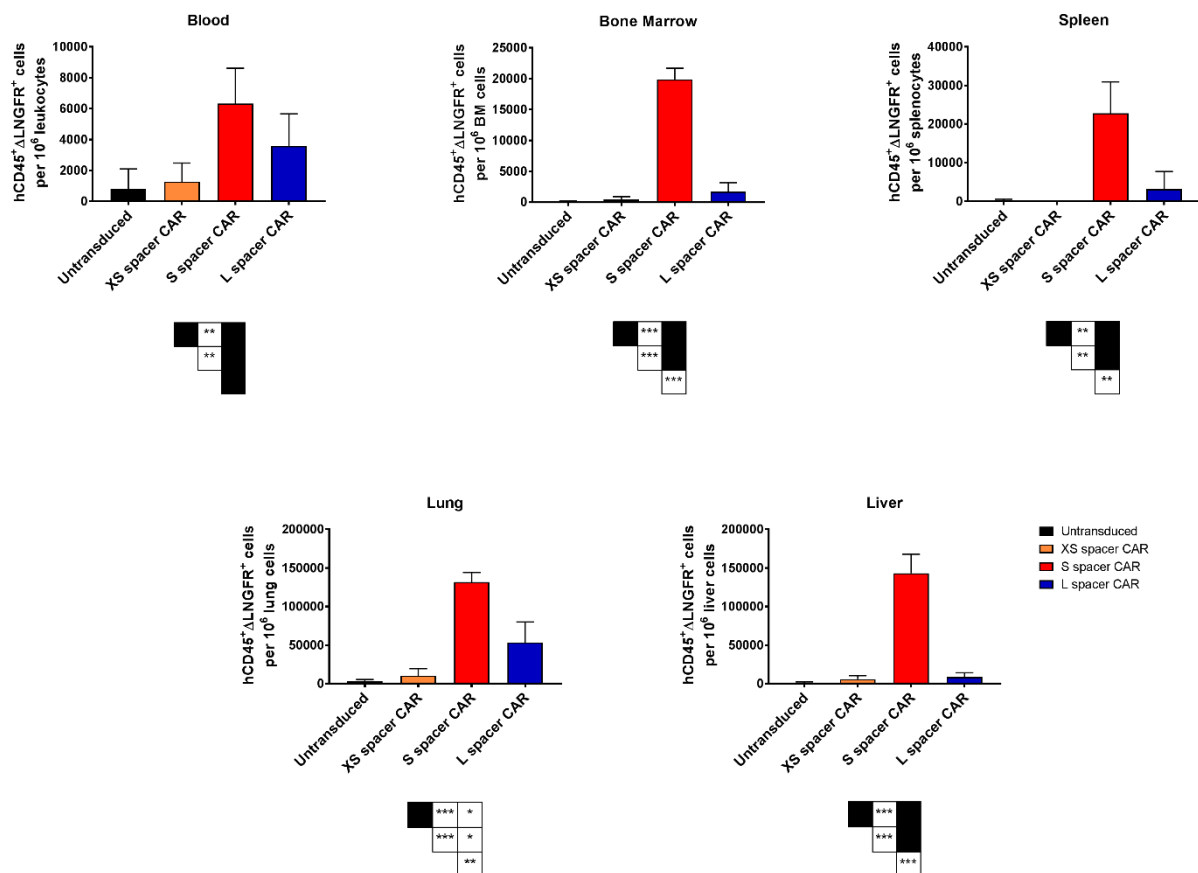


**Figure 25: Organ infiltration by CAR-expressing or untransduced control T cells.** Upon reaching humane endpoint criteria, blood samples were collected and mice were euthanized directly thereafter. Bone marrow, spleen, lung, and liver were collected, processed into single cell suspensions and stained with mAbs for enumeration of human T cell by flow cytometry. For analysis only viable single cells were considered. Plots indicate mean frequency + SD of human CD45<sup>+</sup> (untransduced control) or CD45<sup>+</sup>ΔLNGFR<sup>+</sup> (CAR-expressing) T cells per million cells as measured by flow cytometry of each homogenized organ (n=4).

### 3.9 Characterization of the *in vivo* toxicities mediated by SSEA-4-directed CAR T cells

To understand whether the observed toxicities in the S spacer CAR T cell treated mouse cohort were related to an anti-tumor response or resulted from on target/off tumor recognition, tumor-free NSG™ mice were adoptively transferred with high dose ( $1 \cdot 10^7$ ) XS, S, or L spacer CAR-expressing T cells or untransduced control lymphocytes and toxicity was evaluated via clinical symptoms. Strikingly, adverse events were observed in all cohorts receiving SSEA-4-directed therapy, although different CAR T cells displayed a distinct hierarchy of severity. For the S spacer CAR T cell-treated group, significant toxicity (ruffled fur, hunched posture, tremor, reduced motility) was observed already within a few hours of adoptive transfer and was further accompanied by body weight loss of almost 0.7 g/day. On day 6 following CAR T cell infusion, the mice eventually required euthanasia (Figure 26).

The L spacer CAR-treated mouse cohort showed intermediate levels of toxicity symptoms which appeared several days after adoptive transfer. Initially, the decrease in body weight was mild, but became more pronounced between day 5 and 10. Humane endpoint criteria were reached by day 14 (Figure 26).

Treatment with XS spacer CAR T cells did not display any overt clinical symptoms such as changes in body posture or fur. The body weight dropped only slightly in the first 2-4 days but stabilized thereafter. Despite the reduced severity of adverse events, SSEA-4-directed treatment was lethal in all animals and the mice naturally succumbed to therapy by day 16 (Figure 26).

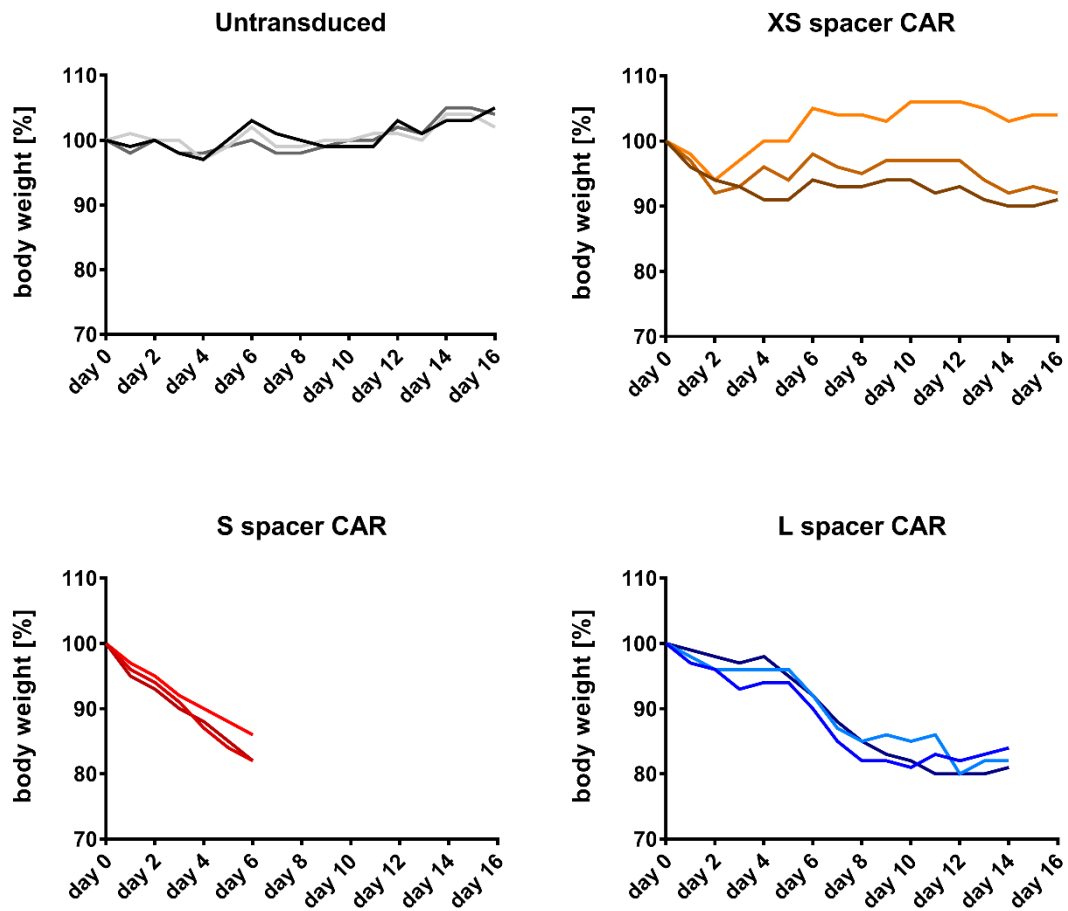


**Figure 26: Body weight development in tumor-free NSG<sup>TM</sup> mice following adoptive transfer of SSEA-4-directed CAR T cells.** Naïve NSG<sup>TM</sup> mice were treated systemically with  $1 \cdot 10^7$  XS, S, or L spacer CAR T cells and body weight development was monitored. For injection of untransduced control T cells, cell number was adjusted to the highest total T cell number injected in the CAR T cell groups.

In addition to physical symptoms, all mouse cohorts receiving SSEA-4-directed CAR T cell therapy showed significantly elevated serum levels of human IFN $\gamma$ . Moreover, the S spacer CAR T cell-treated group exhibited significant increases of human IL-2 and TNF $\alpha$  in peripheral blood (Figure 26). Overall, these data indicated that significant and dangerous on target/off tumor toxicity occurred upon targeting SSEA-4 *in vivo*.

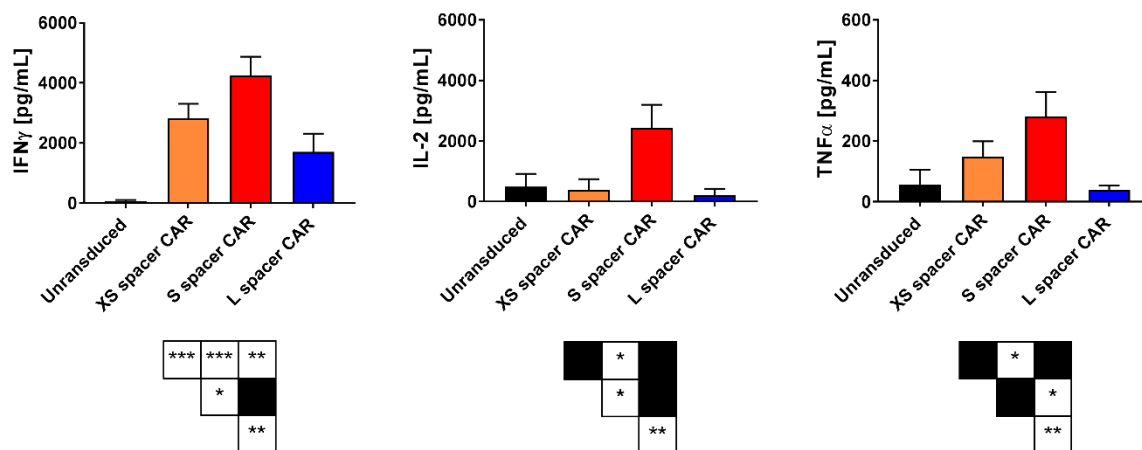


**Figure 26: Blood serum levels of human IFN $\gamma$ , IL-2, and TNF $\alpha$  in NSG<sup>TM</sup> mice.** Non-tumor-bearing NSG<sup>TM</sup> mice were adoptively transferred with  $1 \cdot 10^7$  XS, S, or L spacer CAR T cells or untransduced control T lymphocytes and 6 days later, blood samples were analyzed for the presence of human cytokines as stated in the diagrams (n=3 mice per group).

To investigate the pathology elicited by SSEA-4-directed CAR T cell treatment, formalin preserved internal organs of S spacer CAR and untransduced control T cell-treated mice were subjected to an examination by a pathologist blinded to the treatment conditions. No obvious differences in tissue and organ structure between the groups were detected by him. In an alternative attempt to locate the major sites of on target/off tumor toxicity, bioinformatical expression analysis of the enzyme catalyzing the final step in SSEA-4 synthesis (CMP-*N*-acetylneuraminatate- $\beta$ -galactosamide- $\alpha$ -2,3-sialyltransferase 2, ST3GAL2) was performed by using data derived from The Human Protein Atlas (<https://www.proteinatlas.org>). However, ST3GAL2 showed relatively broad tissue distribution and did not correlate with SSEA-4 expression (data not shown). Therefore, differences in CAR T cell activity between distinct organs were investigated. Small intestine, colon, kidneys, ovaries and stomach were excluded from analysis due to no detection of human T cell infiltrates and although a presence of S spacer CAR T cells was identified in brain and skin, the total human lymphocyte amount in these organs was too low for investigative purposes. For this reason, the primary focus was laid on blood, liver, lung, spleen and bone marrow. Strikingly, compared to human lymphocyte infiltrates in blood, liver and spleen, the bone marrow- and lung-resident CAR T cells exhibited higher levels of  $\Delta$ LNGFR expression as determined by median fluorescence intensity (FI) (Figure 28A). Taking into consideration that transgene transfer had occurred into actively proliferating T cells that had undergone CD3/CD28-stimulated chromatin rearrangement, it was hypothesized that gene integration was favored at genomic sites that are decondensed during proliferation. When T cells return to steady state, the sites are partially recondensed.

However, antigen recognition-triggered CAR T cell proliferation would reopen these sites thus inducing enhanced transgene transcription.

To test whether lung and bone marrow were sites of active CAR T cell proliferation, S spacer CAR or untransduced control T cells were lentivirally engineered to express GFP-luciferase (transduction efficiency 82%) and  $2 \cdot 10^6$  CAR or untransduced T cells were injected i.v. into tumor-free NSG<sup>TM</sup> mice. Thereafter, the luciferin signal was examined regularly over a course of 3 days. Immediately after adoptive transfer, CAR and control T cells trafficked to the lung, where they were retained for several hours. With progressing observation time, however, control T cells left the organ and distributed throughout the mouse body resulting in the loss of a localized luciferin signal. Overall, no proliferation of these cells was detectable. In case of S spacer CAR T cells, however, a fraction of lymphocytes remained retained in the lung and the luciferin signal continuously increased over time indicating active proliferation of the cells was taking place. Moreover, a separate luciferin signal became evident in the bone marrow and exhibited the strongest growth rate (Figure 28B). Thus, it was concluded that lung and bone marrow were the primary sites of CAR T cell proliferation. Analysis of PD-1 expression by T cells infiltrating bone marrow, lung, spleen, and liver further confirmed that CAR T cell expansion was driven by antigen recognition. While in all organs analyzed, untransduced T cells showed only minimal PD-1 expression, CAR T cells significantly upregulated the activation marker and the biggest difference to baseline PD-1 expression in untransduced control T cells was observed in lung and bone marrow. Taken together, the data suggested that bone marrow and lung were the primary sites of on target/off tumor recognition by SSEA-4-directed CAR T cells.

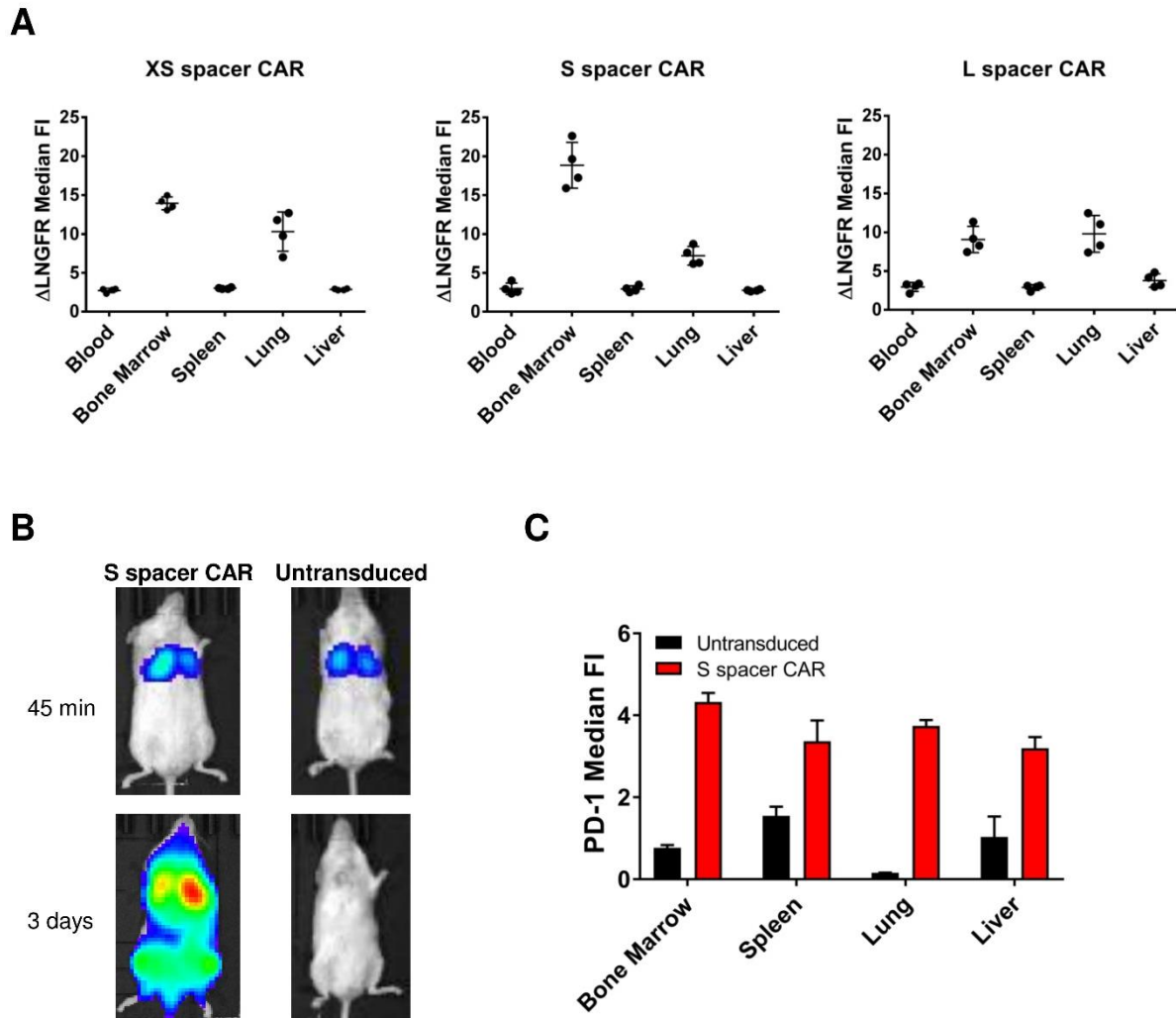


**Figure 28: Localization of SSEA-4-CAR T cell activity following adoptive transfer in NSG<sup>TM</sup> mice.** (A) Median Fluorescent Intensity (FI) of  $\Delta$ LNGFR expression by gene-modified T cells infiltrating different organs. Sixteen (S spacer CAR) or twenty-four (XS and L spacer CAR) days after intravenous CAR T cell administration into NSG<sup>TM</sup> mice, blood, bone marrow, spleen, lung, and liver of the animals were harvested, dissociated to single cell suspensions and  $\Delta$ LNGFR expression was evaluated by flow cytometry. For analysis, gating was performed on viable human CD45<sup>+</sup> single cells expressing  $\Delta$ LNGFR (n=4 mice per group). (B) *In vivo* BLI of T cell trafficking and proliferation. Luciferase-expressing mock and CAR (S spacer) T cells were injected intravenously into NSG<sup>TM</sup> mice and their biodistribution was analyzed at indicated time-points post infusion. Images are representative for two mice analyzed per group. (C) Median Fluorescent Intensity (FI) of PD-1 expression by untransduced and S spacer CAR-transduced T cells infiltrating different organs. Three days after adoptive transfer of T cells in NSG<sup>TM</sup> mice, bone marrow, spleen, lung, and liver were excised, processed into a single-cell suspension and PD-1 expression of the infiltrating human immune cells was analyzed by flow cytometry. For transduced cells, gating was performed on viable human CD45<sup>+</sup>  $\Delta$ LNGFR<sup>+</sup> singlets; for untransduced cells, viable human CD45<sup>+</sup> single cells were considered in the analysis (n=4 mice per group).

### 3.9.1 Identification of SSEA-4-expressing cells in bone marrow

The enhanced proliferation as well as PD-1 expression by CAR T cells in bone marrow suggested that SSEA-4-directed therapy targeted some aspect of bone. Indeed, the total cell number of live bone marrow cells isolated from the femurs and tibias of mice treated with  $1 \cdot 10^7$  SSEA-4-directed (S spacer) CAR T cells was significantly diminished compared to mice treated

with equal numbers of untransduced control T cells (Figure 29A). In addition, SSEA-4-directed treatment led to a distortion of the mouse CD45<sup>+</sup>:CD45<sup>-</sup> ratio within the lineage-negative bone marrow compartment and was associated with strong decrease of mouse CD45<sup>+</sup> cells (Figure 29B) as well as a loss of the CD45<sup>+</sup>Sca-1<sup>bright</sup> population (Figure 29C). Given that SSEA-4 is not expressed by lineage-positive bone marrow cells and encompasses ~0.03% of the lineage-negative compartment (Figure 29D), it was hypothesized that the glycolipid is restrictively produced by hematopoietic progenitor cells. As expected, SSEA-4-positive cells were markedly enriched for co-expression of CD117 and Sca-1 (Figure 29E) which is characteristic for undifferentiated cells (Brown et al., 2015). Besides, expression of CD34, CD48, CD135, and CD150 by the SSEA-4<sup>+</sup>Lin<sup>-</sup>Sca-1<sup>+</sup>CD117<sup>+</sup> population more specifically identified the subset as multipotent progenitor cells (MPPs) (Figure 29F). Further evidence that SSEA-4-directed treatment affected MPP homeostasis was provided by the observation that following CAR treatment, a significantly reduced frequency of low differentiated CD48<sup>high</sup> cells, the ultimate descendent of short-term hematopoietic stem cells (Figure 29F), was observed. While in mice treated with untransduced control T cells the CD48<sup>high</sup> population constituted around 40-48% of the Lin<sup>-</sup>CD45<sup>+</sup>Sca-1<sup>+</sup>CD117<sup>+</sup> compartment, in mice receiving SSEA-4-directed CAR T cell therapy this population dropped to 27-33% (Figure 29G, H).

Importantly, expression of SSEA-4 was also assessed on human CD34<sup>+</sup>CD38<sup>+</sup> cells derived from mobilized stem cell apheresis products of healthy donors (Figure 29I). Around 30 out of 1·10<sup>6</sup> cells were shown to be positive for the glycolipid and although this frequency is drastically low, the mere presence of SSEA-4-expressing hematopoietic progenitor cells poses a high risk that similar adverse events may be observed in SSEA-4-directed treatment modalities for humans as were seen in mice.

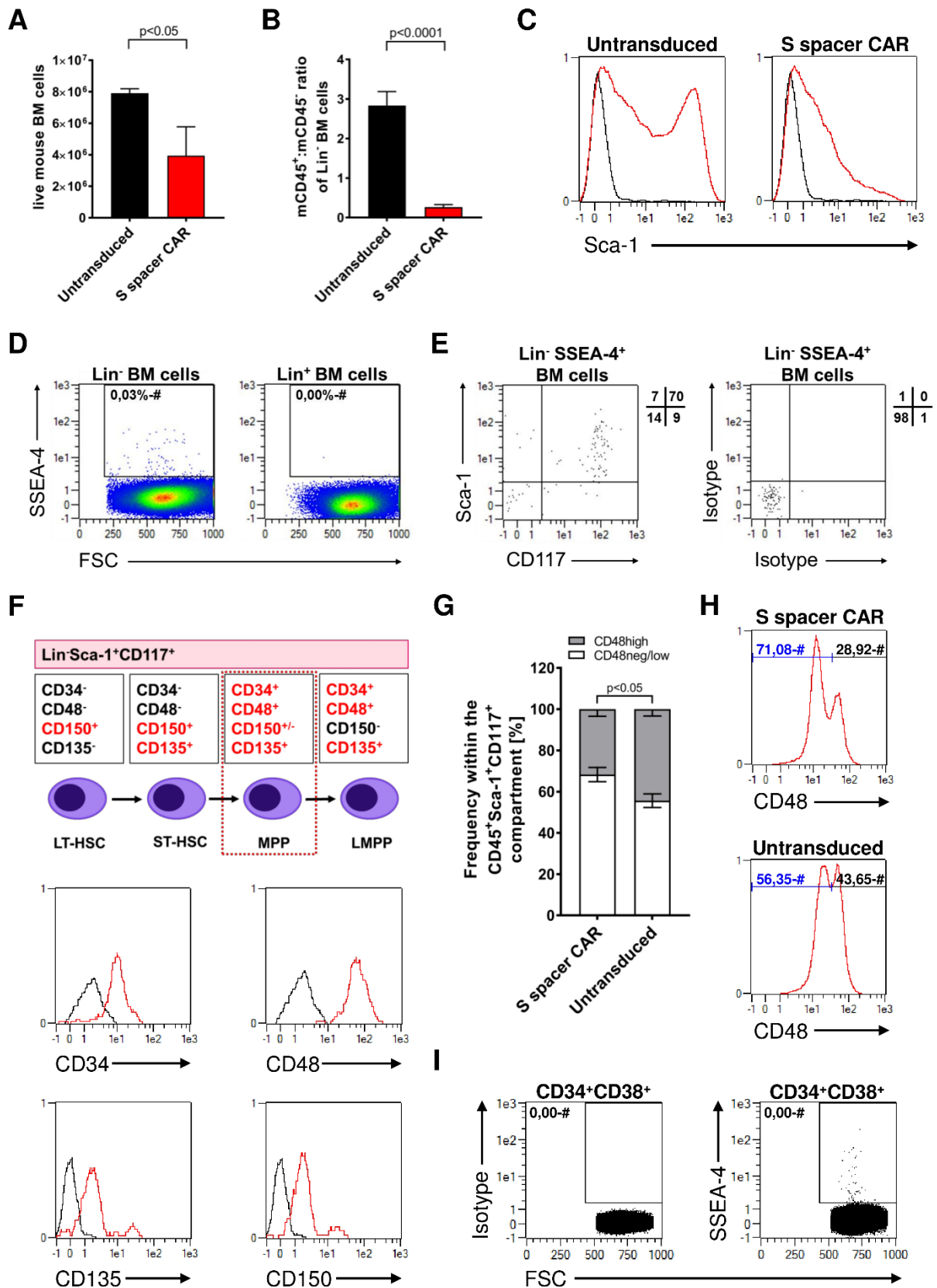


**Figure 27: Bone marrow toxicity following SSEA-4 CAR T cell therapy and phenotypic characterization of bone marrow-resident SSEA-4-expressing cells.** (A) Total bone marrow cell count following treatment with SSEA-4-directed CAR or untransduced control T cell. NSG<sup>TM</sup> mice were treated with  $1 \cdot 10^7$  S spacer CAR-expressing T cells and 3 days later total bone marrow cell number was determined. Control group was treated with untransduced T cells and the administered dose was adjusted to the total cell number used in the CAR T cell group. Data are the average number of cells from the femurs and tibiae of one mouse ( $n=5$  mice per group). (B) Mouse

CD45<sup>+</sup>:mouse CD45<sup>-</sup> ratio of lineage-negative bone marrow cells after therapy. For analysis, only viable single cells were considered and lineage-positive mouse cells were excluded by Ter119<sup>-</sup>, CD5<sup>-</sup>, CD11b<sup>-</sup>, Gr-1<sup>-</sup>, Ly6B<sup>-</sup>, and CD45R-directed mAbs, all conjugated to the same fluorochrome. Therapeutic T cells were excluded by human CD45-labeling. (C) Sca-1-expression in the CD45<sup>+</sup>Lin<sup>-</sup> bone marrow compartment after therapy. Viable single cells were preselected for analysis. The black line represents isotype control and the red line Sca-1 staining. Histograms are representative for 5 samples per group. (D) SSEA-4-expression by lineage-negative and lineage-positive bone marrow cells of untreated NSG<sup>TM</sup> mice. Data are representative for 3 bone marrow samples analyzed. (E) Analysis of Sca-1 and CD117 expression by lineage-negative, SSEA-4-positive bone marrow cells. Numbers in quadrants next to the dot plot represent percentages of positive cells within the respective dot plot quadrant. (F) Subcharacterization of SSEA-4-expressing Lin<sup>-</sup>Sca-1<sup>+</sup>CD117<sup>+</sup> (LSK) cells based on CD34, CD48, CD135, and CD150 expression. Isotype staining is represented by the black line and antigen staining by the red line. (G) Proportion of CD48<sup>high</sup> versus CD48<sup>neg/low</sup> population within the LSK compartment after treatment (n=4 mice per group). (H) Representative histograms for CD48 expression by the LSK compartment after S spacer CAR or untransduced control T cell treatment. (I) Expression of SSEA-4 by human CD34<sup>+</sup>CD38<sup>+</sup> progenitor cells mobilized into peripheral blood. Data is representative for two donors analyzed.

### 3.9.2 Identification of SSEA-4-expressing cells in lung

A novel study has recently described the lung as a second site of hematopoietic activities and a niche for hematopoietic progenitor cells (Lefrançois et al., 2017). Therefore, it was hypothesized that the target population of SSEA-4-directed CAR T cells in the lung may also consist of MPPs – as in bone marrow. To address this, lungs of untreated NSG<sup>TM</sup> mice were processed into single cell suspensions and SSEA-4 expression was analyzed on the CD45-positive and CD45-negative cell subset. Consistent with the findings for bone marrow, the overall frequency of cells expressing the glycolipid was very low, ranging typically between 0.3-0.6%. However, contrary to the expectations, the major antigen signal was located within the CD45-negative compartment (Figure 30A) indicating that the main target population in the lung differed and was not made up of MPPs. To identify the SSEA-4-expressing subset, an antibody screening based on a library of 29 antibodies comprising phenotypic cell surface markers was performed. For this purpose, lung tissue derived from untreated NSG<sup>TM</sup> mice was dissociated into single-cell suspensions and the SSEA-4-positive cell population was characterized for the expression of the selected markers. According to the labeling pattern, each antigen was classified into either no staining (<10% of cells positive), partial staining with two discrete populations, partial staining with a smear of positive cells, and full staining (>90% of cells positive) (Figure 30B). Intriguingly, only 3 markers showed an expression in less than 10% of cells (CD45, CD138, Gr-1) and a partial staining pattern was observed for 22 antigens indicating cellular heterogeneity within the SSEA-4-positive subset. Positivity for CD98 and CD81 in 75% and >90% of cells, respectively, was not indicative as these molecules show a broad cellular distribution and functional versatility (Cantor and Ginsberg, 2012; Levy, 2014; Vences-Catalán et al., 2017). However, co-expression of CD44 by >90% of SSEA-4-positive cells revealed an epithelial origin and co-staining for Prominin-1 (>90% of cells) suggested a low differentiation status. Thus, it was concluded that SSEA-4 expression in lung tissue is mainly restricted to epithelial progenitor cells.

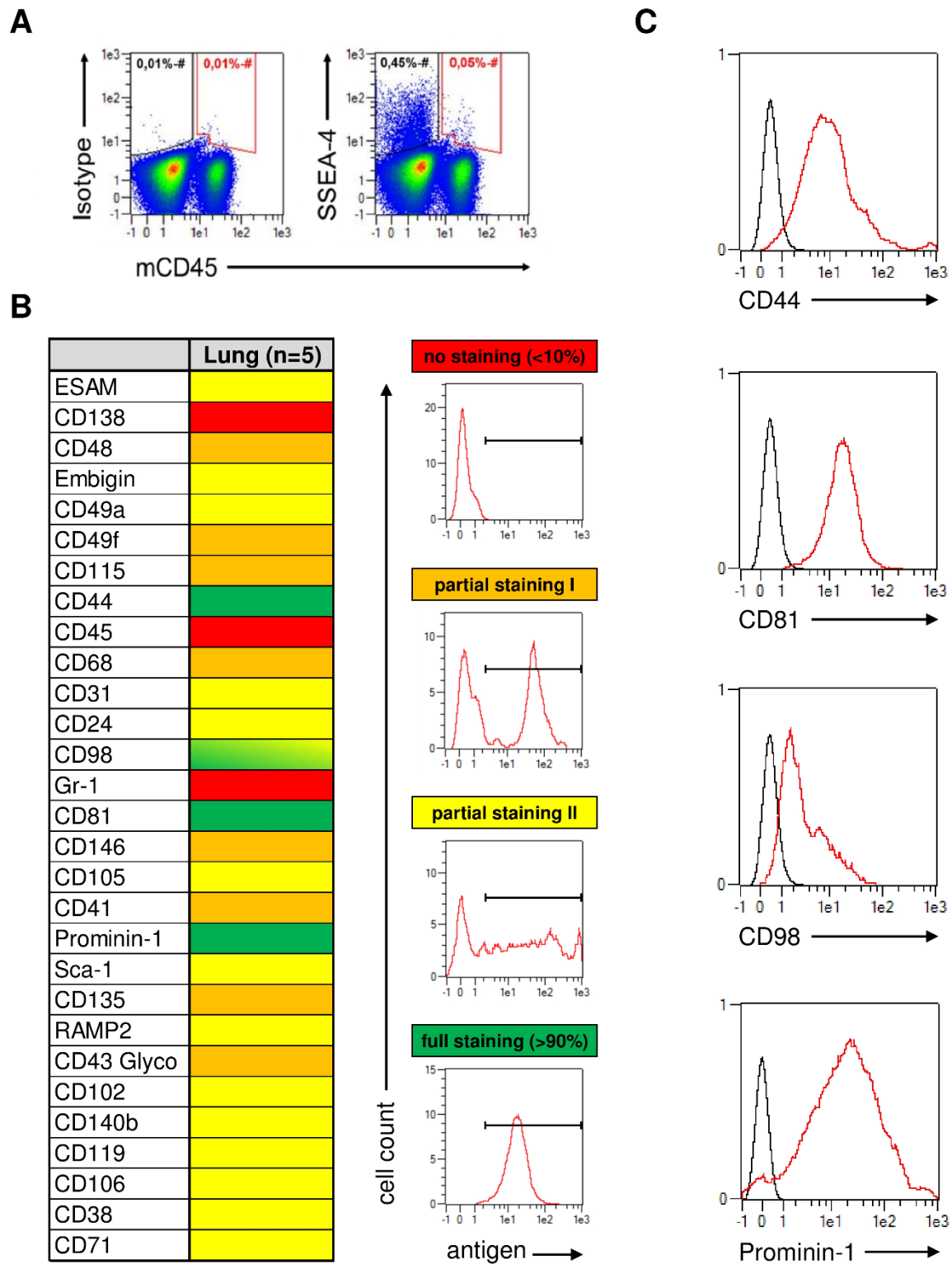


**Figure 30: Phenotypic characterization of SSEA-4-expressing cells in lung tissue.** (A) Expression of SSEA-4 on lung CD45<sup>+</sup> and CD45<sup>-</sup> cells. Lungs of untreated NSG mice were dissociated and the thus obtained single cell suspensions were subjected to flow cytometric analysis for correlated CD45 and SSEA-4 expression. Isotype control was used to assess background staining for SSEA-4. Dead cells and cell aggregates were excluded for analysis. (B) Phenotyping of SSEA-4-expressing lung cells. A library of 29 antibodies was used to identify cell surface markers co-expressed by SSEA-4-positive cells. According to the frequency of antigen-positive cells within the SSEA-4-expressing compartment, markers were categorized into no staining, partial staining with discrete populations, partial staining with smeared population, and full staining. A total of 5 lungs of untreated NSG mice were analyzed. (C) Expression of CD44, CD81, CD98, and Prominin-1 on SSEA-4-positive lung cells as determined by flow cytometry. Gating was performed on viable SSEA-4-positive single cells. Histograms are representative for 5 lungs analyzed.

## 4 Discussion

Due to its poor prognosis and few available treatment options, TNBC represents a significant clinical challenge which is associated with higher mortality compared to other breast cancer subtypes. Several novel therapeutic approaches against TNBC have been explored, including small molecule inhibitors, vaccination, monoclonal antibodies, and adoptive TIL therapies, with only modest benefit thus far (Lee and Djamgoz, 2018). In light of the recent breakthrough in the treatment of hematological malignancies in terminally ill patients using CAR T cell therapy, this study attempted to transfer the CAR technology to the treatment of TNBC. In this context, SSEA-4 was selected as a candidate target antigen for several reasons. First, it is expressed by various TNBCs (Aloia et al., 2015) and other cancers (Saito et al., 1997; Gottschling et al., 2013; Ye et al., 2010; Noto et al., 2013; Lou et al., 2014; Sivasubramanian et al., 2015) thus not only representing an attractive target for a breast cancer subtype that up to now lacks known targetable antigens, but also offering the possibility for a therapy that can be extended to other malignancies. Second, the glycolipid was reported to be expressed by chemoresistant TNBC subpopulations (Aloia et al., 2015) and targeting SSEA-4 offered a complementary treatment approach to chemotherapy, so that a combination of both therapeutic modalities was likely to increase the overall survival rate of cancer patients. Third, the antigen has been suggested to play a critical role in metastatic processes (Sivasubramanian et al., 2015) and elimination of SSEA-4-positive tumor cells held promise to diminish the metastatic potential of cancers. Fourth, although SSEA-4 is strongly expressed by embryonic and mesenchymal stem cells (Breimer et al., 2017; Gang et al., 2007; Pittenger, 1999; Riekstina et al., 2009; Shinohara et al., 2015), we have identified its expression in adult non-malignant tissue to be limited to cell subpopulations in placenta, testis, skin and small intestine (unpublished observation). As placenta and testis are immune privileged organs, potential on target/off tumor toxicities were expected to be restricted to skin and small intestine. In addition, one preclinical study had previously demonstrated that systemic SSEA-4-directed mAb treatment exhibited anti-tumor efficacy against glioblastoma without any reported *in vivo* toxicities (Lou et al., 2014). Against this background, the present study addressed the development and evaluation of several SSEA-4-directed CAR T cell therapies and investigated the CAR structure-to-function relationship with an emphasis on the spacer domain of the synthetic molecules. Besides, it evaluated the suitability and the pitfalls of commonly used flow cytometric methods for the detection of the artificial receptors. The following chapters discuss the findings of this research in the context of current scientific development in the CAR T cell field.

## 4.1 Comparison of different CAR T cell detection methods

The modular design of CARs allows for their building blocks to be easily exchanged, thereby providing the possibility of unlimited receptor versatility. An accompanying challenge of such a receptor changeability is a universal and reliable detection method for the synthetic molecules. While the majority of clinical trials applies quantitative polymerase chain reaction (qPCR) methodology to detect the presence and frequency of gene-modified T cells (Kochenderfer et al., 2010; Morgan et al., 2006; Porter et al., 2011; Maude et al., 2014), in the developmental phase this technique is unwieldy as it provides no information about the expression of the transgene. Therefore, standard laboratory technique is to detect CAR expression by flow cytometry using recombinant antigen-Fc fusion proteins (De Oliveira et al., 2013) or antibodies directed against either an epitope tag (Liu et al., 2016) or the extracellular structure of the receptor such as the spacer region (using an anti-IgG Fc antibody) (Kowolik et al., 2006) or the receptor's scFv domain (using anti-mouse or anti-human F(ab)-specific antibody) (Kunkele et al., 2015). More recently, also the use of Protein L (Zheng et al., 2012) and monoclonal anti-idiotypic antibodies (Jena et al., 2013) has been proposed for CAR expression detection. While all are valid methods, each of them has a disadvantage. The use of recombinant antigens or monoclonal anti-idiotypic antibodies for instance requires the development of a new reagent for each CAR specificity. On the other hand, the introduction of a tag may have a strong impact on the receptors' expression, functionality and potentially immunity, and necessitates an extensive testing beforehand. Consequently, for reasons of convenience, Protein L and anti-mouse/human F(ab) specific antibodies are currently the most widely used reagents to analyze CAR expression. However, an extensive comparison of these agents has not yet been performed and every research center's choice on which one to use is based on an idiosyncratic decision.

Due to the unavailability of a synthetic fluorochrome-conjugated SSEA-4 molecule – which would have been unarguably the best detection agent – an alternative approach for the analysis of SSEA-4-directed CARs had to be applied. In initial expression analyses using HEK293T cells, a Protein L-conjugate was applied, however, the labelling reactions regularly suffered from significant background and limited discrimination of populations with low transfection efficiencies. Subsequent thorough analysis and staining protocol optimization revealed that published work on Protein L for CAR detection used T cell populations where the majority of cells (>70%) expressed the transgene and contained high transgene copy numbers, which in turn helped improving the specific staining index. To ensure appropriate determination of CAR expression on T cells, a comparative analysis of the Protein L- and anti-mouse F(ab)-based staining methods was conducted and set in relation to the expression of the transduction marker  $\Delta$ LNGFR. Strikingly, CAR stainings with Protein L exhibited a spacer-dependent effect: while a complete congruency of L spacer CAR and  $\Delta$ LNGFR expression was detectable, the

frequency of CAR-positive cells within the transgenic population declined with decreasing spacer length – despite equivalent  $\Delta$ LNGFR expression. It is not clear, whether the observed trend is due to a decreased expression of the synthetic receptors on the cell surface or due to an impaired accessibility of the labeling protein to its epitope. In fact, the more proximal the scFv is located to the cell membrane, the more the binding interactions can be affected by the dense glycocalyx. In support of this hypothesis, detection of XS spacer CAR-expressing populations with the polyclonal anti-mouse F(ab)-directed antibody exhibited a reduction in the median FI of the transgene-positive cells compared to  $\Delta$ LNGFR expression. Nevertheless, the overall frequency of the positive population remained comparable to the marker protein, indicating that the glycocalyx may impair but not completely abrogate the binding interactions. In light of the staining data obtained with Protein L, it is debatable whether labeling with the polyclonal anti-mouse F(ab)-directed antibody recognized exclusively functional CARs or may have also resulted in the recognition of improperly folded receptors on the cell surface which escaped Protein L-based detection. To better understand the underlying mechanisms, an extended study analyzing the expression pattern of various CARs incorporating different scFvs is necessary. Although the restriction to SSEA-4-directed CARs is a limitation of the present study, the work clearly illustrates that the detection of functional CARs is not a trivial task and susceptible to artefacts. Thus, the different detection methods employed by different laboratories may lead to discrepant findings and lead to contradictory results in the literature.

## 4.2 Impact of the spacer region on CAR function

Traditionally, the spacer region between the targeting moiety and the transmembrane domain of a CAR molecule has been regarded as an inert structural element that facilitates the positioning of the antigen binding unit outside the T cell glycocalyx (Moritz & Groner, 1995). Accumulating evidence, however, suggests that it can have a significant effect on T cell effector function so that the design of receptors for novel targets needs to consider the localization of the target epitope and based on this customize the spacer length for optimal CAR signaling (Guest et al., 2005; Haso et al., 2013; Hudecek et al., 2016). To determine systematically the optimal spacer length for a SSEA-4-directed CAR, five receptor variants were generated with identical ligand binding and signaling domains, but with alternative spacer regions. Upon transient introduction into HEK293T cells and comparative expression analysis, the three best expressed candidates were selected to progress to the next series of experiments, in which they were investigated for their ability to induce T cell-mediated cytotoxicity and cytokine production. Although all CARs mediated detectable antigen-specific target cell lysis and cytokine release *in vitro*, a clear functional hierarchy was observed. The S spacer CAR was

functionally the most dominant of all SSEA-4-directed CARs examined, followed by the L spacer CAR and subsequently by the XS spacer CAR. *In vivo*, when low CAR T cell doses ( $2 \cdot 10^6$ ) were administered, bioactivity was detected only within the S spacer CAR T cell injected cohort, while high CAR T cell dose infusions ( $10 \cdot 10^6$ ) resulted in reactivity of all CAR variants – with the same hierarchical profile as seen *in vitro*. These data clearly demonstrate a dose-dependent effect of CAR T cell functionality – a phenomenon that has already been described by various investigators (Stemberger et al., 2012; van der Waart et al., 2014; Kagoya et al., 2016; Sabatino et al., 2016). Nevertheless, it cannot be excluded that toxic effects may have appeared at a later time point when low dose XS and L spacer CAR T cells were administered, although this could not be observed in the given experimental setting due to the later development of xenotoxicity.

It is surprising that no obvious correlation between spacer length and CAR potency was observed within this study. As SSEA-4 is a relatively small antigen and the REA101-targeted epitope of the glycolipid is comprised of the three saccharide moieties distal to ceramide (NeuAc $\alpha$ 2-3Gal $\beta$ 1-3GalNac; Figure 3B) – that is half of the extracellular hexasaccharide unit – it was anticipated that a long to intermediate spacer would be required to reach the epitope. Thus, the low reactivity of the XS spacer CAR (spacer 12 amino acids in length) was expected and attributed to an inefficient accessibility of the membrane-proximal scFv to its antigenic determinant. Additionally, as described in 4.1, the possibility of impaired surface expression of this receptor variant remains.

The superior reactivity of the S spacer CAR (spacer 45 amino acids in length) rather than the L spacer CAR (spacer 228 amino acids in length) is less clear. One possible explanation is that the L spacer receptor is too long and therefore hampers efficient downstream signaling upon antigen engagement, while the S spacer CAR may have the optimal length. However, it is important to note that various internal work investigating additional CAR specificities report predominantly a better functional performance of S spacer-incorporating CARs compared to other spacer receptors. Moreover, although a direct comparison of results from CD19-directed CAR T cell clinical trials is difficult due to the various differences in protocols, co-stimulatory signaling, patient groups and disease state, the rough trend can be observed that CAR T cell therapies that demonstrated potent activity in the clinic contained the S spacer sequence (derived from CD8 $\alpha$ ) (Porter et al., 2011; Kalos et al., 2011). By contrast, a clinical trial that utilized the spacer region derived from IgG1 Fc domain demonstrated less impressive anti-tumor efficacy (Savoldo et al., 2011). These observations indicate that not only the length but also the nature of the spacer region affects the receptor's bioactivity. Although the causative reasons have not been entirely elucidated, preliminary work within the scope of this study indicates that the reduced efficacy of IgG Fc spacer-harboring CARs may be due to lower surface stability compared to CD8 $\alpha$ -derived spacer CARs. This is significant as previous

studies analyzing the impact of the spacer region were performed within the framework of Ig-derived sequences and have not been compared to CD8 $\alpha$ -derived spacers (Guest et al., 2005; Hudecek et al., 2016; Künkele et al., 2015). Thus, this study provides evidence that not only structural and spatial elements in CAR T cell:target cell interaction seem to influence a chimeric receptor's potency, but also additional factors which are not entirely understood yet. Presumably, receptor surface stability and spacer flexibility, which can impair ligand affinity, play a role as well. Thus, it is to be appreciated that in their basic form, CARs represent complex molecules and additional work is needed to understand and harness their full potential.

### **4.3 Choice of animal model for testing *in vivo* toxicity of SSEA-4-directed CAR T cells**

Mouse xenograft models are currently the standard testing approach to assess the efficacy of novel CAR T cell therapies. In the majority of studies, however, the human antigen-specific CAR T cells do not cross-react with the cognate murine antigen, in this way failing to provide significant information about potential CAR T cell-mediated autoimmune reactivity. Exceptionally, in the present study, the NSG<sup>TM</sup> mouse-based tumor xenograft model served as a suitable platform to study SSEA-4-directed CAR T cell therapies in the context of both therapeutic efficacy and on target/off tumor toxicity. The highly immunodeficient animal strain allowed a potent engraftment of the human therapeutic cells and the carbohydrate-reactive scFv of the CAR, which is able to cross-recognize its cognate epitope on both human and murine cells, enabled to address and investigate possible on target/off tumor reactivity towards healthy cells. As previous histochemical analysis by ourselves has shown a correlated expression of SSEA-4 between mice and humans, we thus had a clinically relevant xenograft model with predictive value for potential on target/off tumor reactivity in human patients. It was found that adoptive transfer of SSEA-4-directed T cells in mice resulted in only a modest anti-tumor efficacy, but severe on target/off tumor toxicities – a scenario that has often observed with other CAR T cell therapies in the clinical setting (Morgan et al., 2010; Lamers et al., 2006, 2007, 2013). Thus, this study once more emphasizes the need for elaborated toxicity evaluation models in the preclinical setting. Due to the inadequacy of current preclinical models, the majority of clinical trials testing CAR T cell therapies are being initiated “blindly” without knowledgeable preparation for potential adverse events. However, blind translation of a SSEA-4-directed CAR T cell therapy to the clinical setting could have led to catastrophic consequences in patients. Care has to be taken that no further life-threatening therapies enter the clinic. Therefore, it is encouraging that the scientific community has started to appreciate the insufficiency of current animal models and more sophisticated toxicity testing approaches

are now being developed (Berger et al., 2015; Siegler and Wang, 2018). Although this is one step in the right direction, one major missing parameter is the analysis of these toxicities in an immunocompetent host, which would allow the interplay of other components of the immune system in these complex interactions to be studied. To assess e.g. the extent of CRS a humanized NSG™ mouse model with an engrafted human immune system would have been necessary. Nonetheless, such a model would have likely provided only limited information about cytokine-driven adverse events as several human cytokines secreted by activated immune cells mostly do not cross-react with the respective murine receptors. A fully murine model may have equally restricted predictive power due to mouse-human divergence and – in worst case – may underestimate the toxicity associated with CAR T cells. Indeed, a previous study analyzing NKG2DL-directed CARs in various mouse models has demonstrated that while marked adverse events can be observed in BALB/c mice upon treatment, these CAR T cells manifest little toxicity in C57BL/6 mice (VanSeggelen et al., 2015) suggesting that the functionality of CARs may be strain-dependent in murine T cells.

In an attempt to better understand the mechanisms and full spectrum of CRS-based adverse events, Taraseviciute et al. have recently developed a non-human primate model which recapitulates the most significant toxicities of CAR T cell therapy, including CRS and neurotoxicity (Taraseviciute et al., 2018). It is to be expected that this model will soon provide novel insights that may help overcoming the most serious side effects associated with CAR T cell therapy, although, it is likely that the model will find only limited use in the future due to economic and ethical reasons.

#### **4.4 Characterization of SSEA-4-expressing subpopulations targeted by CAR T cells**

Ever since its original description as an embryonic antigen in 1983 (Kannagi et al., 1983), SSEA-4 has been widely used as a marker for stemness and pluripotency. Beyond regenerative medicine research, however, the glycolipid has remained largely unexplored in the last 35 years and knowledge about its function as well as its distribution in normal adult tissue is still limited. Prior to the inception of this project, internal histochemical and flow cytometric screening approaches identified SSEA-4 to be expressed by cell subpopulations in the placenta, testis, skin, and small intestine, indicating a restricted distribution in post-natal tissue. Thus, in the present study, which aimed to evaluate the *in vivo* targeting of SSEA-4 by CAR T cells, potential injury of healthy tissue was expected to be limited to skin and small intestine. Contrary to this supposition, adoptive transfer of SSEA-4-directed CAR T cells into

NSG™ mice resulted in severe toxicities dominated by on target/off tumor recognition in lung and bone marrow with the latter demonstrating hypocellularity and a strong decrease of the CD45<sup>+</sup>Sca-1<sup>bright</sup> population. Subsequent analysis in non-treated mice identified hematopoietic MPPs in the bone marrow and epithelial progenitor cells in the lung to be expressing SSEA-4, providing evidence that the glycolipid is not a restricted embryonic marker, but is also expressed by adult progenitor cells.

Taking into consideration that in oncology, SSEA-4 expression has been described to occur in a variety of tumors, e.g. breast cancer (Aloia et al., 2015; Huang et al., 2013), basaloid lung cancer (Gottschling et al., 2013), ovarian carcinoma (Ye et al., 2010), glioblastoma (Lou et al., 2014) and oral cancer (Noto et al., 2013), our findings described here further support the cancer stem cell theory, which proposes that cancer originates from normal stem or progenitor cells. Indeed, in the lung, SSEA-4 expression highly correlates with Prominin-1 (CD133), a marker for hematopoietic, neuronal and endothelial progenitor cells in both humans and mice (Fargeas et al., 2006). In a colon carcinoma study conducted by Zhu et al. in 2008, Prominin-1-positive cells were shown to expand disproportionately during malignant transformation and that cells within the neoplastic lesions were progeny of Prominin-1 cells. Upon tumor progression, only a fraction of cells retained the Prominin-1-positive phenotype and only a fraction of these cells were proliferating (Zhu et al., 2009). Based on the co-expression of SSEA-4 and Prominin-1 in lung-resident progenitor cells observed in this study, it is tempting to speculate that similar findings may be observed for SSEA-4-expressing cells.

As the approach for the identification of SSEA-4-positive cells conducted within the scope of this study was restrictive, it cannot be certain that all SSEA-4 expressing cells were identified. It is likely that – similar to Prominin-1 – progenitor cells in other tissues express the glycolipid and any potential anti-tumor benefit gained by therapeutic targeting of SSEA-4 would have to be carefully weighed against the ensuing destruction of various progenitor cells. In this context, it is intriguing that a previous study on mAb-based targeting of SSEA-4 demonstrated therapeutic efficacy against glioblastoma without reported *in vivo* toxicities (Lou et al., 2014). Taking into consideration that Lou et al. targeted the same epitope on SSEA-4 as the present work (unpublished data) it is surprising that severe on target/off tumor adverse events were observed only in this study. A possible explanation for this discrepant observation may be the different nature of the therapeutics used. The immune response triggered by T cells is more pronounced than that of antibodies and it is possible that potential adverse events were delayed and may have appeared at a later timepoint in the mAb therapy setting (Lou et al. analyzed the therapeutic efficacy only for 31 days). Furthermore, CAR T cells exhibit a several magnitude higher overall avidity to their antigen than the cognate antibody (Morgan et al., 2010; Watanabe et al., 2015; Turatti et al., 2007; Stone et al., 2012) which in turn decreases the sensitivity threshold. Consequently, mAb may preferentially recognize SSEA-4<sup>high</sup> cells while

CAR T cells may also recognize cells that express the antigen at levels that are hard-to-detect for antibodies. In the present study, it cannot be excluded that SSEA-4-directed CAR T cells might have engaged with antigen-positive cells that were not detected by antibody screening. One observation favoring this hypothesis is the finding that SSEA-4 stainings always gave a slight shift (~1-2%) of the “negative” population towards the positive axis while isotype controls did not (examples in Figure 27D, E). As this shift was observed ubiquitously, it was initially considered unspecific. Alternatively, it is possible that the introduction of the (G<sub>4</sub>S) linker between the V<sub>L</sub> and V<sub>H</sub> regions of the cognate antibody to generate the scFv may have modified the epitope specificity, permitting structurally similar epitopes present on non-target antigens to be cross-recognized by the CAR T cells. Additional work is needed to understand whether these potential mechanisms indeed occurred.

Another aspect to consider between both studies is the administration route of the therapeutics. Lou et al. applied the mAb intraperitoneally which leads to a rapid and convective distribution in the body, while the present study used the intravenous application option. In the latter case, the cells first travel to the lung where they reside for several hours. As this is also the first site of antigen exposure, toxicity appears inevitably before or in parallel to tumor control. In the case of mAb application, the fast distribution kinetics may have enabled that a high amount of the injected dose reaches the tumor site prior to binding to on target/off tumor tissues. Nevertheless, these variables could have only lead to a delay in the toxic effects, but not completely abolished them. It is, therefore, realistic to presume that a combination of the factors discussed above led to the conflicting findings.

## 4.5 Conclusions

The extreme potency of CAR T cells and the severe side effects observed within the scope of this study highlight the essentiality of judicious target antigen selection. Rather than focusing on potential clinical benefit and oncogenic function of a candidate antigen, tumor selectivity needs to be prioritized to ensure an acceptable safety profile for this novel treatment modality. In fact, already in the past, a widespread application of CAR T cell therapy in the solid tumor setting has been impeded by the lack of truly tumor-specific antigens. In an endeavor to circumvent this obstacle, standard practice has become to target antigens that are overexpressed in solid cancers but show minimal expression on normal tissue. However, several clinical trials using this approach have described abundant on target/off tumor toxicities and at the same time only a limited anti-tumor activity – even in settings in which the target antigen is expressed at close to undetectable levels on healthy tissue (Morgan et al., 2010; Lamers et al., 2006, 2007, 2013). With this in mind, investigators need to verify in future

endeavours that sufficient information is known about the expression pattern of a potential target antigen on healthy tissue including the clinical relevance of antigen-expressing subpopulations. Expression by vital cell types – no matter how infrequent their presence in the human body is – has to weigh heavily against a candidate antigen. In this context, it is also imperative to reconsider the restrictedness of embryonic antigens. As exemplified in present work, antigens that are currently described to be specific to embryonic development may indeed be additionally expressed by certain adult tissues. If this tissue is vital to maintain life, therapeutic targeting may have a detrimental outcome. In a similar example, carcinoembryonic antigen (CEA), the expression of which is postulated to decrease after birth is – strictly taken – not a fetal antigen as it is also expressed by cell populations throughout the digestive tract in adults (Hammarström, 1999; Uhlen et al., 2010).

Given that it is difficult to exclude the possibility that a tumor target may be co-expressed on essential healthy tissue, the use of safety mechanisms in CAR therapy can offer an alternative approach to maximize tumor specificity. Indeed, diverse strategies are currently being developed to help overcome the detrimental autoreactivity of CAR T cells, including dual CAR approaches that require the recognition of two different antigens on the tumor cells to effectively activate the engineered T cells or various suicide mechanisms for the ablation of the therapeutic cells upon manifestation of severe on target/off tumor toxicity (Fesnak et al., 2016). However, an accurate evaluation of these different approaches in a clinically relevant model is missing. In this context, SSEA-4 may serve as a model antigen that can not only provide a better understanding of the strengths and shortcomings of the different safety strategies, but also supply a platform for comparative efficacy analyses of these mechanisms. The essentiality of SSEA-4-expressing cells in a mouse model will easily identify “leaky” technologies and eliminate them before they can enter the clinical trial setting, in this way accelerating the translation of the most promising technologies into clinical benefit.

## 5 References

- Adams, S., Gray, R.J., Demaria, S., Goldstein, L., Perez, E.A., Shulman, L.N., Martino, S., Wang, M., Jones, V.E., Saphner, T.J., et al. (2014). Prognostic value of tumor-infiltrating lymphocytes in triple-negative breast cancers from two phase III randomized adjuvant breast cancer trials: ECOG 2197 and ECOG 1199. *Journal of Clinical Oncology* 32(27):2959-2966.
- Ades, F., Zardavas, D., Bozovic-Spasojevic, I., Pugliano, L., Fumagalli, D., de Azambuja, E., Viale, G., Sotiriou, C., and Piccart, M. (2014). Luminal B breast cancer: molecular characterization, clinical management, and future perspectives. *Journal of Clinical Oncology* 32(25):2794-2803.
- Adusumilli, P.S., Cherkassky, L., Villena-Vargas, J., Colovos, C., Servais, E., Plotkin, J., Jones, D.R. and Sadelain, M. (2014). Regional delivery of mesothelin-targeted CAR T cell therapy generates potent and long-lasting CD4-dependent tumor immunity. *Science Translational Medicine* 6(261):261ra151.
- Ahmed, N., Brawley, V., Hegde, M., Bielałowicz, K., Kalra, M., Landi, D., Robertson, C., Gray, T.L., Diouf, O., Wakefield, A., et al. (2017). HER2-specific chimeric antigen receptor–modified virus-specific T cells for progressive glioblastoma: a phase 1 dose-escalation trial. *JAMA Oncology* 3(8):1094-1101.
- Ahmed, N., Brawley, V.S., Hegde, M., Robertson, C., Ghazi, A., Gerken, C., Liu, E., Dakhova, O., Ashoori, A., Corder, A., et al. (2015). Human epidermal growth factor receptor 2 (HER2)–specific chimeric antigen receptor–modified T cells for the immunotherapy of HER2-positive sarcoma. *Journal of Clinical Oncology* 33(15):1688-1696.
- Almeida, J.R., Price, D.A., Papagno, L., Arkoub, Z.A., Sauce, D., Bornstein, E., Asher, T.E., Samri, A., Schnuriger, A., Theodorou, I., et al. (2007). Superior control of HIV-1 replication by CD8<sup>+</sup> T cells is reflected by their Avidity, polyfunctionality, and clonal turnover. *The Journal of Experimental Medicine* 204(10):2473-2485.
- Aloia, A., Petrova, E., Tomiuk, S., Bissels, U., Déas, O., Saini, M., Zickgraf, F.M., Wagner, S., Spaich, S., Sütterlin, M., et al. (2015). The sialyl-glycolipid stage-specific embryonic antigen 4 marks a subpopulation of chemotherapy-resistant breast cancer cells with mesenchymal features. *Breast Cancer Research* 17(1):146.
- Amirache F., Lévy, C., Costa, C., Mangeot, P.E., Torbett, B.E., Wang, C.X., Nègre, D., Cosset, F.L., and Verhoeven, E. (2014). Mystery solved: VSV-G-LVs do not allow efficient gene transfer into unstimulated T cells, B cells, and HSCs because they lack

- the LDL receptor. *Blood* 123(9):1422-1424.
- Anderson, B.O., Shyyan, R., Eniu, A., Smith, R.A., Yip, C.H., Bese, N.S., Chow, L.W., Masood, S., Ramsey, S.D., and Carlson, R.W. (2006). Breast cancer in limited-resource countries: an overview of the breast health global initiative 2005 guidelines. *Breast Journal* 12 Suppl 1:S3-15.
- Ang, W.X., Li, Z., Chi, Z., Du, S.H., Chen, C., Tay, J.C., Toh, H.C., Connolly, J.E., Xu, X.H., and Wang, S. (2017). Intraperitoneal immunotherapy with T cells stably and transiently expressing anti-EpCAM CAR in xenograft models of peritoneal carcinomatosis. *Oncotarget* 8(8):13545-13559.
- Badovinac Črnjević, T., Spagnoli, G., Juretić, A., Jakić-Razumović, J., Podolski, P., and Šarić N. (2012). High expression of MAGE-A10 cancer-testis antigen in triple-negative breast cancer. *Medical Oncology* 29(3):1586-1591.
- Baitsch, L., Baumgaertner, P., Devêvre, E., Raghav, S.K., Legat, A., Barba, L., Wieckowski, S., Bouzourene, H., Deplancke, B., Romero, P., et al. (2011). Exhaustion of tumor-specific CD8<sup>+</sup> T cells in metastases from melanoma patients. *Journal of Clinical Investigation* 121(6):2350-2360.
- Balko, J.M., Giltane, J.M., Wang, K., Schwarz, L.J., Young, C.D., Cook, R.S., Owens, P., Sanders, M.E., Kuba, M.G., Sánchez, V., et al. (2014). Molecular profiling of the residual disease of triple-negative breast cancers after neoadjuvant chemotherapy identifies actionable therapeutic targets. *Cancer Discovery* 4(2):232-245.
- Barber, A., Zhang, T., Megli, C.J., Wu, J., Meehan, K.R., and Sentman, C.L. (2008). Chimeric NKG2D receptor-expressing T cells as an immunotherapy for multiple myeloma. *Experimental Hematology* 36(10):1318-1328.
- Baselga, J. (2010). Treatment of HER2-overexpressing breast cancer. *Annals of Oncology* Vol. 21.
- Bauer, K.R., Brown, M., Cress, R.D., Parise, C.A., and Caggiano, V. (2007). Descriptive analysis of estrogen receptor (ER)-negative, progesterone receptor (PR)-negative, and HER2-negative invasive breast cancer, the so-called triple-negative phenotype: a population-based study from the california cancer registry. *Cancer* 109(9):1721-1728.
- Beard, R.E., Zheng, Z., Lagisetty, K.H., Burns, W.R., Tran, E., Hewitt, S.M., Abate-Daga, D., Rosati, S.F., Fine, H.A., Ferrone, S., et al. (2014). Multiple chimeric antigen receptors successfully target chondroitin sulfate proteoglycan 4 in several different cancer histologies and cancer stem cells. *Journal for Immunotherapy of Cancer* 2:25.

- Beatty, G.L., O'Hara, M.H., Lacey, S.F., Torigian, D.A., Nazimuddin, F., Chen, F., Kulikovskaya, I.M., Soulen, M.C., McGarvey, M., Nelson, A.M., et al. (2018). Activity of mesothelin-specific chimeric antigen receptor T cells against pancreatic carcinoma metastases in a phase 1 trial. *Gastroenterology* S0016-5085(18)30323-8.
- Berger, C., Sommermeyer, D., Hudecek, M., Berger, M., Balakrishnan, A., Paszkiewicz, P.J., Kosasih, P.L., Rader, C., and Riddell, S.R. (2015). Safety of targeting ROR1 in primates with chimeric antigen receptor-modified T cells. *Cancer Immunology Research* 3(2):206-216.
- Berry, D.A., Cronin, K.A., Plevritis, S.K., Fryback, D.G., Clarke, L., Zelen, M., Mandelblatt, J.S., Yakovlev, A.Y., Habbema, J.D., and Feuer, E.J. (2005). Effect of screening and adjuvant therapy on mortality from breast cancer. *The New England Journal of Medicine* 353(17):1784-1792.
- Bianchini, G., Balko, J.M., Mayer, I.A., Sanders, M.E., and Gianni, L. (2016). Triple-negative breast cancer: challenges and opportunities of a heterogeneous disease. *Nature Reviews Clinical Oncology* 13(11):674-690.
- Biffi, A., Bartolomae, C.C., Cesana, D., Cartier, N., Aubourg, P., Ranzani, M., Cesani, M., Benedicenti, F., Plati, T., Rubagotti, E., et al. (2013). Lentiviral vector common integration sites in preclinical models and a clinical trial reflect a benign integration bias and not oncogenic selection. *Blood* 117(20):5332-5339.
- Bleumer, I., Knuth, A., Oosterwijk, E., Hofmann, R., Varga, Z., Lamers, C., Kruit, W., Melchior, S., Mala, C., Ullrich, S., et al. (2004). A phase II trial of chimeric monoclonal antibody G250 for advanced renal cell carcinoma patients. *British Journal of Cancer* 90(5):985-990.
- Blows, F.M., Driver, K.E., Schmidt, M.K., Broeks, A., van Leeuwen, F.E., Wesseling, J., Cheang, M.C., Gelmon, K., Nielsen, T.O., Blomqvist, C., et al. (2010). Subtyping of breast cancer by immunohistochemistry to investigate a relationship between subtype and short and long term survival: a collaborative analysis of data for 10,159 cases from 12 studies. *PLoS Medicine* 7(5):e1000279.
- Bray, F., McCarron, P., and Parkin, D.M. (2004). The changing global patterns of female breast cancer incidence and mortality. *Breast Cancer Research* 6(6):229-239.
- Breimer, M.E., Säljö, K., Barone, A., and Teneberg, S. (2017). Glycosphingolipids of human embryonic stem cells. *Glycoconjugate Journal* 34(6):713-723.
- Brentjens, R.J., Davila, M.L., Riviere, I., Park, J., Wang, X., Cowell, L.G., Bartido, S., Stefanski, J., Taylor, C., Olszewska, M., et al. (2013). CD19-targeted T cells rapidly

- induce molecular remissions in adults with chemotherapy-refractory acute lymphoblastic leukemia. *Science Translational Medicine* 5(177):177ra38.
- Brentjens, R.J., Riviere, I., Park, J.H., Davila, M.L., Wang, X., Stefanski, J., Taylor, C., Yeh, R., Bartido, S., Borquez-Ojeda, O., et al. (2011). Safety and persistence of adoptively transferred autologous CD19-targeted T cells in patients with relapsed or chemotherapy refractory B-cell leukemias. *Blood* 118(18):4817-4828.
- Brown, C.E., Badie, B., Barish, M.E., Weng, L., Ostberg, J.R., Chang, W.C., Naranjo, A., Starr, R., Wagner, J., Wright, C., et al. (2015) Bioactivity and safety of IL13R $\alpha$ 2-redirecated chimeric antigen receptor CD8<sup>+</sup> T cells in patients with recurrent glioblastoma. *Clinical Cancer Research* 21(18):4062-4072.
- Brown, C.E., Alizadeh, D., Starr, R., Weng, L., Wagner, J.R., Naranjo, A., Ostberg, J.R., Blanchard, M.S., Kilpatrick, J., Simpson, J., et al. (2016). Regression of glioblastoma after chimeric antigen receptor T-cell therapy. *New England Journal of Medicine* 375(26):2561-2569.
- Brown, G., Mooney, C.J., Alberti-Servera, L., von Muenchow, L., Toellner, K.M., Ceredig, R., and Rolink, A. (2015). Versatility of stem and progenitor cells and the instructive actions of cytokines on hematopoiesis. *Critical Reviews in Clinical Laboratory Sciences* 52(4):168-179.
- Brudno, J.N., and Kochenderfer, J.N. (2016). Toxicities of chimeric antigen receptor T cells : recognition and management. 127(26):3321-3331.
- Burstein, M. D., Tsimelzon, A., Poage, G.M., Covington, K.R., Contreras, A., Fuqua, S.A., Savage, M.I., Osborne, C.K., Hilsenbeck, S.G., Chang, J.C., et al. (2015). Comprehensive genomic analysis identifies novel subtypes and targets of triple-negative breast cancer. *Clinical Cancer Research* 21(7):1688-1698.
- Cabezón, T., Gromova, I., Gromov, P., Serizawa, R., Timmermans Wielenga, V., Kroman, N., Celis, J.E., and Moreira, J.M. (2013). Proteomic profiling of triple-negative breast carcinomas in combination with a three-tier orthogonal technology approach identifies Mage-A4 as potential therapeutic target in estrogen receptor negative breast cancer. *Molecular & Cellular Proteomics* 12(2):381-394.
- Cantor, J. M., and Ginsberg, M.H. (2012). CD98 at the crossroads of adaptive immunity and cancer. *Journal of Cell Science* 125(6):1373-1382.
- Cardoso, F., Harbeck, N., Fallowfield, L., Kyriakides, S., and Senkus, E. (2012). Locally recurrent or metastatic breast cancer: ESMO clinical practice guidelines for diagnosis, treatment and follow-up. *Annals of Oncology* 23 (SUPPL. 7).

- Carey, L. A., Rugo, H.S., Marcom, P.K., Mayer, E.L., Esteva, F.J., Ma, C.X., Liu, M.C., Storniolo, A.M., Rimawi, M.F. Forero-Torres, A., et al. (2012). TBCRC 001: randomized phase II study of cetuximab in combination with carboplatin in stage IV triple-negative breast cancer. *Journal of Clinical Oncology* 30(21):261-2623.
- Carpenito, C., Milone, M.C., Hassan, R., Simonet, J.C., Lakhai, M., Suhoski, M.M., Varela-Rohena, A., Haines, K.M., Heitjan, D.F., Albelda, S.M., et al. (2009). Control of large, established tumor xenografts with genetically retargeted human T cells containing CD28 and CD137 domains. *Proceedings of the National Academy of Sciences* 106(9):3360-3365.
- Chaffer, C.L., and Weinberg, R.A. (2011). A perspective on cancer cell metastasis. *Science* 331(6024):1559-1564.
- Chinnasamy, D., Yu, Z., Kerkar, S.P., Zhang, L., Morgan, R.A., Restifo, N.P., and Rosenberg, S.A. (2012). Local delivery of interleukin-12 using T cells targeting VEGF receptor-2 eradicates multiple vascularized tumors in mice. *Clinical Cancer Research* 18(6):1672-1683.
- Chinnasamy, D., Yu, Z., Theoret, M.R., Zhao, Y., Shrimali, R.K., Morgan, R.A., Feldman, S.A., Restifo, N.P., and Rosenberg, S.A. (2010). Gene therapy using genetically modified lymphocytes targeting VEGFR-2 inhibits the growth of vascularized syngenic tumors in mice. *Journal of Clinical Investigation* 120(11):3953-3968.
- Chmielewski, M., Hahn, O., Rappl, G., Nowak, M., Schmidt-Wolf, I.H., Hombach, A.A., Abken, H. (2012). T cells that target carcinoembryonic antigen eradicate orthotopic pancreatic carcinomas without inducing autoimmune colitis in mice. *Gastroenterology* 143(4):1095-1107.
- Cho, J.H., Okuma, A., Al-Rubaye, D., Intisar, E., Junghans, R.P., and Wong, W.W. (2018). Engineering Axl specific CAR and synNotch receptor for cancer therapy. *Scientific Reports* 8(1):3846.
- Chow, K.K., Naik, S., Kakarla, S., Brawley, V.S., Shaffer, D.R., Yi, Z., Rainusso, N., Wu, M.F., Liu, H., Kew, Y., et al. (2013). T cells redirected to EphA2 for the immunotherapy of glioblastoma. *Molecular Therapy* 21(3):629-637.
- Cieri, N, Camisa, B., Cocchiarella, F., Forcato, M., Oliveira, G., Provasi, E., Bondanza, A., Bordignon, C., Peccatori, J., Ciceri, F., et al. (2013). IL-7 and IL-15 instruct the generation of human memory stem T cells from naive precursors. *Blood* 121(4):573-584.
- Clemons, M., and Goss, P. (2001). Estrogen and the risk of breast cancer. *The New England*

*Journal of Medicine* 344(4):276-285.

- Cooper, L.J., Topp, M.S., Serrano, L.M., Gonzalez, S., Chang, W.C., Naranjo, A., Wright, C., Popplewell, L., Raubitschek, A., Forman, S.J., et al. (2003). T-Cell clones can be rendered specific for CD19: toward the selective augmentation of the graft-versus-B-lineage leukemia effect. *Blood* 101(4):1637-1644.
- Craddock, J.A., Lu, A., Bear, A., Pule, M., Brenner, M.K., Rooney, C.M., and Foster, A.E. (2010). Enhanced tumor trafficking of GD2 chimeric antigen receptor T cells by expression of the chemokine receptor CCR2b. *Journal of Immunotherapy* 33(8):780-788.
- Creighton, C.J., Li, X., Landis, M., Dixon, J.M., Neumeister, V.M., Sjolund, A., Rimm, D.L., Wong, H., Rodriguez, A., Herschkowitz, J.I., et al. (2009). Residual breast cancers after conventional therapy display mesenchymal as well as tumor-initiating features. *Proceedings of the National Academy of Sciences* 106(33):13820-13825.
- Crompton, J.G., Sukumar, M., Roychoudhuri, R., Clever, D., Gros, A., Eil, R.L., Tran, E., Hanada, K., Yu, Z., Palmer, D.C., et al. (2015). Akt inhibition enhances expansion of potent tumor-specific lymphocytes with memory cell characteristics. *Cancer Research* 75(2):296-305.
- Cummings, M.C., Simpson, P.T., Reid, L.E., Jayanthan, J., Skerman, J., Song, S., McCart Reed, A.E., Kutasovic, J.R., Morey, A.L., et al. (2014). Metastatic progression of breast cancer: insights from 50 years of autopsies. *Journal of Pathology* 232(1):23-31.
- Curigliano, G., Viale, G., Ghioni, M., Jungbluth, A.A., Bagnardi, V., Spagnoli, G.C., Neville, A.M., Nolè, F., Rotmensz, N., and Goldhirsch, A. (2011). Cancer-testis antigen expression in triple-negative breast cancer. *Annals of Oncology* 22(1):98-103.
- Dall, G., Vieusseux, J., Unsworth, A., Anderson, R., and Britt, K. (2015). Low dose, low cost estradiol pellets can support MCF-7 tumour growth in nude mice without bladder symptoms. *Journal of Cancer* 6(12):1331-1336.
- Dall, P., Herrmann, I., Durst, B., Stoff-Khalili, M.A., Bauerschmitz, G., Hanstein, B., and Niederacher, D. (2005). In Vivo cervical cancer growth inhibition by genetically engineered cytotoxic T cells. *Cancer Immunology, Immunotherapy* 54(1):51-60.
- Darcy, P.K., Kershaw, M.H., Trapani, J.A., and Smyth, M.J. (1998). Expression in cytotoxic T lymphocytes of a single-chain anti-carcinoembryonic antigen antibody. Redirected Fas ligand-mediated lysis of colon carcinoma. *European Journal of Immunology* 28(5):1663-1672.

- Davila, M.L., Riviere, I., Wang, X., Bartido, S., Park, J., Curran, K., Chung, S.S., Stefanski, J., Borquez-Ojeda, O., Olszewska, M., et al. (2014). Efficacy and toxicity management of 19-28z CAR T cell therapy in B cell acute lymphoblastic leukemia. *Science Translational Medicine* 6 (224):224ra25.
- Davis, S.L., Eckhardt, S.G., Tentler, J.J., and Diamond, J.R. (2014). Triple-negative breast cancer: bridging the gap from cancer genomics to predictive biomarkers. *Therapeutic Advances in Medical Oncology* 6(3):88-100.
- Dent, R., Hanna, W.M., Trudeau, M., Rawlinson, E., Sun, P., and Narod, S.A. (2009). Pattern of metastatic spread in triple-negative breast cancer. *Breast Cancer Research and Treatment* 115(2):423-428.
- Dent, R., Trudeau, M., Pritchard, K.I., Hanna, W.M., Kahn, H.K., Sawka, C.A., Lickley, L.A., Rawlinson, E., Sun, P., and Narod, S.A. (2007). Triple-negative breast cancer: clinical features and patterns of recurrence. *Clinical Cancer Research* 13(15):4429-4434.
- de Oliveira, S.N., Wang, J., Ryan, C., Morrison, S.L., Kohn, D.B., and Hollis, R.P. (2013). A CD19/Fc fusion protein for detection of anti-CD19 chimeric antigen receptors. *Journal of Translational Medicine* 11:23.
- Eltzschig, H.K. (2013). Extracellular adenosine signaling in molecular medicine. *Journal of Molecular Medicine* 91(2):141-146.
- Eshhar, Z. (2008). The T-body approach: redirecting T cells with antibody specificity. *Handbook of Experimental Pharmacology* 181:329-42.
- Eshhar, Z., Waks, T., Gross, G., and Schindler, D.G. (1993). Specific activation and targeting of cytotoxic lymphocytes through chimeric single chains consisting of antibody-binding domains and the gamma or zeta subunits of the immunoglobulin and T-cell receptors. *Proceedings of the National Academy of Sciences* 90(2):720-24.
- Eshhar, Z., Waks, T., Bendavid, A., and Schindler, D.G. (2001). Functional expression of chimeric receptor genes in human T cells. *Journal of Immunological Methods* 248(1-2):67-76.
- Euhus, D.M., Hudd, C., Laregina, M.C., and Johnson, F.E. (1986). Tumor measurement in the nude mouse. *Journal of Surgical Oncology* 31(4):229-234.
- Fargeas, C.A., Fonseca, A.V., Huttner, W.B., and Corbeil, D. (2006). Prominin-1 (CD133): from progenitor cells to human diseases. *Future Lipidology* 1(2):213-225.
- Feng, K.C., Guo, Y.L., Liu, Y., Dai, H.R., Wang, Y., Lv, H.Y., Huang, J.H., Yang, Q.M., and Han, W.D. (2017). Cocktail treatment with EGFR-specific and CD133-specific chimeric

- antigen receptor-modified T cells in a patient with advanced cholangiocarcinoma. *Journal of Hematology and Oncology* 10(1):1-11.
- Feng, K., Liu, Y., Guo, Y., Qiu, J., Wu, Z., Dai, H., Yang, Q., Wang, Y., and Han, W. (2017). Phase I study of chimeric antigen receptor modified T cells in treating HER2-positive advanced biliary tract cancers and pancreatic cancers. *Protein and Cell*
- Ferlay, J., Soerjomataram, I., Dikshit, R., Eser, S., Mathers, C., Rebelo, M., Parkin, D.M., Forman, D., and Bray, F. (2015). Cancer incidence and mortality worldwide: sources, methods and major patterns in GLOBOCAN 2012. *International Journal of Cancer* 136(5):E359-386.
- Fesnak, A.D., June, C.H., and Levine, B.L. (2016). Engineered T cells: the Promise and Challenges of Cancer Immunotherapy. *Nature Reviews Cancer* 16(9):566-581.
- Finkelshtein, D., Werman, A., Novick, D., Barak, S., and Rubinstein, M. (2013). LDL receptor and its family members serve as the cellular receptors for vesicular stomatitis virus. *Proceedings of the National Academy of Sciences* 110(18):7306-7311.
- Finney, H.M., Lawson, A.D., Bebbington, C.R., and Weir, A.N. (1998). Chimeric receptors providing both primary and costimulatory signaling in T cells from a single gene product. *Journal of Immunology* 161(6):2791-2797.
- Frey, N.V., and Porter, D.L. (2016). Cytokine release syndrome with novel therapeutics for acute lymphoblastic leukemia. *ASH Education Program Book* 2016(1):567-572.
- Fulford, L.G., Reis-Filho, J.S., Ryder, K., Jones, C., Gillett, C.E., Hanby, A., Easton, D., and Lakhani, S.R. (2007). Basal-like grade III invasive ductal carcinoma of the breast: patterns of metastasis and long-term survival. *Breast Cancer Research* 9(1):R4.
- Gang, E.J., Bosnakovski, D., Figueiredo, C.A., Visser, J.W., and Perlingeiro, R.C. (2007). SSEA-4 identifies mesenchymal stem cells from bone marrow. *Blood* 109(4):1743-1751.
- Gardner, R.A., Finney, O., Annesley, C., Brakke, H., Summers, C., Leger, K., Bleakley, M., Brown, C., Mgebroff, S., Kelly-Spratt, K.S., et al. (2017). Intent to treat leukemia remission by CD19CAR T cells of defined formulation and dose in children and young adults. *Blood* 129(25):3322-3331.
- Garrido, F., Cabrera, T., Concha, A., Glew, S., Ruiz-Cabello, F., and Stern, P.L. (1993). Natural history of HLA expression during tumour development. *Immunology Today* 14(10):491-499.
- Gattinoni, L., Zhong, X.S., Palmer, D.C., Ji, Y., Hinrichs, C.S., Yu, Z., Wrzesinski, C., Boni, A., Cassard, L., Garvin, L.M., et al. (2009). Wnt signaling arrests effector T cell

- differentiation and generates CD8+ memory stem cells. *Nature Medicine* 15(7):808-813.
- Geldres, C., Savoldo, B., and Dotti, G. (2016). Chimeric antigen receptor-redirected T cells return to the bench. *Seminars in Immunology* 28(1):3-9.
- Ghoncheh, M., Pournamdar, Z., and Salehiniya, H. (2016). Incidence and mortality and epidemiology of breast cancer in the world. *Asian Pacific Journal of Cancer Prevention* 17(S3):43-46.
- Gilham, D.E., Debets, R., Pule, M., Hawkins, R.E., and Abken, H. (2012). CAR-T cells and solid tumors: tuning T cells to challenge an inveterate foe. *Trends in Molecular Medicine* 18(7):377-384.
- Gottschling, S., Jensen, K., Warth, A., Herth, F.J., Thomas, M., Schnabel, P.A., and Herpel, E. (2013). Stage-specific embryonic antigen-4 is expressed in basaloid lung cancer and associated with poor prognosis. *European Respiratory Journal* 41(3):656-663.
- Goverman, J., Gomez, S.M., Segesman, K.D., Hunkapiller, T., Laug, W.E., and Hood, L. (1990). Chimeric immunoglobulin-T cell receptor proteins form functional receptors: implications for T cell receptor complex formation and activation. *Cell* 60(6):929-939.
- Graille, M., Stura, E.A., Housden, N.G., Beckingham, J.A., Bottomley, S.P., Beale, D., Taussig, M.J., Sutton, B.J., Gore, M.G., and Charbonnier, J.B. (2001). Complex between *Peptostreptococcus magnus* protein L and a human antibody reveals structural convergence in the interaction modes of Fab binding proteins. *Structure* 9(8):679-687.
- Grewal, I.S. (2008). CD70 as a therapeutic target in human malignancies. *Expert Opinion on Therapeutic Targets* 12(3):341-351.
- Gross, G., Waks, T., and Eshhar, Z. (1989). Expression of immunoglobulin-T-cell receptor chimeric molecules as functional receptors with antibody-type specificity. *Proceedings of the National Academy of Sciences* 86(24):10024-10028.
- Gross, G., and Eshhar, Z. (2016). Therapeutic potential of T cell chimeric antigen receptors (CARs) in cancer treatment: counteracting off-tumor toxicities for safe CAR T cell therapy. *Annual Review of Pharmacology and Toxicology* 56(1):59-83.
- Grupp, S.A., Kalos, M., Barrett, D., Aplenc, R., Porter, D.L., Rheingold, S.R., Teachey, D.T., Chew, A., Hauck, B., Wright, J.F., et al. (2013). Chimeric antigen receptor–modified T cells for acute lymphoid leukemia. *New England Journal of Medicine* 368(16):1509-1518.
- Guest, R.D., Hawkins, R.E., Kirillova, N., Cheadle, E.J., Arnold, J., O'Neill, A., Irlam, J., Chester, K.A., Kemshead, J.T., Shaw, D.M., et al. (2005). The role of extracellular

- spacer regions in the optimal design of chimeric immune receptors: evaluation of four different scFvs and antigens. *Journal of Immunother* 28(3):203-211.
- Gust, J., Hay, K.A., Hanafi, L.A., Li, D., Myerson, D., Gonzalez-Cuyar, L.F., Yeung, C., Liles, W.C., Wurfel, M., Lopez, J.A., et al. (2017). Endothelial activation and blood–brain barrier disruption in neurotoxicity after adoptive immunotherapy with CD19 CAR-T cells. *Cancer Discovery* 7(12):1404-1419.
- Hacein-Bey-Abina, S., von Kalle, C., Schmidt, M., McCormack, M.P., Wulffraat, N., Leboulch, P., Lim, A., Osborne, C.S., Pawliuk, R., Morillon, E., et al. (2003). LMO2-associated clonal T cell proliferation in two patients after gene therapy for SCID-X1. *Science* 302(5644):415-419.
- Hackett, P.B., Largaespada, D.A., and Cooper, L.J. (2010). A transposon and transposase system for human application. *Molecular Therapy* 18(4):674-683.
- Hammarström, S. (1999). The carcinoembryonic antigen (CEA) family: structures, suggested functions and expression in normal and malignant tissues. *Seminars in Cancer Biology* 9(2):67-81.
- Hartmann, J., Schüßler-Lenz, M., Bondanza, A., and Buchholz, C.J. (2017). Clinical development of CAR T cells—challenges and opportunities in translating Innovative treatment concepts. *EMBO Molecular Medicine* 9(9):1183-1197.
- Haso, W., Lee, D.W., Shah, N.N., Stetler-Stevenson, M., Yuan, C.M., Pastan, I.H., Dimitrov, D.S., Morgan, R.A., Fitzgerald, D.J., Barrett, D.M., et al. (2013). Anti-CD22 – chimeric antigen receptors targeting B-cell precursor acute lymphoblastic leukemia. *Blood* 121(7):1165-1175.
- Heczey, A., Louis, C.U., Savoldo, B., Dakhova, O., Durett, A., Grilley, B., Liu, H., Wu, M.F., Mei, Z., Gee, A., et al. (2017). CAR T cells administered in combination with lymphodepletion and PD-1 inhibition to patients with neuroblastoma. *Molecular Therapy* 25(9):2214-2224.
- Henderson, I.C. (2013). Comparisons between different polychemotherapy regimens for early breast cancer: meta-analyses of long-term outcome among 100 000 women in 123 randomised trials. *Breast Diseases A Year Book Quarterly* 24(1):76-78.
- Hennigs, A., Riedel, F., Gondos, A., Sinn, P., Schirmacher, P., Marmé, F., Jäger, D., Kauczor, H.U., Stieber, A., Lindel, K., et al. (2016). Prognosis of breast cancer molecular subtypes in routine clinical care: a large prospective cohort study. *BMC Cancer* 16(1):734.

- Hombach, A., Hombach, A.A., and Abken, H. (2010). Adoptive immunotherapy with genetically engineered T cells: modification of the IgG1 Fc spacer domain in the extracellular moiety of chimeric antigen receptors avoids off-target activation and unintended initiation of an innate immune response. *Gene Therapy* 17(10):1206-1213.
- Hombach, A., Koch, D., Sircar, R., Heuser, C., Diehl, V., Kruis, W., Pohl, C., and Abken, H. (1999). A chimeric receptor that selectively targets membrane-bound carcinoembryonic antigen (mCEA) in the presence of soluble CEA. *Gene Therapy* 6(2):300-304.
- Hombach, A., Sircar, R., Heuser, C., Tillmann, T., Diehl, V., Kruis, W., Pohl, C., and Abken, H. (1998). Chimeric anti-TAG72 receptors with immunoglobulin constant Fc domains and gamma or zeta signalling chains. *International Journal of Molecular Medicine* 2(1):99-103.
- Hombach, A., Heuser, C., Gerken, M., Fischer, B., Lewalter, K., Diehl, V., Pohl, C., and Abken, H. (2000). T cell activation by recombinant FcepsilonRI gamma-chain immune receptors: an extracellular spacer domain impairs antigen-dependent T cell activation but not antigen recognition. *Gene Therapy* 7(12):1067-1075.
- Hong, H., Stastny, M., Brown, C., Chang, W.C., Ostberg, J.R., Forman, S.J., and Jensen, M.C. (2014). Diverse solid tumors expressing a restricted epitope of L1-CAM can be targeted by chimeric antigen receptor redirected T lymphocytes. *Journal of Immunotherapy* 37(2):93-104.
- Howe, S.J., Mansour, M.R., Schwarzwaelder, K., Bartholomae, C., Hubank, M., Kempinski, H., Brugman, M.H., Pike-Overzet, K., Chatters, S.J., de Ridder, D., et al. (2008). Insertional mutagenesis combined with acquired somatic mutations causes leukemogenesis following gene therapy of SCID-X1 patients. *Journal of Clinical Investigation* 118(9):3143-3150.
- Hua, C.K., Gacerez, A.T., Sentman, C.L., and Ackerman, M.E. (2017). Development of unique cytotoxic chimeric antigen receptors based on human scFv targeting B7H6. *Protein Engineering, Design & Selection* 30(10):713-721.
- Huang, G., Yu, L., Cooper, L.J., Hollomon, M., Huls, H., and Kleinerman, E.S. (2012). Genetically modified T cells targeting interleukin-11 receptor  $\alpha$ -chain kill human osteosarcoma cells and induce the regression of established osteosarcoma lung metastases. *Cancer Research* 72(1):271-281.
- Huang, X., Park, H., Greene, J., Pao, J., Mulvey, E., Zhou, S.X., Albert, C.M., Moy, F., Sachdev, D., Yee, D., et al. (2015). IGF1R- and ROR1-specific CAR T cells as a potential therapy for high risk sarcomas. *PLoS ONE* 10(7):e0133152.

- Huang, Y.L., Hung, J.T., Cheung, S.K., Lee, H.Y., Chu, K.C., Li, S.T., Lin, Y.C., Ren, C.T., Cheng, T.J., Hsu, T.L., et al. (2013). Carbohydrate-based vaccines with a glycolipid adjuvant for breast cancer. *Proceedings of the National Academy of Sciences* 110(7):2517-2522.
- Hudecek, M., Sommermeyer, D., Kosasih, P.L., Silva-Benedict, A., Liu, L., Rader, C., Jensen, M.C., and Riddell, S.R. (2015). The nonsignaling extracellular spacer domain of chimeric antigen receptors is decisive for in vivo antitumor activity. *Cancer Immunology Research* 3(2):125-135.
- Hudecek, M., Lupo-Stanghellini, M.T., Kosasih, P.L., Sommermeyer, D., Jensen, M.C., Rader, C., and Riddell, S.R. (2013). Receptor affinity and extracellular domain modifications affect tumor recognition by ROR1-specific chimeric antigen receptor T cells. *Clinical Cancer Research* 19(12):3153-3164.
- Huls, M.H., Figliola, M.J., Dawson, M.J., Olivares, S., Kebriaei, P., Shpall, E.J., Champlin, R.E., Singh, H., and Cooper, L.J. (2013). Clinical application of sleeping beauty and artificial antigen presenting cells to genetically modify T cells from peripheral and umbilical cord blood. *Journal of Visualized Experiments*, 72:e50070.
- Ibrahim, E.M., Al-Foheidi, M.E., Al-Mansour, M.M., and Kazkaz, G.A. (2014). The prognostic value of tumor-infiltrating lymphocytes in triple-negative breast cancer: a meta-analysis. *Breast Cancer Research and Treatment* 148(3):467-476.
- Imai, C., Mihara, K., Andreansky, M., Nicholson, I.C., Pui, C.H., Geiger, T.L., and Campana, D. (2004). Chimeric receptors with 4-1BB signaling capacity provoke potent cytotoxicity against acute lymphoblastic leukemia. *Leukemia* 18(4):676-684.
- Irving, B.A., and Weiss, A. (1991). The cytoplasmic domain of the T cell receptor  $\zeta$  chain is sufficient to couple to receptor-associated signal transduction pathways. *Cell* 64(5):891-901.
- Jaalouk, D.E., Crosato, M., Brodt, P., and Galipeau, J. (2006). Inhibition of histone deacetylation in 293GPG packaging cell line improves the production of self-inactivating MLV-derived retroviral vectors. *Virology Journal* 3:1-12.
- James, S.E., Greenberg, P.D., Jensen, M.C., Lin, Y., Wang, J., Till, B.G., Raubitschek, A.A., Forman, S.J., and Press, O.W. (2008). Antigen sensitivity of CD22-specific chimeric TCR is modulated by target epitope distance from the cell membrane. *The Journal of Immunology* 180(10):7028-7238.
- Jena, B., Maiti, S., Huls, H., Singh, H., Lee, D.A., Champlin, R.E., and Cooper, L.J. (2013). Chimeric antigen receptor (CAR)-specific monoclonal antibody to detect CD19-specific

- T cells in clinical trials. *PLoS ONE* 8(3):e57838.
- Jensen, M.C., Popplewell, L., Cooper, L.J., DiGiusto, D., Kalos, M., Ostberg, J.R., and Forman, S.J. (2010). Antitransgene rejection responses contribute to attenuated persistence of adoptively transferred CD20/CD19-specific chimeric antigen receptor redirected T cells in humans. *Biology of Blood and Marrow Transplantation* 16(9):1245-1256.
- Jiang, Z., Jiang, X., Chen, S., Lai, Y., Wei, X., Li, B., Lin, S., Wang, S., Wu, Q., Liang, Q., et al. (2017). Anti-GPC3-CAR T cells suppress the growth of tumor cells in patient-derived xenografts of hepatocellular carcinoma. *Frontiers in Immunology* 7:690.
- Johnson, L.A., Scholler, J., Ohkuri, T., Kosaka, A., Patel, P.R., McGettigan, S.E., Nace, A.K., Dentchev, T., Thekkat, P., Loew, A., et al. (2015). Rational development and characterization of humanized anti-EGFR variant III chimeric antigen receptor T cells for glioblastoma. *Science Translational Medicine* 7(275):275ra22.
- Jonnalagadda, M., Mardiros, A., Urak, R., Wang, X., Hoffman, L.J., Bernanke, A., Chang, W.C., Bretzlaff, W., Starr, R., Priceman, S., et al. (2015). Chimeric antigen receptors with mutated IgG4 Fc spacer avoid Fc receptor binding and improve T cell persistence and antitumor efficacy. *Molecular Therapy* 23(4):757-768.
- Junghans, R.P., Ma, Q., Rathore, R., Gomes, E.M., Bais, A.J., Lo, A.S., Abedi, M., Davies, R.A., Cabral, H.J., Al-Homsi, A.S., et al. (2016). Phase I trial of anti-PSMA designer CAR-T cells in prostate cancer: possible role for interacting interleukin 2 T Cell pharmacodynamics as a determinant of clinical response. *Prostate* 76(14):1257-1270.
- Kagoya, Y., Nakatsugawa, M., Yamashita, Y., Ochi, T., Guo, T., Anczurowski, M., Saso, K., Butler, M.O., Arrowsmith, C.H., and Hirano, N. (2016). BET bromodomain inhibition enhances T cell persistence and function in adoptive immunotherapy models. *Journal of Clinical Investigation* 126(9):3479-3494.
- Kaiser, A.D., Assenmacher, M., Schröder, B., Meyer, M., Orentas, R., Bethke, U., and Dropulic, B. (2015). Towards a commercial process for the manufacture of genetically modified T cells for therapy. *Cancer Gene Therapy* 22(2):72-78.
- Kakarla, S., Chow, K.K., Mata, M., Shaffer, D.R., Song, X.T., Wu, M.F., Liu, H., Wang, L.L., Rowley, D.R., Pfizenmaier, K., et al. (2013). Antitumor effects of chimeric receptor engineered human T cells directed to tumor stroma. *Molecular Therapy* 21(8):1611-1620.
- Kalimutho, M., Parsons, K., Mittal, D., López, J.A., Srihari, S., and Khanna, K.K. (2015). Targeted therapies for triple-negative breast cancer: combating a stubborn disease.

*Trends in Pharmacological Sciences* 36(12):822-846.

- Kalos, M., Levine, B.L., Porter, D.L., Katz, S., Grupp, S.A., Bagg, A., and June, C.H. (2011). T cells with chimeric antigen receptors have potent antitumor effects and can establish memory in patients with advanced leukemia. *Science Translational Medicine* 3(95):95ra73.
- Kannagi, R., Cochran, N.A., Ishigami, F., Hakomori, S., Andrews, P.W., Knowles, B.B., and Solter, D. (1983). Stage-specific embryonic antigens (SSEA-3 and -4) are epitopes of a unique globo-series ganglioside isolated from human teratocarcinoma cells. *The EMBO Journal* 2(12):2355-2361.
- Katz, S.C., Burga, R.A., McCormack, E., Wang, L.J., Mooring, W., Point, G.R., Khare, P.D., Thorn, M., Ma, Q., Stainken, B.F., et al. (2015). Phase I hepatic immunotherapy for metastases study of intra-arterial chimeric antigen receptor-modified T-cell therapy for CEA+ liver metastases. *Clinical Cancer Research* 21(14):3149-3159.
- Kershaw, M.H., Westwood, J.A., Parker, L.L., Wang, G., Eshhar, Z., Mavroukakis, S.A., White, D.E., Wunderlich, J.R., Canevari, S., Rogers-Freezer, L., et al. (2006). A phase I study on adoptive immunotherapy using gene-modified T cells for ovarian cancer. *Clinical Cancer Research* 12(20 Pt 1):6106-6115.
- Kochenderfer, J.N., Dudley, M.E., Feldman, S.A., Wilson, W.H., Spaner, D.E., Maric, I., Stetler-Stevenson, M., Phan, G.Q., Hughes, M.S., Sherry, R.M., et al. (2012). B-cell depletion and remissions of malignancy along with cytokine-associated toxicity in a clinical trial of anti-CD19 chimeric-antigen-receptor-transduced T cells. *Blood* 119(12):2709-2720.
- Kochenderfer, J.N., Dudley, M.E., Kassim, S.H., Somerville, R.P., Carpenter, R.O., Stetler-Stevenson, M., Yang, J.C., Phan, G.Q., Hughes, M.S., Sherry, R.M., et al. (2015). Chemotherapy-refractory diffuse large B-cell lymphoma and indolent B-cell malignancies can be effectively treated with autologous T cells expressing an anti-CD19 chimeric antigen receptor. *Journal of Clinical Oncology* 33(6):540-549.
- Kochenderfer, J.N., Feldman, S.A., Zhao, Y., Xu, H., Black, M.A., Morgan, R.A., Wilson, W.H., and Rosenberg, S.A. (2009). Construction and preclinical evaluation of an anti-CD19 chimeric antigen receptor. *Journal of Immunotherapy* 32(7):689-702.
- Kochenderfer, J.N., Wilson, W.H., Janik, J.E., Dudley, M.E., Stetler-Stevenson, M., Feldman, S.A., Maric, I., Raffeld, M., Nathan, D.A., Lanier, B.J., et al. (2010). Eradication of B-lineage cells and regression of lymphoma in a patient treated with autologous T cells genetically engineered to recognize CD19. *Blood* 116(20):4099-4102.

- Kohn, D.B., Sadelain, M., and Glorioso, J.C. (2003). Occurrence of leukaemia following gene therapy of X-linked SCID. *Nature Reviews Cancer* 3(7):477-488.
- Korde, L.A., Zujewski, J.A., Kamin, L., Giordano, S., Domchek, S., Anderson, W.F., Bartlett, J.M., Gelmon, K., Nahleh, Z., Bergh, J., et al. (2010). Multidisciplinary meeting on male breast cancer: summary and research recommendations. *Journal of Clinical Oncology* 28(12):2114-2122.
- Kowolik, C.M., Topp, M.S., Gonzalez, S., Pfeiffer, T., Olivares, S., Gonzalez, N., Smith, D.D., Forman, S.J., Jensen, M.C., and Cooper, L.J. (2006). CD28 costimulation provided through a CD19-specific chimeric antigen receptor enhances in vivo persistence and antitumor efficacy of adoptively transferred T cells. *Cancer Research* 66(22):10995 LP-11004.
- Krenciute, G., Krebs, S., Torres, D., Wu, M.F., Liu, H., Dotti, G., Li, X.N., Lesniak, M.S., Balyasnikova, I.V., and Gottschalk, S. (2016). Characterization and functional analysis of scFv-based chimeric antigen receptors to redirect T cells to IL13R $\alpha$ 2-positive Glioma. *Molecular Therapy* 24(2):354-363.
- Kumar, R., Sharma, A., and Tiwari, R.K. (2012). Application of microarray in breast cancer: an overview. *Journal of Pharmacy and Bioallied Sciences* 4(1):21-26.
- Künkele, A., Johnson, A.J., Rolczynski, L.S., Chang, C.A., Hoglund, V., Kelly-Spratt, K.S., and Jensen, M.C. (2015). Functional tuning of CARs reveals signaling threshold above which CD8<sup>+</sup> CTL antitumor potency is attenuated due to cell Fas-FasL-dependent AICD. *Cancer Immunology Research* 3(4):368-379.
- Künkele, A., Taraseviciute, A., Finn, L.S., Johnson, A.J., Berger, C., Finney, O., Chang, C.A., Rolczynski, L.S., Brown, C., Mgebroff, S., et al. (2017). Preclinical assessment of CD171-directed CAR T-cell adoptive therapy for childhood neuroblastoma: CE7 epitope target safety and product manufacturing feasibility. *Clinical Cancer Research* 23(2):466-477.
- Kwa, M.J., and Adams, S. (2018). Checkpoint inhibitors in triple-negative breast cancer (TNBC): where to go from here. *Cancer* 124(10):2086-2103.
- Lamers, C.H., Sleijfer, S., van Steenbergen, S., van Elzaker, P., van Krimpen, B., Groot, C., Vulto, A., den Bakker, M., Oosterwijk, E., Debets, R., et al. (2013). Treatment of metastatic renal cell carcinoma with CAIX CAR-engineered T cells: clinical evaluation and management of on-target toxicity. *Molecular Therapy* 21(4):904-912.
- Lamers, C.H., Klaver, Y., Gratama, J.W., Sleijfer, S., and Debets, R. (2016). Treatment of metastatic renal cell carcinoma (mRCC) with CAIX CAR-engineered T-cells-a

- completed study overview. *Biochemical Society Transactions* 44(3):951-959.
- Lamers, C.H., Langeveld, S.C., Groot-van Ruijven, C.M., Debets, R., Sleijfer, S., and Gratama, J.W. (2007). Gene-modified T cells for adoptive immunotherapy of renal cell cancer maintain transgene-specific immunefunctions in vivo. *Cancer Immunology, Immunotherapy* 56(12):1875-1883.
- Lamers, C.H., Sleijfer, S., Vulto, A.G., Kruit, W.H., Kliffen, M., Debets, R., Gratama, J.W., Stoter, G., and Oosterwijk, E. (2006). Treatment of metastatic renal cell carcinoma with autologous T-lymphocytes genetically retargeted against carbonic anhydrase IX: first clinical experience. *Journal of Clinical Oncology* 24(13):e20-22.
- Lawrence, R.T., Perez, E.M., Hernández, D., Miller, C.P., Haas, K.M., Irie, H.Y., Lee, S.I., Blau, C.A., and Villén, J. (2015). The proteomic landscape of triple-negative breast cancer. *Cell Reports* 11(4):630-644.
- Lee, A., and Djamgoz, M.B.A. (2018). Triple negative breast cancer: emerging therapeutic modalities and novel combination therapies. *Cancer Treatment Reviews* 62:110-122.
- Lee, D.W., Kochenderfer, J.N., Stetler-Stevenson, M., Cui, Y.K., Delbrook, C., Feldman, S.A., Fry, T.J., Orentas, R., Sabatino, M., Shah, N.N., et al. (2015). T cells expressing CD19 chimeric antigen receptors for acute lymphoblastic leukaemia in children and young adults: a phase 1 dose-escalation trial. *The Lancet* 385(9967):517-528.
- Lefrançois, E., Ortiz-Muñoz, G., Caudrillier, A., Mallavia, B., Liu, F., Sayah, D.M., Thornton, E.E., Headley, M.B., David, T., Cughlin, S.R., et al. (2017). The lung is a site of platelet biogenesis and a reservoir for haematopoietic progenitors. *Nature* 544(7648):105-109.
- Lehmann, B.D., Bauer, J.A., Chen, X., Sanders, M.E., Chakravarthy, A.B., Shyr, Y., and Pietenpol, J.A. (2011). Identification of human triple-negative breast cancer subtypes and preclinical models for selection of targeted therapies. *Journal of Clinical Investigation* 121(7):2750-2767.
- Letourneur, F., and Klausner, R.D. (1991). T-Cell and basophil activation through the cytoplasmic tail of T-cell-receptor zeta family proteins. *Proceedings of the National Academy of Sciences of the United States of America* 88(20):8905-8909.
- Levy, S. (2014). Function of the tetraspanin molecule CD81 in B and T cells. *Immunologic Research* 58(2-3):179-185.
- Li, H., and Zhao, Y. (2017). Increasing the safety and efficacy of chimeric antigen receptor T cell therapy. *Protein & Cell* 8(8):573-589.
- Li, K., Pan, X., Bi, Y., Xu, W., Chen, C., Gao, H., Shi, B., Jiang, H., Yang, S., Jiang, L., et al.

- (2015). Adoptive immunotherapy using T lymphocytes redirected to glypican-3 for the treatment of lung squamous cell carcinoma. *Oncotarget* 7(3):2496-2507.
- Li, N., Liu, S., Sun, M., Chen, W., Xu, X., Zeng, Z., Tang, Y., Dong, Y., Chang, A.H., and Zhao, Q. (2018). Chimeric antigen receptor-modified T cells redirected to EphA2 for the immunotherapy of non-small cell lung cancer. *Translational Oncology* 11(1):11-17.
- Liedtke, C., Mazouni, C., Hess, K.R., André, F., Tordai, A., Mejia, J.A., Symmans, W.F., Gonzalez-Angulo, A.M., Hennessy, B., Green, M., et al. (2008). Response to neoadjuvant therapy and long-term survival in patients with triple-negative breast cancer. *Journal of Clinical Oncology* 26(8):1275-1281.
- Litterman, A.J., Zellmer, D.M., LaRue, R.S., Jameson, S.C., and Largaespada, D.A. (2014). Antigen-specific culture of memory-like CD8 T cells for adoptive immunotherapy. *Cancer Immunology Research* 2(9):839-845.
- Liu, L., Sommermeyer, D., Cabanov, A., Kosasih, P., Hill, T., and Riddell, S.R. (2016). Inclusion of Strep-tag II in design of antigen receptors for T-cell immunotherapy. *Nature Biotechnology* 34(4):430-434.
- Loi, S., Pommey, S., Haibe-Kains, B., Beavis, P.A., Darcy, P.K., Smyth, M.J., and Stagg, J. (2013). CD73 promotes anthracycline resistance and poor prognosis in triple negative breast cancer. *Proceedings of the National Academy of Sciences* 110(27):11091-11096.
- Loi, S., Michiels, S., Salgado, R., Sirtaine, N., Jose, V., Fumagalli, D., Kellokumpu-Lehtinen, P.L., Bono, P., Kataja, V., Desmedt, C., et al. (2014). Tumor infiltrating lymphocytes are prognostic in triple negative breast cancer and predictive for trastuzumab benefit in early breast cancer: results from the FinHER trial. *Annals of Oncology* 25(8):1544-1550.
- Loi, S., Sirtaine, N., Piette, F., Salgado, R., Viale, G., van Eenoo, F., Rouas, G., Francis, P., Crown, J.P., Hitre, E., et al. (2013). Prognostic and predictive value of tumor-infiltrating lymphocytes in a phase III randomized adjuvant breast cancer trial in node-positive breast cancer comparing the addition of docetaxel to doxorubicin with doxorubicin-based chemotherapy: BIG 02-98. *Journal of Clinical Oncology* 31(7):860-867.
- Lou, Y.W., Wang, P.Y., Yeh, S.C., Chuang, P.K., Li, S.T., Wu, C.Y., Khoo, K.H., Hsiao, M., Hsu, T.L., and Wong, C.H. (2014). Stage-specific embryonic antigen-4 as a potential therapeutic target in glioblastoma multiforme and other cancers. *Proceedings of the National Academy of Sciences* 111(7):2482-2487.
- Louis, C.U., Savoldo, B., Dotti, G., Pule, M., Yvon, E., Myers, G.D., Rossig, C., Russel, H.V., Diouf, O., Liu, E., et al. (2011). Antitumor activity and long-term fate of chimeric antigen receptor-positive T cells in patients with neuroblastoma. *Blood* 118(23):6050-6056.

- Magee, M.S., and Snook, A.E. (2014). Challenges to chimeric antigen receptor (CAR)-T cell therapy for cancer. *Discovery Medicine* 18(100):265-271.
- Maier, J. (2013). Clinical immunotherapy of B-cell malignancy using CD19-targeted CAR T-cells. *Current Gene Therapy* 14(1):35-43.
- Maier, J., Brentjens, R.J., Gunset, G., Riviere, I., Sadelain, M. (2002). Human T-lymphocyte cytotoxicity and proliferation directed by a single chimeric TCR $\zeta$ /CD28 receptor. *Nature Biotechnology* 20(1):70-75.
- Maiti, S.N., Huls, H., Singh, H., Dawson, M., Figliola, M., Olivares, S., Rao, P., Zhao, Y.J., Multani, A., Yang, G., et al. (2013). Sleeping beauty system to redirect T-cell specificity for human applications. *Journal of Immunotherapy* 36(2):112-123.
- Masuda, H., Masuda, N., Kodama, Y., Ogawa, M., Karita, M., Yamamura, J., Tsukuda, K., Doihara, H., Miyoshi, S., Mano, M., et al. (2011). Predictive factors for the effectiveness of neoadjuvant chemotherapy and prognosis in triple-negative breast cancer patients. *Cancer Chemotherapy and Pharmacology* 67(4):911-917.
- Maude, S.L., Frey, N., Shaw, P.A., Aplenc, R., Barrett, D.M., Bunin, N.J., Chew, A., Gonzalez, V.E., Zheng, Z., Lacey, S.F., et al. (2014). Chimeric antigen receptor T cells for sustained remissions in leukemia. *New England Journal of Medicine* 371(16):1507-1517.
- Maus, M.V., Haas, A.R., Beatty, G.L., Albelda, S.M., Levine, B.L., Liu, X., Zhao, Y., Kalos, M., and June, C.H. (2013). T cells expressing chimeric antigen receptors can cause anaphylaxis in humans. *Cancer Immunology Research* 1(1):26-31.
- Mezzanzanica, D., Canevari, S., Mazzoni, A., Figini, M., Colnaghi, M.I., Waks, T., Schindler, D.G., and Eshhar, Z. (1998). Transfer of chimeric receptor gene made of variable regions of tumor-specific antibody confers anticarbohydrate specificity on T cells. *Cancer Gene Therapy* 5(6):401-407.
- Milone, M.C., Fish, J.D., Carpenito, C., Carroll, R.G., Binder, G.K., Teachey, D., Samanta, M., Lakhal, M., Gloss, B., Danet-Desnoyers, G., et al. (2009). Chimeric receptors containing CD137 signal transduction domains mediate enhanced survival of T cells and increased antileukemic efficacy in vivo. *Molecular Therapy* 17(8):1453-1464.
- Min, I.M., Shevlin, E., Vedvyas, Y., Zaman, M., Wyrwas, B., Scognamiglio, T., Moore, M.D., Wang, W., Park, S., Park, S., et al. (2017). CAR T therapy targeting ICAM-1 eliminates advanced human thyroid tumors. *Clinical Cancer Research* 23(24):7569-7583.
- Mittal, D., Sinha, D., Barkauskas, D., Young, A., Kalimutho, M., Stannard, K., Caramia, F.,

- Haibe-Kains, B., Stagg, J., Khanna, K.K., et al. (2016). Adenosine 2B receptor expression on cancer cells promotes metastasis. *Cancer Research* 76(15):4372-4382.
- Moon, E.K., Carpenito, C., Sun, J., Wang, L.C., Kapoor, V., Predina, J., Powell, D.J., Riley, J.L., June, C.H., and Albelda, S.M. (2011). Expression of a functional CCR2 receptor enhances tumor localization and tumor eradication by retargeted human T cells expressing a mesothelin-specific chimeric antibody receptor. *Clinical Cancer Research* 17(14):4719-4730.
- Morgan, R.A., Dudley, M.E., Wunderlich, J.R., Hughes, M.S., Yang, J.C., Sherry, R.M., Royal, R.E., Topalian, S.L., Kammula, U.S., Restifo, N.P., et al. (2006). Cancer regression in patients after transfer of genetically engineered lymphocytes. *Science* 314(5796):126-129.
- Morgan, R.A., Yang, J.C., Kitano, M., Dudley, M.E., Laurencot, C.M., and Rosenberg, S.A. (2010). Case Report of a serious adverse event following the administration of T cells transduced with a chimeric antigen receptor recognizing ERBB2. *Molecular Therapy* 18(4):843-851.
- Morgenroth, A., Cartellieri, M., Schmitz, M., Günes, S., Weigle, B., Bachmann, M., Abken, H., Rieber, E.P., and Temme, A. (2007). Targeting of tumor cells expressing the prostate stem cell antigen (PSCA) using genetically engineered T-cells. *The Prostate* 67(10):1121-1131.
- Moritz, D., and Groner, B. (1995). A spacer region between the single chain antibody-and the CD3 $\zeta$ -chain domain of chimeric T cell receptor components is required for efficient ligand binding and signaling activity. *Gene Therapy* 2(8):539-546.
- Newick, K., Moon, E., and Albelda, S.M. (2016). Chimeric Antigen Receptor T-Cell Therapy for Solid Tumors. *Molecular Therapy, Oncolytics* 3:16006.
- Niederman, T.M., Ghogawala, Z., Carter, B.S., Tompkins, H.S., Russell, M.M., and Mulligan, R.C. (2002). Antitumor activity of cytotoxic T lymphocytes engineered to target vascular endothelial growth factor receptors. *Proceedings of the National Academy of Sciences of the United States of America* 99(10):7009-7014.
- Nik-Zainal, S., Davies, H., Staaf, J., Ramakrishna, M., Glodzik, D., Zou, X., Martincorena, I., Alexandrov, L.B., Martin, S., Wedge, D.C., et al. (2016). Landscape of somatic mutations in 560 breast cancer whole-genome sequences. *Nature* 534(7605):47-54.
- Noto, Z., Yoshida, T., Okabe, M., Koike, C., Fathy, M., Tsuno, H., Tomihara, K., Arai, N., Noguchi, M. and Nikaido, T. (2013). CD44 and SSEA-4 positive cells in an oral cancer cell line HSC-4 possess cancer stem-like cell characteristics. *Oral Oncology* 49(8):787-

795.

- O'Reilly, E.A., Gubbins, L., Sharma, S., Tully, R., Guang, M.H., Weiner-Gorzel, K., McCaffrey, J., Harrison, M., Furlong, F., Kell, M., et al. (2015). The fate of chemoresistance in triple negative breast cancer (TNBC). *BBA Clinical* 3:257-275.
- O'Rourke, D.M., Nasrallah, M.P., Desai, A., Melenhorst, J.J., Mansfield, K., Morrisette, J.J.D., Martinez-Lage, M., Brem, S., Maloney, E., Shen, A., et al. (2017). A single dose of peripherally infused EGFRvIII-directed CAR T cells mediates antigen loss and induces adaptive resistance in patients with recurrent glioblastoma. *Science Translational Medicine* 9(399).
- Pal, S.K., Childs, B.H., and Pegram, M. (2011). Triple negative breast cancer: unmet medical needs. *Breast Cancer Research and Treatment* 125(3):627-636.
- Pal, S.K., and Mortimer, J. (2009). Triple-negative breast cancer: novel therapies and new directions. *Maturitas* 63(4):269-274.
- Parise, C.A., and Caggiano, V. (2014). Breast cancer survival defined by the ER/PR/HER2 subtypes and a surrogate classification according to tumor grade and immunohistochemical biomarkers. *Journal of Cancer Epidemiology* 2014:469251.
- Park, J.R., DiGiusto, D.L., Slovak, M., Wright, C., Naranjo, A., Wagner, J., Meechoovet, H.B., Bautista, C., Chang, W.C., Ostberg, J.R., et al. (2007). Adoptive transfer of chimeric antigen receptor re-directed cytolytic T lymphocyte clones in patients with neuroblastoma. *Molecular Therapy* 15(4):825-833.
- Park, Y.P., Jin, L., Bennett, K.B., Wang, D., Fredenburg, K.M., Tseng, J.E., Chang, L.J., Huang, J., and Chan, E.K.L. (2018). CD70 as a target for chimeric antigen receptor T cells in head and neck squamous cell carcinoma. *Oral Oncology* 78:145-150.
- Parkhurst, M.R., Yang, J.C., Langan, R.C., Dudley, M.E., Nathan, D.A., Feldman, S.A., Davis, J.L., Morgan, R.A., Merino, M.J., Sherry, R.M., et al. (2011). T cells targeting carcinoembryonic antigen can mediate regression of metastatic colorectal cancer but induce severe transient colitis. *Molecular Therapy* 19(3):620-626.
- Patel, S.D., Moskalenko, M., Smith, D., Maske, B., Finer, M.H., and McArthur, J.G. (1999). Impact of chimeric immune receptor extracellular protein domains on T cell function. *Gene Therapy* 6(3):412-419.
- Peng, W., Ye, Y., Rabinovich, B.A., Liu, C., Lou, Y., Zhang, M., Whittington, M., Yang, Y., Overwijk, W.W., Lizee, G., et al. (2010). Transduction of tumor-specific T cells with CXCR2 chemokine receptor improves migration to tumor and antitumor immune

- responses. *Clinical Cancer Research* 16(22):5458-5468.
- Peppercorn, J., Perou, C.M., and Carey, L.A. (2008). Molecular Subtypes in breast cancer evaluation and management: divide and conquer. *Cancer Investigation* 26(1):1-10.
- Perou, C.M., Sørile, T., Eisen, M.B., van de Rijn, M., Jeffrey, S.S., Ress, C.A., Pollack, J.R., Ross, D.T., Johnsen, H., Akslen, L.A., et al. (2000). Molecular portraits of human breast tumours. *Nature* 406(6797):747-752.
- Pfeifer, R., Al Rawashdeh, W., Brauner, J., Lock, D., Kaiser, A., Hardt, O., Bosio, A., Assenmacher, M., Johnston, I.C.D. (2018). Targeting stage-specific embryonic antigen 4 (SSEA-4) in TNBC by CAR T cells reveals unforeseen on target/off tumor toxicities in adult mice. *in submission*
- Pittenger, M.F. (1999). Multilineage potential of adult human mesenchymal stem cells. *Science* 284(5411):143-147.
- Porter, D.L., Levine, B.L., Kalos, M., Bagg, A., and June, C.H. (2011). Chimeric antigen receptor-modified T cells in chronic lymphoid leukemia. *The New England Journal of Medicine* 365(8):725-733.
- Porter, D.L., Hwang, W.T., Frey, N.V., Lacey, S.F., Shaw, P.A., Loren, A.W., Bagg, A., Marcucci, K.T., Shen, A., Gonzalez, V., et al. (2015). Chimeric antigen receptor T cells persist and induce sustained remissions in relapsed refractory chronic lymphocytic leukemia. *Science Translational Medicine* 7(303):303ra139.
- Posey, A.D., Schwab, R.D., Boesteanu, A.C., Steentoft, C., Mandel, U., Engels, B., Stone, J.D., Madsen, T.D., Schreiber, K., Haines, K.M., et al. (2016). Engineered CAR T cells targeting the cancer-associated Tn-glycoform of the membrane mucin MUC1 control adenocarcinoma. *Immunity* 44(6):1444-1454.
- Priceman, S.J., Gerdt, E.A., Tilakawardane, D., Kennewick, K.T., Murad, J.P., Park, A.K., Jeang, B., Yamaguchi, Y., Yang, X., Urak R., et al. (2018). Co-stimulatory signaling determines tumor antigen sensitivity and persistence of CAR T cells targeting PSCA+ metastatic prostate cancer. *Oncotarget* 9(2):e1380764.
- Pule, M.A., Savoldo, B., Myers, G.D., Rossig, C., Russell, H.V., Dotti, G., Huls, M.H., Liu, E., Gee, A.P., Mei, Z., et al. (2008). Virus-specific T cells engineered to coexpress tumor-specific receptors: persistence and antitumor activity in individuals with neuroblastoma. *Nature Medicine* 14(11):1264-1270.
- Pure, E., and Lo, A. (2016). Can targeting stroma pave the way to enhanced antitumor immunity and immunotherapy of solid tumors? *Cancer Immunology Research* 4(4):269-

278.

- Riekstina, U., Cakstina, I., Parfejevs, V., Hoogduijn, M., Jankovskis, G., Muiznieks, I., Muceniece, R., and Ancans, J. (2009). Embryonic stem cell marker expression pattern in human mesenchymal stem cells derived from bone marrow, adipose tissue, heart and dermis. *Stem Cell Reviews and Reports* 5(4):378-386.
- Romeo, C., and Seed, B. (1991). Cellular immunity to HIV activated by CD4 fused to T cell or Fc receptor polypeptides. *Cell* 64(5):1037-1046.
- Sabatino, M., Hu, J., Sommariva, M., Gautam, S., Fellowes, V., Hocker, J.D., Dougherty, S., Qin, H., Klebanoff, C.A., Fry, T.J., et al. (2016). Generation of clinical-grade CD19-specific CAR-modified CD81 memory stem cells for the treatment of human B-cell malignancies. *Blood* 128(4):519-528.
- Saha, S., Nakazawa, Y., Huye, L.E., Doherty, J.E., Galvan, D.L., Rooney, C.M., and Wilson, M.H. (2012). piggyBac transposon system modification of primary human T cells. *Journal of Visualized Experiments* 69:e4235.
- Saito, S., Orikasa, S., Satoh, M., Ohyama, C., Ito, A., and Takahashi, T. (1997). Expression of globo-series gangliosides in human renal cell carcinoma. *Japanese Journal of Cancer Research* 88(7):652-659.
- Savoldo, B., Ramos, C.A., Liu, E., Mims, M.P., Keating, M.J., Carrum, G., Kamble, R.T., Bollard, C.M., Gee, A.P., Mei, Z., et al. (2011). CD28 costimulation improves expansion and persistence of chimeric antigen receptor-modified T cells in lymphoma patients. *Journal of Clinical Investigation* 121(5):1822-1826.
- Scholler, J., Brady, T.L., Binder-Scholl, G., Hwang, W.T., Plesa, G., Hege, K.M., Vogel, A.N., Kalos, M., Riley, J.L., Deeks, S.G., et al. (2012). Decade-long safety and function of retroviral-modified chimeric antigen receptor T cells. *Science Translational Medicine* 4(132):132ra53.
- Schuberth, P.C., Hagedorn, C., Jensen, S.M., Gulati, P., van den Broek, M., Mischo, A., Soltermann, A., Jüngel, A., Marroquin Belaunzaran, O., Stahel, R., et al. (2013). Treatment of malignant pleural mesothelioma by fibroblast activation protein-specific re-directed T cells. *Journal of Translational Medicine* 11:187.
- Seder, R.A., Darrah, P.A., and Roederer, M. (2008). T-cell quality in memory and protection: implications for vaccine design. *Nature Reviews Immunology* 8(4):247-258.
- Sergina, N.V., Rausch, M., Wang, D., Blair, J., Hann, B., Shokat, K.M., and Moasser, M.M. (2007). Escape from HER-family tyrosine kinase inhibitor therapy by the kinase-inactive

- HER3. *Nature* 445(7126):437-441.
- Shinohara, Y., Furukawa, J., and Miura, Y. (2015). Glycome as Biomarkers. *General Methods in Biomarker Research and Their Applications* 1–2:111–140.
- Shirasu, N., Yamada, H., Shibaguchi, H., Kuroki, M., and Kuroki, M. (2012). Molecular characterization of a fully human chimeric T-cell antigen receptor for tumor-associated antigen EpCAM. *Journal of Biomedicine and Biotechnology* 2012:853879.
- Shultz, L.D., Lyons, B.L., Burzenski, L.M., Gott, B., Chen, X., Chaleff, S., Kotb, M., Gillies, S.D., King, M., Mangada, J., et al. (2005). Human lymphoid and myeloid cell development in NOD/LtSz-scid IL2R gamma null mice engrafted with mobilized human hemopoietic stem cells. *The Journal of Immunology* 174(10):6477-6489.
- Shultz, L.D., Goodwin, N., Ishikawa, F., Hosur, V., Lyons, B.L., and Greiner, D.L. (2014). Human cancer growth and therapy in immunodeficient mouse models. *Cold Spring Harbor Protocol* 2014(7):694-708.
- Siegler, E.L., and Wang, P. (2018). Preclinical models in chimeric antigen receptor-engineered T cell therapy. *Human Gene Therapy* 29(5):534-546.
- Singh, H., Figliola, M.J., Dawson, M.J., Huls, H., Olivares, S., Switzer, K., Mi, T., Maiti, S., Kebriaei, P., Lee, D.A., et al. (2011). Reprogramming CD19-specific T cells with IL-21 signaling can improve adoptive immunotherapy of B-lineage malignancies. *Cancer Research* 71(10):3516-3527.
- Sitkovsky, M.V., Hatfield, S., Abbott, R., Belikoff, B., Lukashev, D., and Ohta, A. (2014). Hostile, hypoxia-A2-adenosinergic tumor biology as the next barrier to overcome for tumor immunologists. *Cancer Immunology Research* 2(7):598-605.
- Sivasubramaniyan, K., Harichandan, A., Schilbach, K., Mack, A.F., Bedke, J., Stenzl, A., Kanz, L., Niederfellner, G., and Bühring, H.J. (2015). Expression of stage-specific embryonic antigen-4 (SSEA-4) defines spontaneous loss of epithelial phenotype in human solid tumor cells. *Glycobiology* 25(8):902-917.
- Slovin, S.F., Wang, X., Hullings, M., Arauz, G., Bartido, S., Lewis, J.S., Schöder, H., Zanzonico, P., Scher, H.I., Riviere, I., et al. (2013). Chimeric antigen receptor (CAR<sup>+</sup>) modified T cells targeting prostate-specific membrane antigen (PSMA) in patients (pts) with castrate metastatic prostate cancer (CMPC). *Journal of Clinical Oncology* 31(6):72-72.
- Stemberger, C., Dreher, S., Tschulik, C., Piossek, C., Bet, J., Yamamoto, T.N., Schiemann, M., Neuenhahn, M., Martin, K., Schlapschy, M., et al. (2012). Novel serial positive

- enrichment technology enables clinical multiparameter cell sorting. *PLoS ONE* 7(4):e35798.
- Stewart, B.W., and Wild, C.P. (2014). World Cancer Report 2014. *World Health Organization, Geneva*.
- Stone, J.D., Aggen, D.H., Schietinger, A., Schreiber, H., and Kranz, D.M. (2012). A sensitivity scale for targeting T cells with chimeric antigen receptors (CARs) and bispecific T-cell engagers (BiTEs). *Oncot Immunology* 1(6):863-873.
- Sukumar, M., Liu, J., Ji, Y., Subramanian, M., Crompton, J.G., Yu, Z., Roychoudhuri, R., Palmer, D.C., Muranski, P., Karoly, E.D., et al. (2013). Inhibiting glycolytic metabolism enhances CD8+ T cell memory and antitumor function. *Journal of Clinical Investigation* 123(10):4479-4488.
- Sun, X.X., and Yu, Q. (2015). Intra-tumor heterogeneity of cancer cells and its implications for cancer treatment. *Acta Pharmacologica Sinica* 36(10):1219-1227.
- Tamma, S., Huang, X., Wong, M., Milone, M.C., Ma, L., Levine, B.L., June, C.H., Wagner, J.E., Blazar, B.R., and Zhou, X. (2010). 4-1BB and CD28 signaling plays a synergistic role in redirecting umbilical cord blood T cells against B-cell malignancies. *Human Gene Therapy* 21(1):75-86.
- Taraseviciute, A., Tkachev, V., Ponce, R., Turtle, C.J., Snyder, J.M., Liggitt, H.D., Myerson, D., Gonzalez-Cuyar, L., Baldessari, A., English, C., et al. (2018) Chimeric antigen receptor T cell-mediated neurotoxicity in non-human primates. *Cancer Discovery* CD-17-1368.
- Tchou, J., Zhao, Y., Levine, B.L., Zhang, P.J., Davis, M.M., Melenhorst, J.J., Kulikovskaya, I., Brennan, A.L., Liu, X., Lacey, S.F., et al. (2017). Safety and efficacy of intratumoral injections of chimeric antigen receptor (CAR) T cells in metastatic breast cancer. *Cancer Immunology Research* 5(12):1152-1161.
- Thiery, J.P. (2002). Epithelial–mesenchymal transitions in tumour progression. *Nature Reviews Cancer* 2(6):442-454.
- Tomayko, M.M., and Reynolds, C.P. (1989) Determination of subcutaneous tumor size in athymic (nude) mice. *Cancer Chemotherapy and Pharmacology* 24(3):148-154.
- Tran, E., Chinnasamy, D., Yu, Z., Morgan, R.A., Lee, C.C., Restifo, N.P., and Rosenberg, S.A. (2013). Immune targeting of fibroblast activation protein triggers recognition of multipotent bone marrow stromal cells and cachexia. *The Journal of Experimental Medicine* 210(6):1125-1135.

- Turatti, F., Figini, M., Balladore, E., Alberti, P., Casalini, P., Marks, J.D., Canevari, S., and Mezzanzanica, D. (2007). Redirected activity of human antitumor chimeric immune receptors is governed by antigen and receptor expression levels and affinity of interaction. *Journal of Immunotherapy* 30(7):68-693.
- Turner, N., Lambros, M.B., Horlings, H.M., Pearson, A., Sharpe, R., Natrajan, R., Geyer, F.C., van Kouwenhove, M., Kreike, B., Mackay, A., et al. (2010). Integrative molecular profiling of triple negative breast cancers identifies amplicon drivers and potential therapeutic targets. *Oncogene* 29(14):2013-2023.
- Turtle, C.J., Hanafi, L.C., Berger, C., Gooley, T.A., Cherian, S., Hudecek, M., Sommermeyer, D., Melville, K., Pender, B., Budiarto, T.M., et al. (2016). CD19 CAR – T cells of defined CD4+ :CD8+ composition in adult B cell ALL patients. *The Journal of Clinical Investigations* 126(6):2123-2138.
- Uhlen, M., Oksvold, P., Fagerberg, L., Lundberg, E., Jonasson, K., Forsberg, M., Zwahlen, M., Kampf, C., Wester, K., Hober, S., et al. (2010). Towards a knowledge-based human protein atlas. *Nature Biotechnology* 28(12):1248-1250.
- van der Waart, A.B., van de Weem, N.M., Maas, F., Kramer, C.S., Kester, M.G., Falkenburg, J.H., Schaap, N., Jansen, J.H., van der Voort, R., Gattinoni, L., et al. (2014). Inhibition of Akt signaling promotes the generation of superior tumor-reactive T cells for adoptive immunotherapy. *Blood* 124(23):3490-3500.
- van Schalkwyk, M.C., Papa, S.E., Jeannon, J.P., Guerrero Urbano, T., Spicer, J.F., and Maher, J. (2013). Design of a phase I clinical trial to evaluate intratumoral delivery of ErbB-targeted chimeric antigen receptor T-cells in locally advanced or recurrent head and neck cancer. *Human Gene Therapy Clinical Development* 24(3):134-142.
- vanSeggelen, H., Hammill, J.A., Dvorkin-Gheva, A., Tantalos, D.G., Kwiecien, J.M., Denisova, G.F., Rabinovich, B., Wan, Y., Bramson, J.L. (2015). T cells engineered with chimeric antigen receptors targeting NKG2D ligands display lethal toxicity in mice. *Molecular Therapy* 23(10):1600-1610.
- Vences-Catalán, F., Duault, C., Kuo, C.C., Rajapaksa, R., Levy, R., and Levy, S. (2017). CD81 as a tumor target. *Biochemical Society Transactions* 45(2):531-535.
- Venkitaraman, A.R. (2002). Cancer susceptibility and the functions of BRCA1 and BRCA2. *Cell* 108(2):171-182.
- Villa, G.R., and Mischel, P.S. (2016). Old player, new partner: EGFRvIII and cytokine receptor signaling in glioblastoma. *Nature Neuroscience* 19(6):765-767.

- Voduc, K.D., Cheang, M.C., Tyldesley, S., Gelmon, K., Nielsen, T.O., and Kennecke, H. (2010). Breast cancer subtypes and the risk of local and regional relapse. *Journal of Clinical Oncology* 28(10):1684-1691.
- Wang, J., Jensen, M., Lin, Y., Sui, X., Chen, E., Lindgren, C.G., Till, B., Raubitschek, A., Forman, S.J., Qian, X., et al. (2007). Optimizing adoptive polyclonal T cell immunotherapy of lymphomas, using a chimeric T cell receptor possessing CD28 and CD137 costimulatory domains. *Human Gene Therapy* 18(8):712-725.
- Wang, L.C., Lo, A., Scholler, J., Sun, J., Majumdar, R.S., Kapoor, V., Antzis, M., Cotner, C.E., Johnson, L.A., Durham, A.C., et al. (2014). Targeting fibroblast activation protein in tumor stroma with chimeric antigen receptor T cells can inhibit tumor growth and augment host immunity without severe toxicity. *Cancer Immunology Research* 2(2):154-166.
- Wang, X., Naranjo, A., Brown, C.E., Bautista, C., Wong, C.W., Chang, W.C., Aguilar, B., Ostberg, J.R., Riddell, S.R., Forman, S.J., et al. (2012). Phenotypic and functional attributes of lentivirus-modified CD19-specific human CD8<sup>+</sup> central memory T cells manufactured at clinical scale. *Journal of Immunotherapy* 35(9):689-701.
- Wang, Y., Geldres, C., Ferrone, S., and Dotti, G. (2015). Chondroitin sulfate proteoglycan 4 as a target for chimeric antigen receptor-based T-cell immunotherapy of solid tumors. *Expert Opinion on Therapeutic Targets* 19(10):1339-1350.
- Watanabe, K., Terakura, S., Martens, A.C., van Meerten, T., Uchiyama, S., Imai, M., Sakemura, R., Goto, T., Hanajiri, R., Imahashi, N., et al. (2015). Target antigen density governs the efficacy of anti-CD20-CD28-CD3 $\zeta$  chimeric antigen receptor-modified effector CD8<sup>+</sup> T cells. *The Journal of Immunology* 194(3):911-920.
- Wei, F., Zhong, S., Ma, Z., Kong, H., Medvec, A., Ahmed, R., Freeman, G.J., Krosgaard, M., and Riley, J.L. (2013). Strength of PD-1 signaling differentially affects T-cell effector functions. *Proceedings of the National Academy of Sciences* 110(27):E2480-E2489.
- Weijtens, M.E., Willemsen, R.A., van Krimpen, B.A., and Bolhuis, R.L. (1998). Chimeric scFv/gamma receptor-mediated T-cell lysis of tumor cells is coregulated by adhesion and accessory molecules. *International Journal of Cancer* 77(2):181-187.
- Whilding, L.M., Parente-Pereira, A.C., Zabinski, T., Davies, D.M., Petrovic, R.M.G., Kao, Y.V., Saxena, S.A., Romain, A., Costa-Guerra, J.A., Violette, S., et al. (2017). Targeting of aberrant  $\alpha\beta 6$  integrin expression in solid tumors using chimeric antigen receptor-engineered T cells. *Molecular Therapy* 25(1):259-273.
- Wikstrand, C.J., Hale, L.P., Batra, S.K., Hill, M.L., Humphrey, P.A., Kurpad, S.N., McLendon,

- R.E., Moscatello, D., Pegram, C.N., Reist, C.J., et al. (1995). Monoclonal antibodies against EGFRvIII are tumor specific and react with breast and lung carcinomas and malignant gliomas. *Cancer Research* 55(14):3140-3148.
- Wu, M.R., Zhang, T., DeMars, L.R., and Sentman, C.L. (2015). B7H6-specific chimeric antigen receptors lead to tumor elimination and host antitumor immunity. *Gene Therapy* 22(8):675-684.
- Xu, X.J., Song, D.G., Poussin, M., Ye, Q., Sharma, P., Rodríguez-García, A., Tang, Y.M., and Powell, D.J. (2016). Multiparameter comparative analysis reveals differential impacts of various cytokines on CAR T cell phenotype and function ex vivo and in vivo. *Oncotarget* 7(50):82354-82368.
- Xu, Y., Zhang, M., Ramos, C.A., Durett, A., Liu, E., Dakhova, O., Liu, H., Creighton, C.J., Gee, A.P., Heslop, H.E., et al. (2014). Closely related T-memory stem cells correlate with in vivo expansion of CAR.CD19-T cells and are preserved by IL-7 and IL-15. *Blood* 123(24):3750-3759.
- Yaghoubi, S.S., Jensen, M.C., Satyamurthy, N., Budhiraja, S., Paik, D., Czernin, J. and Gambhir, S.S. (2009). Noninvasive detection of therapeutic cytolytic T cells with 18F-FHBG PET in a patient with glioma. *Nature Clinical Practice Oncology* 6(1):53-58.
- Ye, F., Li, Y., Hu, Y., Zhou, C., Hu, Y., and Chen, H. (2010). Stage-specific embryonic antigen 4 expression in epithelial ovarian carcinoma. *International Journal of Gynecological Cancer : Official Journal of the International Gynecological Cancer Society* 20(6):958-964.
- You, F., Jiang, L., Zhang, B., Lu, Q., Zhou, Q., Liao, X., Wu, H., Du, K., Zhu, Y., Meng, H., et al. (2016). Phase 1 clinical trial demonstrated that MUC1 positive metastatic seminal vesicle cancer can be effectively eradicated by modified anti-MUC1 chimeric antigen receptor transduced T cells. *Science China Life Sciences* 59(4):386-397.
- Yvon, E., Del Vecchio, M., Savoldo, B., Hoyos, V., Dutour, A., Anichini, A., Dotti, G., and Brenner, M.K. (2009). Immunotherapy of metastatic melanoma using genetically engineered GD2-specific T cells. *Clinical Cancer Research* 15(18):5852-5860.
- Zhang, C., Wang, Z., Yang, Z., Wang, M., Li, S., Li, Y., Zhang, R., Xiong, Z., Wei, Z., Shen, J. et al. (2017). Phase I escalating-dose trial of CAR-T therapy targeting CEA+ metastatic colorectal cancers. *Molecular Therapy* 25(5):1248-1258.
- Zhang, T., Barber, A., and Sentman, C.L. (2007). Chimeric NKG2D-modified T cells inhibit systemic T-cell lymphoma growth in a manner involving multiple cytokines and cytotoxic pathways. *Cancer Research* 67(22):11029-11036.

- Zhang, T., Lemoi, B.A., and Sentman, C.L. (2005). Chimeric NK-receptor-bearing T cells mediate antitumor immunotherapy. *Blood* 106(5):1544-1551.
- Zheng, Z., Chinnasamy, N. and Morgan, R.A. (2012). Protein L: a novel reagent for the detection of chimeric antigen receptor (CAR) expression by flow cytometry. *Journal of Translational Medicine* 10(1):29.
- Zhou, X., Li, J., Wang, Z., Chen, Z., Qiu, J., Zhang, Y., Wang, W., Ma, Y., Huang, N., Cui, K., et al. (2013). Cellular immunotherapy for carcinoma using genetically modified EGFR-specific T lymphocytes. *Neoplasia* 15(5):544-553.
- Zhu, L., Gibson, P., Currle, D.S., Tong, Y., Richardson, R.J., Bayazitov, I.T., Poppleton, H., Zakharenko, S., Ellison, D.W., and Gilbertson, R.J. (2009). Prominin 1 marks intestinal stem cells that are susceptible to neoplastic transformation. *Nature* 457(7229):603-607.
- Zhu, X., Prasad, S., Gaedicke, S., Hettich, M., Firat, E., and Niedermann, G. (2015). Patient-derived glioblastoma stem cells are killed by CD133-specific CAR T cells but induce the T cell aging marker CD57. *Oncotarget* 6(1):171-184.
- Zuccolotto, G., Fracasso, G., Merlo, A., Montagner, I.M., Rondina, M., Bobisse, S., Figini, M., Cingarlini, S., Colombatti, M., Zanovello, P., et al. (2014). PSMA-specific CAR-engineered T cells eradicate disseminated prostate cancer in preclinical models. *PLoS ONE* 9(10):e109427

## Acknowledgement

A body of work like the one presented here would not have been possible without the help and support of many people. First and foremost, I would like to express my sincere gratitude to Dr. Ian Johnston for his mentorship and continuous guidance as well as his open door policy which was of permanent enormous help during the whole time of my PhD studies. He has always found the right combination of being encouraging and critical, impelling and understanding, and has always put his trust in me, thereby promoting my independent growth. The friendly relationship we had throughout my PhD studies was highly supportive and his warm-hearted personality and positive attitude made it easier for me to overcome certain drawbacks in my project(s).

My PhD studies would have been a lot harder if it was not for Dr. Stefan Stevanović and Dr. Hans-Georg Rammensee who accepted me as an intern, then as a HiWi, and later as a diploma student in their department while I was still a graduate student in Tübingen. In this way they equipped me with the fundamentals of T cell biology and launched my scientific career. I am particularly grateful to them for agreeing to be my academic supervisors during my PhD studies, for being always open to my request and reviewing this thesis.

I would also like to cordially thank Dr. Olaf Hardt and Dr. Andrew Kaiser for valuable and highly appreciated scientific input as well as the support during my studies. Despite their busy schedules, they always found time to discuss aspects and challenges of my project, gave insightful advice and asked hard questions which incited me to widen my research from various perspectives.

Moreover, I am very much in debt of Dr. Wa'el Al Rawashdeh, who shared his immense knowledge and expertise in *in vivo* experiments with me. Although he was new at Miltenyi Biotec GmbH when I started my *in vivo* work and had to face lots of novelty and projects himself, he, too, used to make time to help me and his insightful observation as well as our constructive scientific meetings on the project had enormous impact on my development. I came to value him a lot – both as a colleague and a friend. Equally, I am thankful to his team member Janina Brauner, who readily helped me with the *in vivo* experiments when it was just too much. Janina and Wa'el, thank you also for helping me out with the i.v. injections 😊

I would also like to thank all members of the Students' Club at Miltenyi Biotec GmbH for critical comments and fruitful discussions that fundamentally helped me to grow scientifically over the last years. In particular, I am grateful to Nicole Cordes and Bettina Kotter for going through parts of the thesis.

A special thank you goes to Maria Delso Vallejo and Patrícia Domingues, my former office colleagues and true friends. I very much appreciated their scientific input and our stimulating

discussions...but also their loyalty, patience, and encouragement. I will always remember the great time we three had together.

A big thank you goes also to Kerstin von Kolontaj for giving me such a warm welcome when I joined Miltenyi Biotec GmbH and for introducing me to BodyAttack as a balance to work. I really miss our meet ups for sports!

I would also like to acknowledge Roland for being a true and supportive friend these last years and the recent "care package"...I can really use it now 😊

Finally, I would like to express my deepest gratitude to my family for giving me the opportunity to follow my dreams and supporting me in every possible way along my path. You always let me make my own decision and your understanding, faith, and love have always been heart-balm for me in difficult situations. I love you all so much!

It's been a tough, demanding and exciting journey and only with all your help and support I was able to make it happen. Thank you all for this and please know that I consider myself both fortunate and blessed to have you all in my life!